The Institute of Paper Chemistry

Appleton, Wisconsin

Doctor's Dissertation

An Investigation of the Physical-Chemical Mechanism of Selective Delignification of Wood with Peracetic Acid

James S. Albrecht

June, 1971

AN INVESTIGATION OF THE PHYSICAL-CHEMICAL MECHANISM OF SELECTIVE DELIGNIFICATION OF WOOD WITH PERACETIC ACID

A thesis submitted by

James S. Albrecht

B.A. 1966, Grinnell College

M.S. 1968, Lawrence University

in partial fulfillment of the requirements
of The Institute of Paper Chemistry
for the degree of Doctor of Philosophy
from Lawrence University
Appleton, Wisconsin

June, 1971

TABLE OF CONTENTS

SUMMARY

The peracetic acid delignification of acetone-extracted loblolly pinewood (Pinus taeda L.) wood wafers was investigated with coincident emphasis on physical and chemical changes occurring in both the wood and the solubilized reaction products. Delignification was achieved by subjecting thin wood wafers to a continuous stream of fresh peracetic acid in 3.0% aqueous solution at 60°C. Quantitative analysis for lignin and carbohydrate materials showed that about 7% of the reaction products solubilized by 80% yield of the residual wood was unoxidized carbohydrates; the remainder was from the lignin portion of the wood. Lignin-stained microtome cross sections of the partially delignified wood wafers showed that the reaction proceeded uniformly across the thin (0.5 mm. thick) radial dimension of the wafers.

The solute exclusion technique was applied to show that the change in pore volume of the wood wafers upon peracetic acid delignification to 80% yield was comparable to that observed with kraft pulping. An improved estimation of the size of dextran (solute) molecules in solution was applied to solute exclusion studies in the literature to yield a relationship between estimated median pore width and yield.

Stagewise delignification of loblolly pinewood wafers was accomplished by collecting the solubilized reaction products from the continuous flow reactor. Gel permeation chromatography of the solubilized reaction products showed that, as reaction proceeded, there was a shift in the distribution curve of the lignin fragments toward larger molecules. A composite product liquor, containing all the solubilized reaction products down to 80% yield, was fractionated on the GPC column for use in column calibration. Intrinsic viscosity and number-average molecular weight of the fractions were determined, but neither yielded a smooth decreasing function with increasing fraction number. The absorptivity at 275 nm.

was also found to vary as a function of fraction number, verifying that there existed some chemical differences between the fractions.

The porous sphere model for a cross-linked polymer in solution was applied to the $[\eta]$-$\bar{M}_n$ data over a limited range to yield a relationship between hydrodynamic radius of the solubilized lignin and fraction number. When the GPC elution curves of the successive reaction stages were compared to the estimated median pore width curve, a corresponding size change was noted, and from this it was concluded that pore size serves as a restricting mechanism in the extraction of lignin fragments from loblolly pinewood by peracetic acid.

Chemical analysis of the lignin fractions showed that 0.3-0.6 carboxyl groups per C_9 unit were introduced during the delignification reaction. The number of methoxyl groups and free phenolic hydroxyl groups decreased to about 30% of the amount in unreacted softwood lignin.

Ultraviolet spectroscopy of the solubilized lignin in solution showed that there was almost complete destruction of α-carbonyl and α-ethylenic structures. Interpretation of the UV spectra was consistent with the methoxyl and carboxyl contents of the lignin.

Infrared spectroscopy of the solubilized lignin by the pressed disk technique showed that oxidation of the aromatic ring to form carboxyl groups and lactones occurred, in addition to the side-chain oxidation previously indicated. As also noted in the UV, the same bands appeared to be present in all the fractions, but the ratios of their intensities varied, verifying the lack of chemical uniformity for the fractions.

Quantitative carbohydrate analyses of the solubilized lignin showed that 5 to 10% of the material in all the fractions was unoxidized carbohydrate. At

no time was it possible to separate this carbohydrate from the lignin present in the fractions. It was also shown that, in general, the relative percent of carbohydrate solubilized increased as delignification proceeded. The amount of araban in a fraction, however, remained constant with stagewise delignification.

It is postulated that when peracetic acid reacts with softwood lignin, solubilization occurs at a carboxyl content of about 0.3 equivalents per C_9 unit. However, pore size serves as a restricting mechanism to the transport of water-soluble lignin fragments out of the cell wall. In the earliest stages of the reaction, these lignin fragments are trapped within the cell wall, exposed to active peracetic acid for an extended period of time. Thus, the lignins first extracted from the wood are rather highly oxidized, low molecular weight structures. As the reaction proceeds, the size of the cell wall pores increases, and solubilized lignin fragments are not trapped within the cell wall for as long as in the earliest stages of the reaction. As a result, the observed trend is toward larger, less oxidized lignin fragments being extracted as delignification proceeds.

INTRODUCTION

In the chemical pulping of wood, the active agent in the cooking liquor reacts with and makes soluble lignin and part of the carbohydrates present in the wood. The two major commercial chemical pulping processes, kraft and acid sulfite, result in what is termed "nonselective" delignification of wood. In both processes, approximately equal quantities of carbohydrate and lignin are dissolved from the wood, resulting in a yield of about 50%.

Wood has also been treated with chemicals which are more selective in their point of chemical attack than are the commercial pulping agents. Increased selectivity for the lignin component of wood results in less carbohydrate dissolved and a higher pulp yield. Peracetic acid has been shown in experimental pulping studies (1-4) to be highly specific in its attack upon wood. Under relatively mild conditions, compared to the commercial pulping processes, most of the lignin can be dissolved from wood with only small losses of hemicelluloses present.

Many investigations have been made on changes taking place in the chip which result ultimately in liberation of papermaking pulps. Changes in both the solid and liquid phases during pulping reactions have been studied as a function of yield. These studies have included consideration of dissolved materials and changes in the wood fibers including cell wall porosity. However, no studies have been reported in which pore size modification is directly related to the size of lignin fragments liberated as pulping proceeds.

This investigation is concerned with the reaction between peracetic acid and coniferous wood, with particular emphasis on both the nature of the dissolved lignin fragments and the changes in cell wall porosity.

LITERATURE REVIEW

PREPARATION AND PROPERTIES OF PERACETIC ACID

Peracetic acid has been prepared commercially by two procedures (5). Oxidation of acetic acid or acetic anhydride with hydrogen peroxide may be made to yield either solutions of peracetic acid in diluted acetic acid or nearly pure peracetic acid.

$$(CH_3CO)_2O + 3H_2O_2 \rightleftharpoons 2CH_3COOOH + 3H_2O \quad (1)$$

$$CH_3COOH + H_2O_2 \rightleftharpoons CH_3COOOH + H_2O \quad (2)$$

Alternatively, acetaldehyde has been oxidized by oxygen to yield peracetic acid solution in organic solvents. The following series of reactions takes place:

$$CH_3CHO + O_2 \longrightarrow CH_3COOOH \quad (3)$$

$$CH_3COOOH + CH_3CHO \rightleftharpoons CH_3CH(OH)\text{-}O\text{-}O\text{-}CO\text{-}CH_3 \quad (4)$$

$$CH_3CH(OH)\text{-}O\text{-}O\text{-}CO\text{-}CH_3 \longrightarrow 2\ CH_3COOH \quad (5)$$

Peracetic acid in aqueous solution forms a particularly stable five-membered ring (6-7).

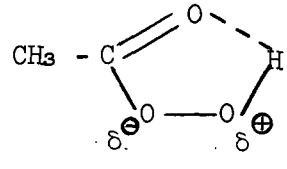

The outer peroxy oxygen is thought to possess a partial positive charge. The reactions of peracetic acid may be considered to be the attack of the peroxy oxygen upon electron-rich sites. Tracer studies by Benton, et al. (7a) suggested that the attacking species is not the hydroxyl cation $(OH)^+$ released upon ionization.

Many chemical structures are susceptible to the electrophilic attack of peracetic acid. Of particular concern in the delignification of wood are the π-electrons of the aromatic rings and of the side-chain carbonyl and olefin groups in lignin. These types of reactions are illustrated below. Ring substitution:

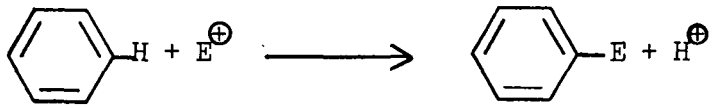

Ring cleavage:

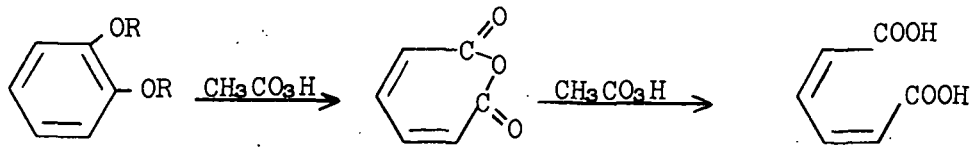

Side-chain carbonyl oxidation:

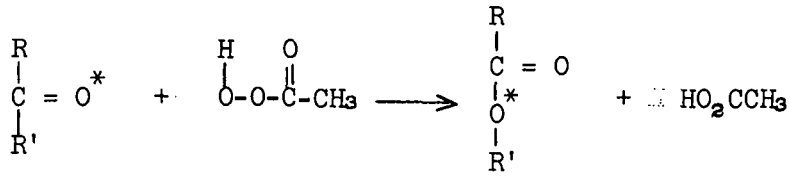

Side-chain olefin oxidation:

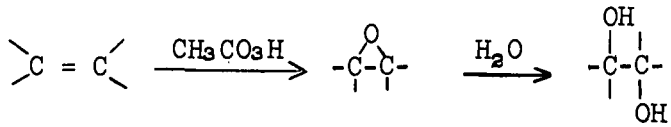

The oxidation reactions of peracetic acid have been reviewed in detail by Farrand (8).

REACTIONS OF PERACETIC ACID WITH MODEL COMPOUNDS OF LIGNIN[a]

Model compound studies of peracetic acid oxidation reactions have shown that both side-chain oxidation and ring cleavage may occur. Ring substitution has a significant effect on the reaction pathway and oxidation products formed.

Side-Chain Oxidation

Several Japanese workers (9-11) have shown that when model compounds of softwood lignin were oxidized with peracetic acid, side-chain oxidation proceeded with α-carbonyl formation from a hydroxyl group on the carbon atom alpha to the aromatic ring. Further oxidation to carboxyl groups at this position was also suggested (10).

Ring Oxidation

Ishikawa, et al., (10) found that small amounts of muconic, maleic, and oxalic acids were formed from all lignin model compounds oxidized with peracetic acid. Demethoxylation and ring cleavage evidently led to these products.

---

[a] Throughout this paper, the following conventional notation for the carbon atoms of the guaiacylpropane structure of softwood lignin will be used.

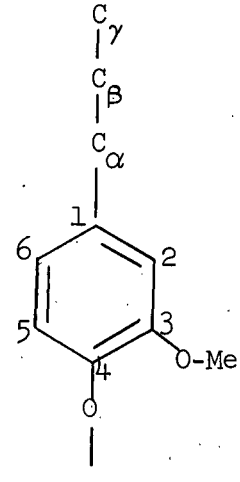

Hatakeyama, et al., (9) found that degradation of vanillyl alcohol (I) by peracetic acid resulted in ring cleavage and formation of muconic acids as well as side-chain oxidation. Reaction with veratryl alcohol (II), however, resulted in only side-chain oxidation.

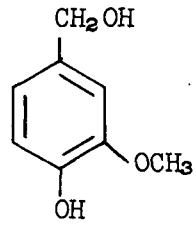

I

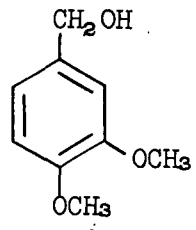

II

Sakai and Kondo (12) measured the rates of reaction of several model compounds. Their results suggested that sensitivity to ring-oxidation increased with the increase of electron-donating substituents.

Farrand (8) oxidized certain 4-methylphenols and their methyl ethers and accounted for about one-half of the total theoretical product in aromatic ring oxidations. The reactions were run in 10% peracetic acid (73% acetic acid, 17% water, and 0.1% hydrogen peroxide) at 25°C. The model compounds studied, in decreasing order of reactivity, were 4-methyl-o-quinone (III), 4-methylcatechol (IV), 2-methoxy-p-cresol (V), 4-methylveratrole (VI), p-cresol (VII), and p-methylanisole (VIII).

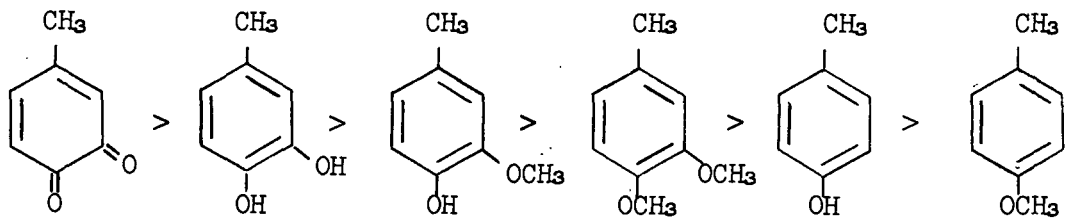

III IV V VI VII VIII

Approximate half lives (hr.) at 25°C.:

0.01	0.2	4	5	25	100

Increasing numbers of oxygen-containing substituents on an aromatic ring increased reactivity to electrophilic attack by peracetic acid. Thus, the rate of delignification of hardwoods would be expected to be more rapid than that of softwoods. The presence of a hydroxyl group on the ring caused a faster reaction than the corresponding methylated compound. In softwood lignin, therefore, guaiacyl nuclei with a free phenolic hydroxyl at C-4 would be expected to react faster than those which are etherified at C-4.

Farrand identified three classes of reaction products: neutral products (quinones and hydroxy compounds), muconic acids, and the lactones of muconic acids. Quinones were isolated from the product mixtures of the less reactive substrates. Ortho-quinones (IX, X) were suggested as intermediates, and para-quinones (XI) were found to be semistable reaction products. In softwood lignin, formation of o-quinones would involve cleavage of the ether linkage of the polymer at the C-4 ether bond.

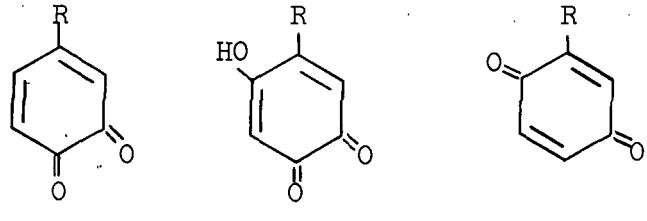

IX X XI

where R is a substituted C_3 group.

A reaction scheme was proposed which involved initial hydroxylation of the ring to form 3,4-dioxy or 3,4,6-trioxy intermediates, which rapidly reacted to form more highly oxidized products. Evidence for 2,3,4-trioxy intermediates was not obtained, possibly for steric reasons.

Muconic acids were found to be principal reaction products in all cases, since most quinone structures are more reactive than the starting materials.

Generally, carboxylic acid products were isolated as lactones, with the exception of cis,trans-β-methylmuconic acid (XII).

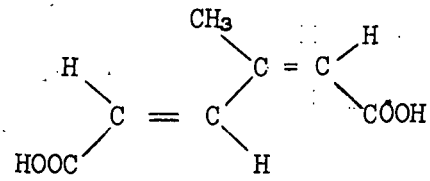

XII

In the oxidation of softwood lignins, various muconic acid structures might be formed (XIII) by ring cleavage of the o-quinone (IX).

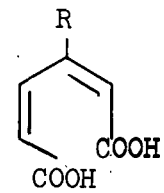

R = substituted C_3

XIII

Formation of β-(XIV) or γ-(XV) alkyl γ-lactones from softwood lignins was suggested by Farrand's work. These structures are isomers of muconic acids and may be formed under mild conditions.

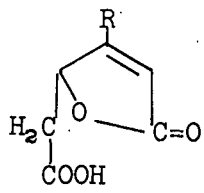

XIV

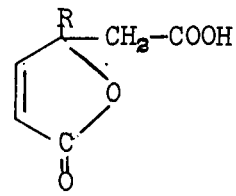

XV

If oxidation were via the p-quinone pathway, γ-hydroxy lactones (XVI) might be favored over the corresponding muconic acids.

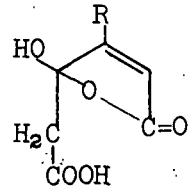

XVI

The overall reaction scheme for peracetic acid oxidation of 4-methyl phenols and their methyl esters is reproduced in Fig. 1.

REACTIONS OF PERACETIC ACID WITH THE COMPONENTS OF WOOD

Lignin Degradation Studies

Sarkanen, et al., (13-14) investigated the oxidative delignification of both softwood and hardwood meals by peracetic acid solution. The batch reaction conditions employed were rather severe (10% peracetic acid at 75°C. for four hours). Yield of Douglas-fir was 69.0%, and yield of red alder was 67.2% (14). The solutions obtained were dried under vacuum, extracted with acetone and then water, to obtain a water-soluble fraction.

The analytical compositions of these highly degraded lignins were very similar. Methoxyl contents were reduced by oxidation to less than one-third that of milled wood lignin. Correspondingly, the absorptivity at 280 nm. indicated the amount of unoxidized nuclei to be as high as one-fourth to one-third of the original aromatic rings. Phenolic hydroxyl content was found to be less than one-half percent. Ionization difference spectra showed a low order of absorbance. The presence of small amounts of acetoxyl groups at the 2- or 6-positions on the ring was suggested by the spectra of methylated peracetic acid lignins. However, carryover of acetic acid through the entire extraction and methylation procedure could account for this result.

It was concluded (14) that oxidation of lignin by peracetic acid required an oxidative ring opening mechanism which would yield the same or similar product structures from both guaiacyl- and syringylpropane units. However, considering the long exposure of the wood meal to the active liquor, secondary reactions of the solubilized reaction products undoubtedly occurred. The very high degree of

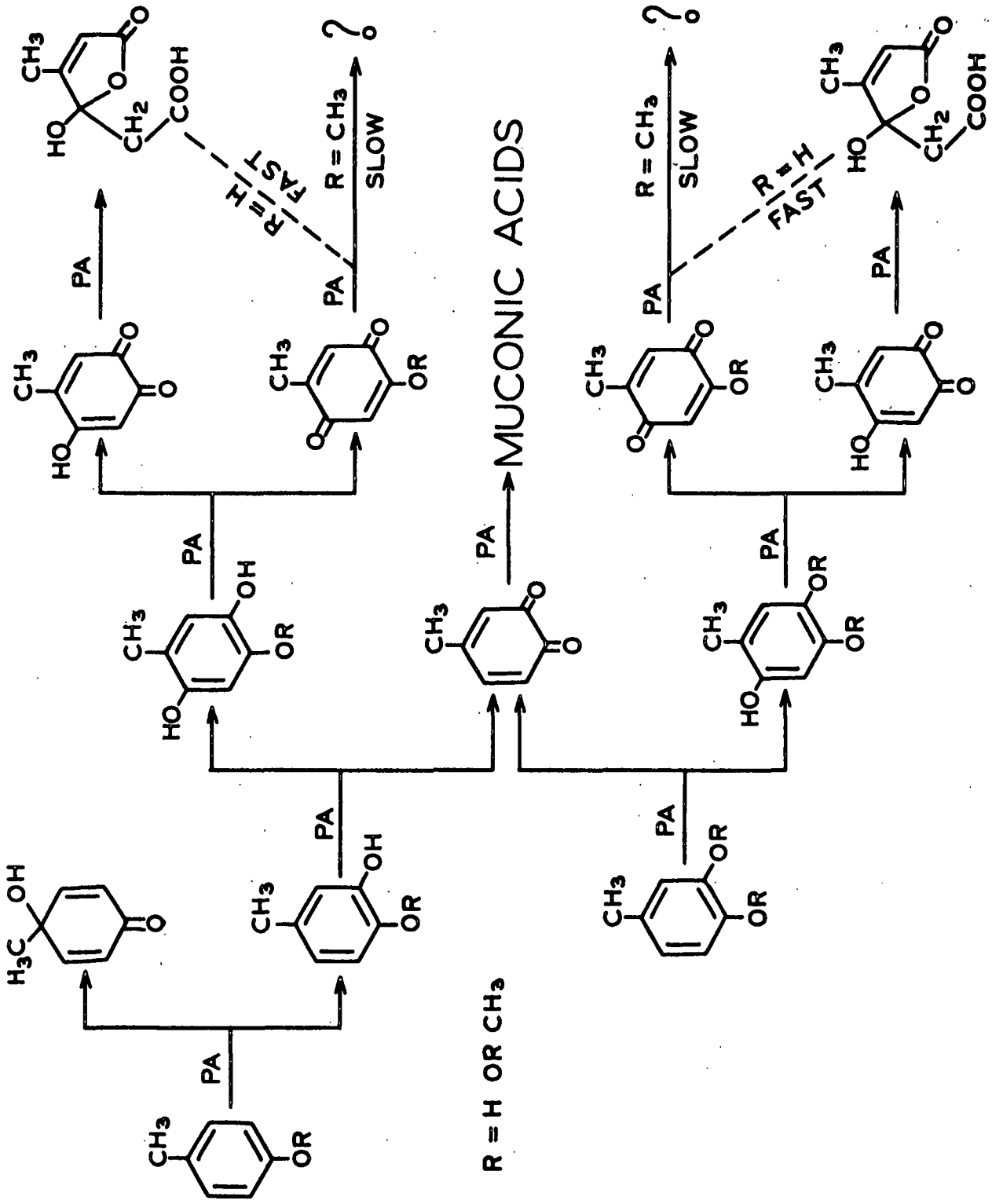

Figure 1. Overall Reaction Scheme for Peracetic Acid Oxidation of 4-Methyl Phenols and Their Methyl Ethers (8)

oxidation (about 2.5 carboxylic functions per C_9 unit) requires that a major portion of the products formed be of very low molecular weight. No molecular weights were obtained to confirm this, nor was any identification of low molecular weight products reported. Under the severe reaction conditions employed, it seems likely that much of the product residue collected was comprised of highly condensed reaction products, as was also suggested in model compound studies (10). No fractionation of the water-soluble fraction was attempted, nor is it clear how peracetic acid and acetic acids were removed from the product mixture.

The oxidation of lignin in wood and of isolated lignins has been studied extensively by several Japanese workers (15-21). Generally, lower temperatures and peracetic acid concentrations were used than were used by Sarkanen, and some information about the progress of delignification reactions was obtained. In these studies, the hydrogen peroxide content was about 30% of the peracetic acid concentration and might have played a significant role in the oxidations occurring.

Ishikawa, et al., (15) reacted pine groundwood pulp with peracetic acid solutions at 40°C. for prolonged periods. Delignification of the pulp resulted in formation of a water-soluble lignin product. Dioxane lignins were isolated from the pulp at several points in the reaction, and the changes in infrared, ultraviolet, and ultraviolet difference spectra were noted. Significant decreases in absorption of this extracted lignin were apparent at 280 nm. in the ultraviolet spectra and at Δ250 nm. in the ultraviolet difference spectra. In addition, oxidation of dioxane lignin from an untreated groundwood pulp was undertaken. The degraded product was separated into water-insoluble and water-soluble parts. The functional group contents of these lignins are presented in Table I. Both side-chain and oxidative ring opening were postulated in these

reactions. Oxidation of the aromatic ring was suggested to involve demethoxylation and formation of quinone intermediates which were in turn converted to muconic acid structures.

TABLE I

ANALYSIS OF DIOXANE LIGNIN OXIDIZED WITH PERACETIC ACID (15)

	Groundwood Pulp Dioxane Lignin	The Degraded Product	
		H_2O-Insoluble Part	H_2O-Soluble Part
OMe, %	14.52	9.73	6.90
Total phenolic OH/C_9 unit	0.33	0.50	0.28
Carboxyl/C_9 unit	0.10	0.35	0.45

Ishikawa, et al., (16) oxidized pine dioxane lignin with peracetic acid and compared the water-soluble and water-insoluble parts obtained. Their results are summarized in Table II. The solubilized lignin had a greater carboxyl content but lesser contents of methoxyl groups and phenolic groups without paraconjugation than the lignin which remained water-insoluble. [In the literature, conjugated phenolic hydroxyl groups are those hydroxyl groups at the C-4 position of rings which are conjugated to unsaturated groups on the side chain. Carbonyl groups alpha to the ring and α-β-ethylenic groups are responsible for this unsaturation. Nonconjugated phenolic hydroxyl groups do not have this unsaturation para to the C-4 hydroxyl. This convention appears in both Japanese (15-16, 19) and American (22-23) literature.] Both ring opening and side chain oxidation occurred. In the first stage of the reaction, the open vanillin-yielding moieties were preferentially attacked. This suggests that the most reactive sites of the softwood lignin structure are the C-O linkages of the side chains of guaiacyl units with a free phenolic hydroxyl at C-4.

TABLE II

FUNCTIONAL GROUPS PRESENT IN PINE DIOXANE LIGNIN OXIDIZED WITH PERACETIC ACID (16)

	H_2O-Insoluble Fraction			H_2O-Soluble Fraction		
Time, hr.	0	2.5	24	0	2.5	24
Yield, %	100	73	38	0	12	25
COOH/C_9 (before NaOH hydrolysis)		0.19	0.30		0.39	0.48
COOH/C_9 (after NaOH hydrolysis)		0.41	> 0.50		0.43	0.50
OMe, % (before NaOH hydrolysis)	15.0	7.8	6.0	15.0	6.0	4.0
OMe, % (after NaOH hydrolysis)		5.5	5.0		4.0	2.5
Nonconjugated phenolic hydroxyl/C_9	0.19	0.22	0.13	0.19	0.17	0.09

Sakai and Kondo (18) reacted peracetic acid with dioxane lignins from pine and birch woods. Infrared and ultraviolet spectra were obtained as reaction proceeded. A close relationship was observed between the rate of demethylation and the solubilization of the lignin. It was suggested that the rate-determining step in the reaction was the loss of loosely-bound methoxyl groups. In a faster stage of the reaction, the structural units of aromatic nuclei having conjugated groups were destroyed selectively.

In a succeeding study (19), pine and birch dioxane lignins were oxidized by peracetic acid, and the products obtained were examined for functional group contents and molecular weight distribution. The results were summarized as follows: (1) The phenolic hydroxyl content of water-insoluble fractions had a broad maximum ear the reaction time of one hour and then decreased to the content of the original

dioxane lignin. (2) To dissolve in water, the lignin oxidation products must have carboxyl contents exceeding a certain amount (e.g., 0.25 equiv./equiv. mol. wt. for pine, 0.20 equiv./equiv. mol.wt. for birch where equiv. mol.wt. = 200). Thus, the carboxyl group content seems to be the limiting factor in lignin solubilization. (3) The molecular weight distribution curves of water-soluble fractions were much lower than those of the original dioxane lignin and water-insoluble fractions, but it is not likely that molecular weight is the limiting factor in lignin solubilization.

The solubilization of dioxane lignin was said to progress as follows. The molecular weight of lignin decreased upon scission of the lignin polymer, following the breaking of the aryl-alkyl ether bond (consequently a demethylation reaction takes place, and catechol nuclei are formed). At the same time, the molecular weight is also decreased by the formation of a muconic acid structure and its ester structure and the formation of carboxyl groups (ester groups in some cases) following the oxidation of side chains. At this stage, the fractions containing more than a specific amount of carboxyl groups become water-soluble and dissolve, but those without sufficient carboxyl groups remain insoluble.

Hatakeyama, et al., (20-21) degraded lignosulfonic acid and thiolignin with peracetic acid. Both ring opening oxidation and side-chain oxidation alpha to the ring were observed, as was decreased molecular weight. Absorptivity at 280 nm. dropped to 6.5-7.0 l./g. cm.

In summary, there have been no studies reported of peracetic acid delignification of wood in which the water-soluble reaction products were isolated directly from a continuous flow reaction. It would be of interest to characterize the delignification of wood by peracetic acid in terms of the change in lignin fragments dissolved as reaction proceeds.

Oxidation of Hemicelluloses and Extractives

Prolonged treatment of pulps by peracetic acid under severe reaction conditions results in the oxidation of hemicelluloses as well as lignin (17, 24). Under milder conditions major solubilization of hemicelluloses from wood does not occur until most of the lignin has been removed. Haas, et al., (2) reported the loss of hemicelluloses with progressive delignification of wood (Table III). The relative loss of arabinan was particularly high by 75.8% yield.

Leopold (3) prepared holocellulose fibers by peracetic acid treatment of both wood meal and chips of loblolly pinewood. At about 75% yield, more than 90% of the total carbohydrate material was retained in the chip (Table IV).

Oxidation of extractives in wood by peracetic acid was shown to be significant by Endo, et al., (25). This shows the necessity of extracting wood prior to investigating delignification phenomena.

LIGNIN MACROMOLECULES IN SOLUTION

The recent development of gel permeation chromatography (GPC) has greatly aided in the investigation of lignin fragments solubilized during the chemical pulping of wood, as discussed below.

The Principles of Gel Permeation Chromatography

Several excellent reviews of the principles of gel permeation chromatography have been published (26-28). In brief, gel permeation chromatography is a liquid-liquid partition chromatographic process in which solute molecules distribute themselves between the liquid contained in the gel pores and the liquid outside of the gel, i.e., in the interstitial volume. GPC fractionation of polymer molecules is achieved according to a separation related to the size in solution of the molecules. Three general mechanisms have been proposed to describe the

TABLE III

DELIGNIFICATION OF GERMAN PINE BY 10% PERACETIC ACID AT 90°C. (2)

Time, min.	Yield, %	Content (g./100 g. original wood)							Material Balance
		Lignin[a]	Pentosan[b]	Galactan	Mannan	Xylan	Araban	Glucan[c]	
0	100.0	27.0	7.7	1.0	8.7	4.1	1.3	55.6	100.0
30	75.8	2.4	6.2	1.5[a]	7.9	4.7[a]	0.4	57.8[a]	102.2
75	62.9	0.3	4.7	0.4	5.1	3.3	0.1	52.4	96.8

[a] In this determination lignin value is probably low due to the acid-soluble portion of the lignin. All sugar contents must remain constant or decrease from the initial value; therefore, galactan, xylan, and glucan values at 75.8% yield all appear slightly high.

[b] Pentosans present in wood: araban, xylan.

[c] Glucan calculated by difference: Glucan = Yield - (Lignin + Pentosan + Galactan + Mannan)

TABLE IV

COMPARISON OF PERACETIC ACID HOLOCELLULOSES PREPARED FROM LOBLOLLY PINEWOOD CHIPS AND WOOD MEAL (3)

Holocellulose	Yield, %	% Retention of				
		Glucan	Galactan	Mannan	Araban	Xylan
From wood meal	75.3	99	80	91	88	94
From wood chips						
Summerwood	71.7	100	72	93	50	99
Springwood	75.2	100	50	97	40	99

GPC separation process: 1) the steric exclusion mechanism, 2) the restricted diffusion mechanism, and 3) mechanisms based on thermodynamic theories. The relative importance of each depends upon the particular operating parameters of the system.

According to the steric exclusion mechanism, advanced by Laurent and Killander (29), it is assumed that different fractions of the total pore volume are accessible to different size molecules, because the gel particles contain a distribution of pore sizes. Large molecules are excluded from most pores, and they elute from the column in early fractions. Small molecules enter a relatively large number of pores and elute in later fractions. A second assumption of the steric exclusion mechanism is that there is no concentration gradient between molecules within and outside the pores of the gel due to a finite rate of diffusion of the solute. The process would, therefore, be expected to be flow-rate insensitive (not diffusion controlled) over a relatively wide range of linear velocities. This is indeed what is most often observed experimentally. The total liquid volume in the column is thus the sum of V_o, the interstitial volume (or void volume), and V_x, the total pore volume.

$$V_t = V_o + V_x \tag{6}$$

The fraction of the pore volume which is accessible to a given solute molecule may be calculated from V_o, V_t, and V_e, the elution volume of the solute molecule.

$$K_{av} = \frac{V_e - V_o}{V_x} = \frac{V_e - V_o}{V_t - V_o} \tag{7}$$

V_o is determined experimentally by eluting a very large (completely excluded) molecule through the column. V_t may be calculated, or it may be determined experimentally by eluting a very small molecule through the column. In the

absence of interaction (sorption) of the solute and the gel, the molecular radius of the eluting species may be related to the inverse error function complement of the column partition coefficient (30).

In the restricted diffusion mechanism, the process is assumed to be, to a significant degree, controlled by the rate of solute diffusion. As a result, observed elution volume is influenced by flow rate, as is also the shape of broad chromatographic elution curves of polydisperse mixtures. Yau (31) found that the chromatographic distribution coefficient could be expressed as a product of the diffusion and exclusion effects:

$$K_{GPC} \ (= K_{av}) = K_D K_X \tag{8}$$

K_D is flow rate dependent, but K_X is not. At slow enough flow rates, K_D approaches unity and K_{GPC} approximates K_X – that is, separation is based on exclusion effects alone.

Thermodynamic theories for GPC fractionation generally involve independent estimates of solute and pore size or considerations of enthalpy and entropy contributions to the distribution coefficient.

Characterization of Solubilized Lignin by Gel Permeation Chromatography

Most applications of gel permeation chromatography to lignin chemistry have dealt with the characterization of lignosulfonates (32-41).

Forss (32-35) and Stenlund (36-38) fractionated lignosulfonates from spent sulfite liquors on Sephadex, a cross-linked dextran gel which swells in water. Early work (32-33) showed that lignosulfonates, fractionated according to molecular weight, showed little difference in UV absorption, absorptivity at 280 nm., or methoxyl content. From this work were deduced the repeating structural units of

spruce lignin (34). Fractionation was shown to be according to molecular size in solution (36). The logarithm of weight-average molecular weight was linearly related to elution volume. Most recent work (37-38) has shown that there are marked polyelectrolyte effects in the GPC fractionation of lignosulfonates in water media, but these effects can be eliminated by using an electrolyte solution as eluent.

Gupta and McCarthy (40-41) examined the effect of several electrolyte environments upon the GPC elution curves of sodium lignosulfonates, using Sephadex gel columns. The sizes of the polymer molecules in terms of equivalent Einstein spheres, $\underline{r}_\eta$, were estimated from measured molecular weights (by ultracentrifuge sedimentation equilibrium) and from intrinsic viscosities calculated from these molecular weights. These radii ranged from about 7 to 70 A. For a lignosulfonate of a particular molecular weight, $\underline{r}_\eta$ was estimated to be up to two times greater in water than in 0.1M NaCl solution – behavior expected for a polymeric network containing negative charge sites in an environment of varying ionic strength. Although some analytical characterization of the unfractionated sodium lignosulfonate was obtained, no comparative analysis of the fractionated polymer was undertaken.

Pla (42-43) fractionated lignins obtained from a sodium benzoate cook of hardwoods on Sephadex, obtaining four fractions. The fractions all had the same elemental composition, methoxyl content, infrared spectra, and absorption intensity at 280 nm. The linear relationship found between the logarithm of intrinsic viscosity and the logarithm of molecular weight suggested that the lignin molecules assumed a rather compact shape.

Brown, et al., (44-46) studied the molecular size distributions of lignins liberated enzymatically from wood by treatment with brown rot fungi, which selectively

solubilize the carbohydrates of wood. Several conclusions were drawn. First, the lignin polymer in wood is finite rather than "infinite" in molecular size. Second, the average molecular weight of the lignin liberated increased with increasing weight loss during enzymatic decay. Finally, it was shown that lignins in wood are probably distributed across the cell walls with a high molecular weight component located in the middle lamella and a low molecular weight component in the secondary wall.

In summary, the only lignin materials which have been characterized according to molecular size in solution are lignosulfonates, and in this case the validity of the Einstein solid-sphere model was not demonstrated. Furthermore, no attempts have been made to obtain narrow molecular-weight fractions of solubilized lignin and to characterize the chemical modifications which had occurred during delignification.

Evidence for a Lignin-Carbohydrate Linkage in Wood

Significant contributions to the knowledge of the existence of a chemical bond between lignin and carbohydrate in wood has been gained recently with the aid of gel permeation techniques (47-49). Earlier evidence for the existence of a lignin-carbohydrate linkage has been reviewed by Linnell, et al., (50). Linnell himself studied the structure of glucomannan extracted from black spruce holocellulose with sodium hydroxide. A small percentage of lignin was found to be associated with the glucomannan, and since it could not be removed by fractionation, nor its aromatic character destroyed by further treatment with sodium chlorite, it was assumed that a chemical bond exists between lignin and glucomannan. A model involving cross-linking of linear glucomannan chains by small branch units of lignin successfully explained the viscosity-molecular weight data obtained (51).

Loras (47) studied the removal of lignin and carbohydrate materials during chlorination and subsequent alkali extraction of sulfite pulp. The solubilized material was fractionated on gel permeation columns, and elution of both lignin and total organic material monitored. It was found that most of the material solubilized upon chlorination was lignin, and also that the proportion between lignin and carbohydrate was nearly the same for all fractions. The carbohydrate present seemed to be associated with lignin in the elution of material extracted with alkali also.

Kosikova, et al., (48) isolated a homogeneous fraction of lignin-carbohydrate complex from sprucewood chips by a procedure involving repeated methylation, methanol and chloroform extractions, and chromatographic fractionation. The ratio of lignin to carbohydrate in the complex was 2:1. In this form, 4.5% of the lignin originally present in the wood was isolated. Based on the mild isolation procedures used, it was proposed that the linkages between lignin and carbohydrate existed as originally present in wood. The main part of the lignin in the isolated complex appeared to be bound by phenyl glycosidic linkages to the carbohydrates.

Kringstad and Cheng (49) investigated water-soluble lignin-hemicellulose complexes isolated from spruce chlorite holocellulose of 3% lignin content. When the isolated complex containing 25% lignin was eluted through a GPC column, the molecular weight distribution curve for the polysaccharide present was always accompanied by a lignin distribution curve of the same shape. Studies of simple mixtures of these components, and of enzymatic degradation of the complex, suggested the existence of covalent lignin-carbohydrate bonds. Selective enzymatic degradation of the carbohydrate present in the complex always resulted in a substantial decrease in the molecular weight of the lignin present. Kringstad and Cheng concluded that the lignin-carbohydrate complex is a graft copolymer

consisting of polysaccharides (principally glucomannan) as backbone chains with more or less degraded lignin branches attached by covalent bonds. However, this model does not necessarily have to be representative for the lignin-hemicellulose copolymer in wood, which could very well have been formed from a "three-dimensional" lignin-hemicellulose copolymer of "infinite" molecular weight by a splitting of the lignin molecule during holopulping.

When barium acetate in aqueous ethanol was added to the hydrolyzate of the lignin-glucomannan complex, approximately 70% of the total lignin originally present in the complex could be recovered in this low molecular weight precipitate. The lignin contained 15% carbohydrates. Analysis showed a significant enrichment in D-galactose in this product. D-galactose is attached by α-1-6 linkage as monomeric branches on the linear glucomannan chain.

Brownell (48a) investigated the stability of the lignin-carbohydrate complex of milled sprucewood and found that the results were inconsistent with a lignin-carbohydrate linkage of the acid-labile acetal, hemiacetal, or ketal type or with an ester or other alkali-labile bond. An ether bond was suggested as a possibility.

The evidence for lignin-carbohydrate linkages was also reviewed by Kringstad and Cheng (49).

Pulping Studies Using Continuous Flow Delignification

Goring, et al., (52-53) applied a continuous flow method to studies of delignification of spruce sawdust. Both sulfite (52) and kraft (53) pulping were investigated. The sawdust was placed in a reaction chamber and subjected to a continuous stream of fresh cooking liquor. The effluent was collected in a series of fractions representing the material solubilized at successive stages of the reaction. After removal of carbohydrates and small lignin fragments by dialysis,

the lignins were characterized by several physical and chemical properties as a function of degree of reaction. For both lignosulfonates and solubilized kraft lignins, the methoxyl contents, ultraviolet absorption, sulfur contents, and neutralization equivalents were found not to vary with extent of lignin removal, indicating in each case that the fractions were chemically quite similar. However, determination of weight-average molecular weight of the various reaction stage fractions indicated a marked increase in $\underline{M}_w$ of the lignin as yield decreased. $\underline{M}_w$ ranged from 10,000 to 140,000 for six fractions obtained from sulfite cooking, and from 1,800 to 51,000 for seven kraft pulping fractions.

In addition, the molecular size distributions of the kraft lignins solubilized in successive stages of reaction were estimated by elution through four Sephadex columns of increasing porosity. The GPC elution profiles obtained were analyzed according to the theory of Laurent and Killander (29) to yield a molecular size distribution in terms of effective molecular radius, $\underline{r}_s$. The value of $\underline{r}_s$ ranged from 4 to 46 A. for the various gel zones. It was found that all fractions contained some low molecular weight material, with the proportion of high molecular weight substance increasing with decreasing yield. A quite substantial 1000-fold change in molecular volume was noted for the full range of kraft lignins solubilized.

Szabo and Goring (54) treated the kraft and sulfite delignification of wood in terms of degradation of a three-dimensional lignin gel network, applying the Flory theory of trifunctional polymerization in reverse. By postulating the joint degradation of two gels, one corresponding to the secondary wall lignin and the other to the middle lamella lignin, approximate agreement was obtained between the theoretically predicted behavior and the experimentally determined results, both in the topochemistry of delignification (55) and in the molecular weight of the lignin dissolved at successive stages of the cook (52-53).

The Porous Sphere Model for Cross-Linked Polymers in Solution

Seely (56) has proposed a mathematical model which treats a hypothetical polymer molecule as a porous sphere. This model has been found to be useful in explaining the hydrodynamic behavior of molecules which are highly branched or cross-linked, and it was successfully applied by Seely to data from the literature of branched dextrans, the triacetate derivatives of a lignin-containing natural glucomannans, and lignosulfonic acids. It therefore promised to be a useful approach in estimating the molecular size distribution of lignin solubilized by peracetic acid from GPC elution curves.

The porous sphere model requires that the internal structure of the polymer molecule be uniform – that is, the permeability, K, must be constant throughout the sphere. This suggests a relatively rigid branched or cross-linked structure of uniform chemical composition. The first step in applying this model to a polydisperse polymer is to obtain a series of narrow molecular weight fractions of the polymer. Intrinsic viscosity and molecular weight are then determined independently of each other for the fractions. Seely's relation may be used conveniently in linear form:

$$1/[\eta] = (1/A) + (B/A)M^{-2/3} \qquad (9)$$

where $1/A$ and B/A are the intercept and the slope respectively, of the plot of the inverse intrinsic viscosity, $[\eta]$, versus molecular weight, M, to the negative two-thirds power. The permeability, K, and hydrodynamic radius, a, are calculated directly from A and B according to Seely, as follows:

$$K = \frac{B}{10[N \cdot 4\pi\rho_1(1-\varepsilon)/3]^{2/3}} \text{ cm.}^2 \qquad (10)$$

where

$\underline{N}$ = Avogadro's number

ρ_1 = solid density

ε = porosity

$\rho_1 \cdot (1-\varepsilon) = 5/(2\underline{A})$ g./cm.^{3}

$$a = (10K/B)^{1/2} M^{1/3} \text{cm.} \qquad (11)$$

CHEMICAL DELIGNIFICATION AND CELL WALL POROSITY

Cell Wall Structure and Lignin Distribution

The physical structure of wood, both in the dry state and in the swollen, wet state appears to be better understood in terms of recent studies. Davies (57) studied cell wall porosity by examining the retention of metal particles within cell walls by observation with the electron microscope. He concluded that when wood is in the wet state, the microfibrils within the cell wall are in a swollen condition and only touch one another intermittently. As water is withdrawn during drying, microfibrils move together, and the cell wall shrinks. Several workers (58-62) have shown that the density of the cell wall of fibers dried from water approaches that of its components – that is, 1.5 g./cc., implying that the dry cell wall is essentially nonporous. When wood is rewet, the microfibrils move apart, but not necessarily to the same position as before. It was postulated that there are no permanent capillaries in the wall, but that solutions move in the wet wall and occupy all the spaces between microfibrils in the swollen state. These capillaries in the cell wall, or pores, appeared to be of molecular size, or about 10^{-4} times the diameter of the lumen of a softwood tracheid.

Proctor, et al., (55) used the ultraviolet microscope to follow the topochemical pattern of the removal of lignin from sprucewood in kraft, acid sulfite,

and neutral sulfite pulping. Kraft and acid sulfite pulping resulted first in preferential lignin removal from the secondary wall, then in rapid removal of lignin from the middle lamella after half the total lignin had been dissolved. No such topochemical preference was found in the removal of lignin by neutral sulfite up to 50% delignification. No concentration gradients of lignin were produced in the secondary wall by any of the processes. Moreover, the middle lamella was resistant to solution even when it came into direct contact with the liquor at the margin of the pit cavity. This suggests that diffusion through the secondary wall, either of chemicals in or of lignin macromolecules out, did not play the dominant role in controlling the rate of the pulping reaction. Later studies from the same laboratory (63-64) suggested that, for these processes, delignification is a chemically controlled mechanism, by the high activation energy of alkali cooking and by the dependence of rate upon chemical structure of the lignin gel.

Effect of Lignin Removal on Cell Wall Porosity

Stone (65) attempted to classify cell wall pores according to three types: those which traverse the cell wall, those which are on one surface only, and those which are internal. Although this rigid classification is overly restricting for wood sections in a swelling solvent, the review which Stone presented of techniques used to investigate cell wall porosity was comprehensive and critical.

The only apparent means of quantitatively examining the pore size characteristics of water-swollen wood appears to be by the diffusion of solutes. The solute exclusion technique offers the distinct advantage that drying of the wood sample is not required. It has been shown that even solvent exchange drying does not preserve the entire pore structure of the wood (66).

According to the principles of solute exclusion, macromolecular solute fractions of narrow distribution can be used to relate relative percentage of total pore volume measurable to the size of the diffusing solute molecule which can penetrate the structure. The technique involves allowing a dilute polymer solution of known concentration to diffuse into a wood sample of known moisture content and measuring the polymer concentration when equilibrium is reached (Fig. 2). The water within those pores of the wood which are smaller than the macromolecule will be "inaccessible." At large enough molecular diameter, no diffusion at all will occur, and total pore volume, the "fiber saturation point," may be obtained. Both fiber saturation point and the macromolecular diameter at the fiber saturation point are expected to increase with decreasing yield.

Stone and Scallan (58, 66-68) studied the effect of component removal upon the porous structure of the cell wall of wood. Initially, pore volume was determined by mercury porosimetry (59). Surface area was determined by nitrogen absorption of solvent exchange dried pulps using B.E.T. theory (69). It was concluded that lignin and carbohydrate removal by kraft and sulfite leaves small pores in the swollen cell wall of 20 to 40 A. size. Porosity increased with lignin removal down to 67% yield, but at lower yields the cell wall contracted. However, when progressive delignification was accomplished with a selective delignification agent such as sodium chlorite, no maximum pore volume, but only a continual increase with lower yield, was noted.

Later, Stone and Scallan (66-67) employed the solute exclusion technique to compare the kraft and sulfite processes in terms of porosity changes with progressive delignification. The diameter of the dextran molecules used as solute was taken to be that calculated from their diffusion coefficients by the Einstein-Stokes formula:

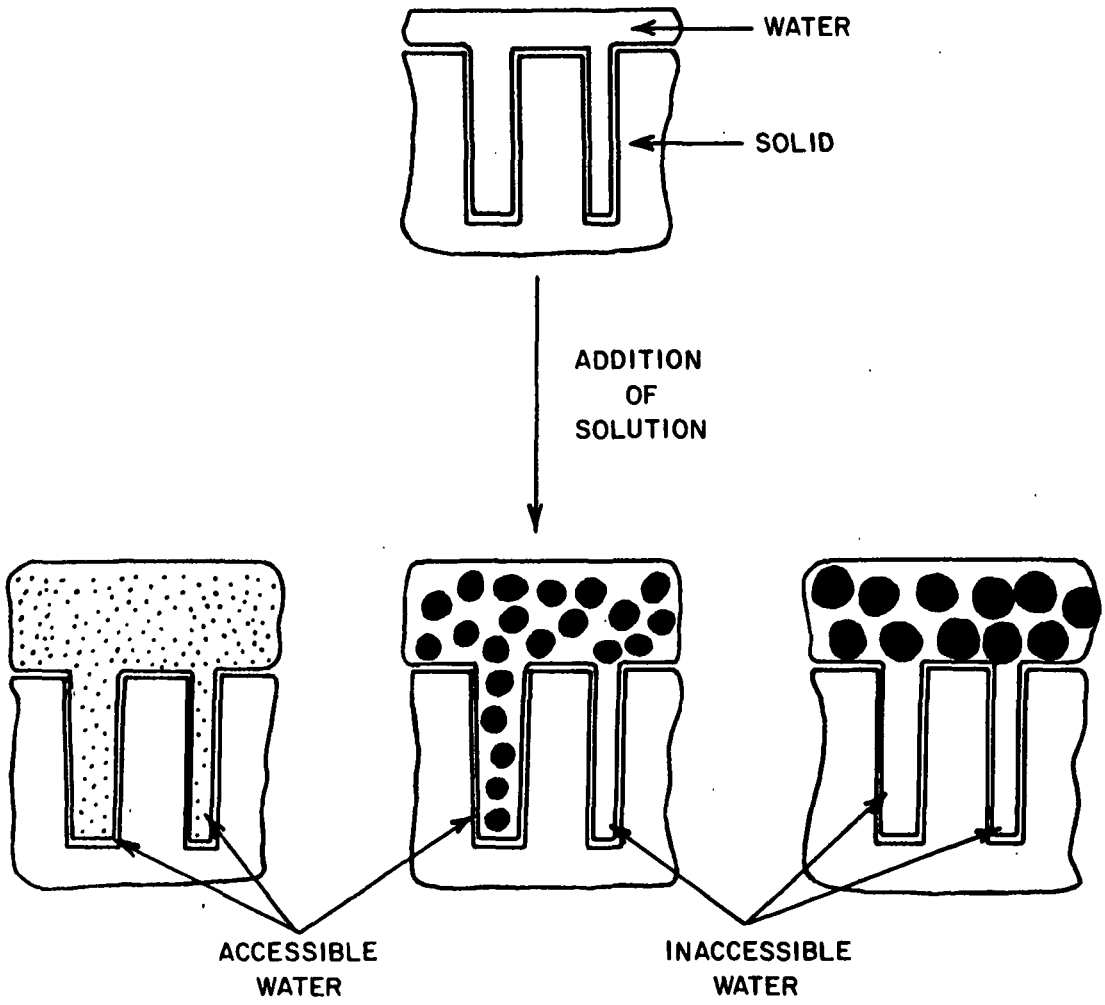

Figure 2. Pore-Size Distribution by the Solute Exclusion Technique (67)

$$\text{Diameter} = \frac{RT}{3\pi\eta DN} \qquad (12)$$

where

$\underline{R}$ = gas constant

$\underline{T}$ = temperature

η = intrinsic viscosity

$\underline{D}$ = diffusion coefficient

$\underline{N}$ = Avogadro's number

Pore width was assumed to be equal to this calculated molecular diameter. Then "inaccessible water," or cumulative pore volume, was plotted as a function of pore width. Pore volume increased with increasing molecular diameter of the solute molecule until a maximum was reached at the point when the solute molecule was completely excluded from the cell wall. Thereafter, no further increase in molecular diameter had any effect on the value of inaccessible water, and the plateau formed was the so-called "fiber saturation point." In general, the fiber saturation point increased with decreasing yield to a maximum at 65%, verifying earlier conclusions. This is illustrated for sulfite and kraft pulping in Fig. 3a. To judge whether swelling had occurred, by which is meant an increase in cell wall volume, the total volume of solid plus water associated with one gram of wood as it is pulped is considered. This value is computed by adding the fiber saturation point plus the specific volume of the solid material (0.667 cc./g. – i.e., the inverse of cell wall solid density, 1.5 g./cc.) and multiplying this quantity by yield. The substantially greater swelling of cell wall with sulfite pulping compared to kraft pulping is illustrated in Fig. 3b.

The pore volume measured by solute exclusion was always greater than that obtained earlier by nitrogen absorption. This discrepancy was rationalized by suggesting that micropores in the cell wall structure were closed upon solvent-

exchange drying, leaving only macropores to be measured by nitrogen absorption. The change with kraft pulping in macro- and micropore water volume and solid volume of one gram of sprucewood is shown in Fig. 4. As the solid material dissolved, the volume of water in the micropores decreased slightly while that in the macropores first increased, then decreased.

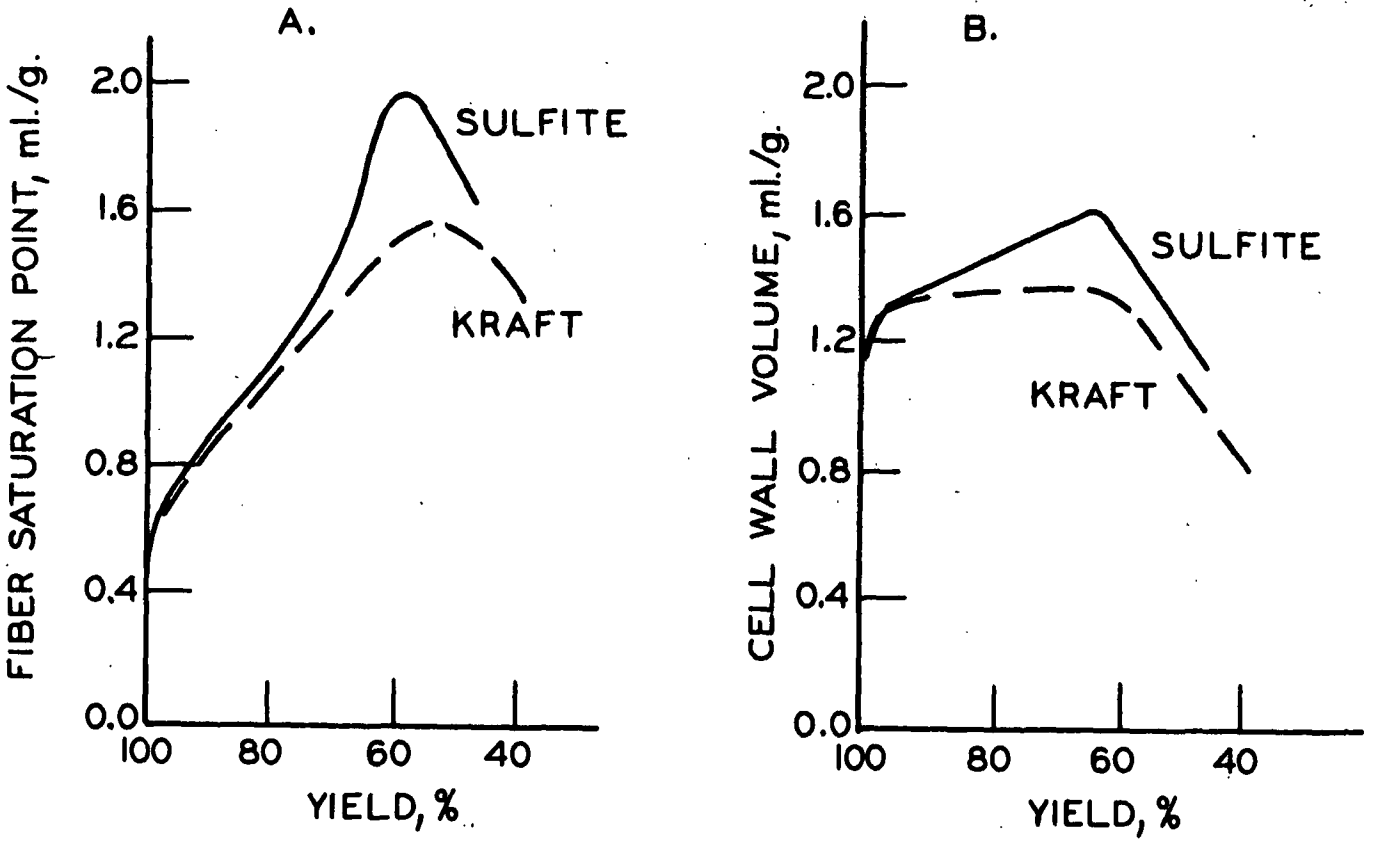

Figure 3. Effect of Kraft and Sulfite Pulping upon Porosity of Black Sprucewood. a) Fiber Saturation Point Versus Yield, b) Cell Wall Volume Versus Yield (67)

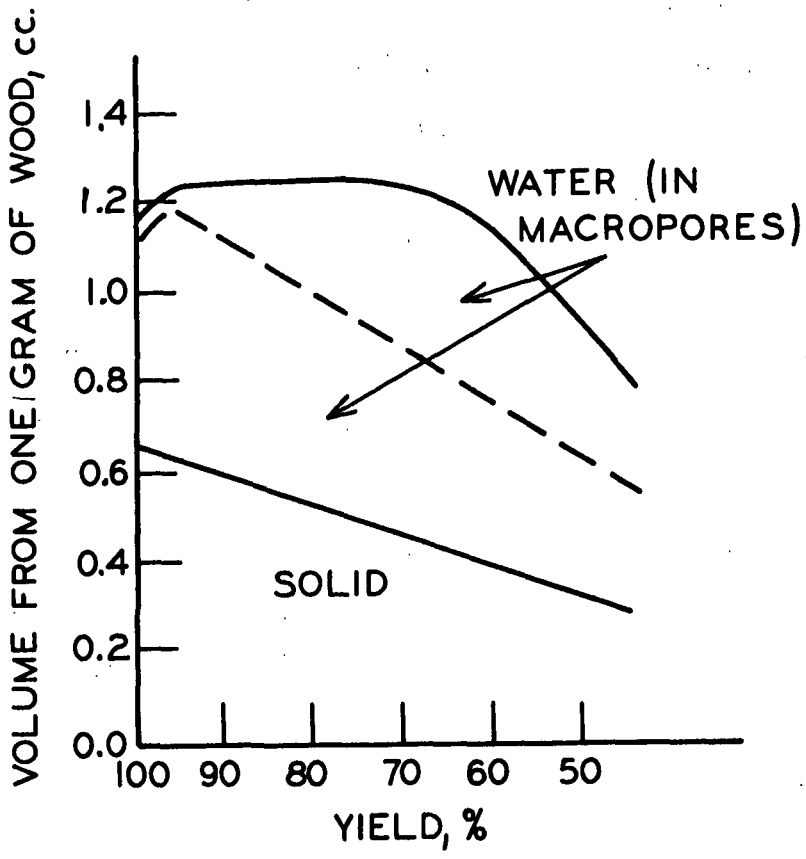

Figure 4. Volumetric Changes Brought About by Kraft Pulping of One Gram of Black Sprucewood (66)

Using this information, Stone and Scallan (68) proposed a model for the water-swollen cell wall of wood composed of many layers of lamellae of cellulose-rich material, all concentric with the cell axis. Surrounding the cellulose-rich microfibrils within the lamellae is an amorphous mantle of microporous lignin-hemicellulosic material. These micropores were considered to be less than 25 A. in diameter. Between the lamellae are regions of macropores, having widths greater than 25 A. Upon drying, the lamellae move together, and the disordered material shrinks to form a solid, nonporous wall. Reswelling of the fibers in water results in a complete recovery of the micropore volume but a substantial loss of macropore volume. Before pulping, water within the cell wall of wood fibers is contained

almost wholly within micropores. As the wood is pulped, larger pores, or macropores, are progressively created not only at the expense of a volume of solid material, but also at the expense of the microporous system. Overall swelling of the cell wall subsequently may occur.

Feist and Tarkow (70-72) used polyethylene glycol as the penetrating macromolecule in their solute exclusion studies. When Sitka spruce was treated by the sodium chlorite holocellulose method, the fiber saturation point was found to increase continuously with decreasing lignin content (Table V). At yields above about 78%, the change in fiber saturation point as a function of yield appeared to closely parallel the curves for kraft and sulfite pulping (Fig. 3a). At lower yields, holopulping resulted in cell wall swelling which was intermediate between the moderate swelling reported for kraft pulping and the much greater swelling with sulfite pulping (66).

TABLE V

SITKA SPRUCE HOLOCELLULOSE AND FIBER SATURATION POINT (72)

Lignin Content, %	Lignin Removed, %	Estimated Yield, %[a]	Fiber Saturation Point, %
29.05	0	100.0	35
21.54	26	92.5	63
16.98	42	88.0	70
10.66	63	81.5	94
5.53	81	76.5	130
3.27	89	74.2	140
1.11	96	72.1	180

[a] Yield is estimated assuming zero carbohydrate loss.

DISCUSSION

DELIGNIFICATION BY PERACETIC ACID AND EXAMINATION OF SOFTWOOD WAFERS

SELECTION OF WOOD AND PREPARATION OF WAFERS

In order to provide a reasonably uniform wood substrate for reaction, it was desirable to use only the springwood from a softwood species. The wood used had to be in chip form in order to apply the solute exclusion technique. In order to make possible uniform penetration of the active delignifying agent into the wood and bring about uniform reaction, very thin wood wafers were shaved from a fresh log of nineteen-year-old loblolly pine (Pinus taeda L.) which had rather widely spaced growth rings. Loblolly pine is a common softwood species in the southern states and is of some importance as a source of pulpwood. In addition, valuable comparison to the studies by Leopold (3) could be made.

Blocks of the sapwood portion of the loblolly pine log were shaved along the plane tangential to the pith to obtain wafers of approximate radial thickness 0.5 mm. or 10-15 springwood fiber diameters. Shaving the chips along the tangential plane made it possible to separate the wood into pure springwood and mixed summerwood-springwood wafers. The wafers were extracted with acetone to eliminate extraneous materials present and then were air dried. Prepared in this manner, the wafers were stable indefinitely at room temperature. Details on the preparation of the wafers may be found in the experimental section.

SELECTION AND PREPARATION OF PERACETIC ACID

The selection of peracetic acid was based on several considerations. Under mild conditions, peracetic acid has been shown to selectively delignify loblolly pinewood with minimal degradation of hemicelluloses present (3). A principal advantage of

using a selective delignification reagent in this study was that it simplified analysis of the solubilized reaction products, eliminating the dialysis step needed to remove carbohydrates, which was necessary in studies of conventional pulping processes (52-53). No purification steps were necessary at all, and the entire product solution from the reaction could be investigated using gel permeation chromatography techniques.

Peracetic acid was chosen as the selective delignification reagent principally because the present knowledge of its specific reaction mechanism with wood is quite limited. However, valuable comparison to studies reported in the literature review of peracetic acid oxidation of isolated lignins and lignin model compounds might be realized.

Finally, practical considerations prompted the selection of peracetic acid. No inorganic salts are present in dilute peracetic acid solutions. Delignification with peracetic acid promised to be adaptable to a nonpressurized, moderate temperature reaction which could be run in chiefly standard pyrex glassware. In addition, peracetic acid could be generated at high purity in aqueous solution by a method developed by FMC Corporation (73) and used previously by Farrand (8). The generation and analysis of peracetic acid solutions are discussed in the experimental section and in Appendix I.

DESIGN OF THE CONTINUOUS FLOW REACTION APPARATUS

A continuous flow reaction apparatus has been designed and constructed. This allowed the delignification reaction to be run under single-pass, continuous flow conditions with constant collection of the solubilized reaction products.

A photograph of the continuous flow apparatus is presented in Fig. 5. The apparatus was built entirely of pyrex glass, teflon, stainless steel, and

Figure 5. Continuous Flow Reaction Apparatus

polyethylene to minimize decomposition of the hot peracetic acid solution. Flow of peracetic acid solution was maintained at a constant rate by a constant-head device, fed from a reservoir at the top of the reaction apparatus. The solution was brought to reaction temperature by passing it through a glass coil submerged in a constant-temperature bath which could be raised into position to surround the coil and reaction vessel. From the coil, the hot liquor passed into the reaction vessel. The reaction vessel itself was constructed from standard-taper joints and adaptors and could be disassembled as shown in Fig. 6 to allow packing of the wood wafers. The wafers were held within the reaction vessel between two teflon plates, perforated with small holes to allow flow of the reaction liquor. Beyond the reaction vessel, condensers were positioned in the flow line to cool the hot liquor. Finally, a receiver was placed at the end of the flow line in which to collect and quench the liquor containing the solubilized reaction products.

A detailed description of the components of the continuous flow reaction apparatus is presented in Appendix II.

ESTABLISHING REACTION PROCEDURES AND UNIFORMITY WITHIN THE WOOD WAFERS

The delignification reaction was run under single-pass, continuous flow conditions to allow continuous collection of effluent product liquor. This made possible the comparison of solubilized reaction products of successive stages of the reaction without requiring the repeated filtration and washing procedures necessary to separate the residue from each successive liquor, as is the case in an incremental batch pulping method. In addition, the effluent liquor could be quickly cooled and residual peracetic acid quenched immediately to minimize secondary reactions occurring after solubilized reaction products were removed from the wood.

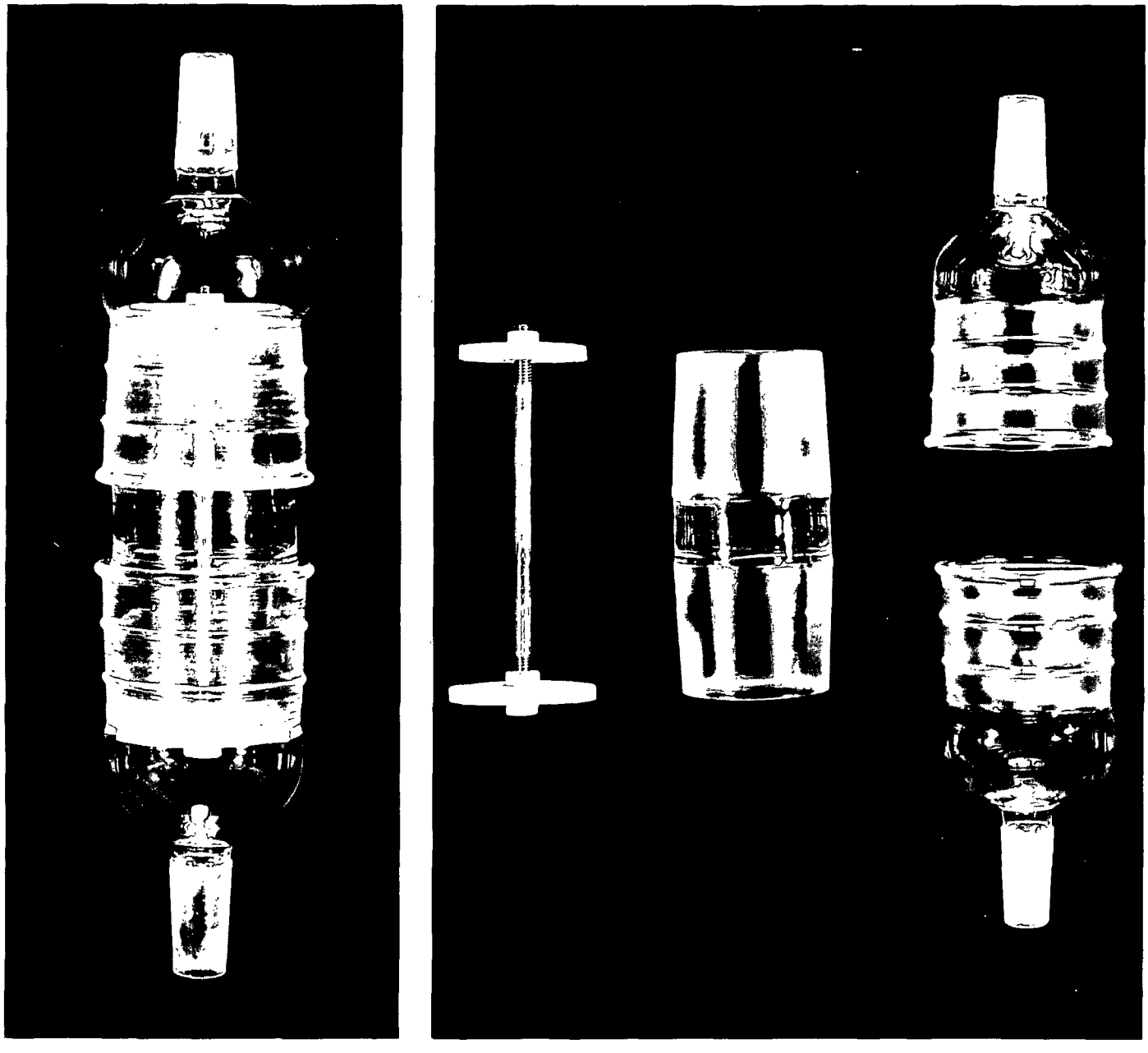

Figure 6. Reaction Vessel in Assembled and Exploded Views

Certain reaction objectives were desirable in the system:

(1) reaction uniformity within the wood wafers;
(2) reaction uniformity within the reaction vessel;
(3) minimal carbohydrate loss into solution;
(4) slow, reproducible rate of delignification;
(5) minimal change in pH within the reaction vessel; and
(6) minimal degradation of lignin fragments once made soluble.

A series of preliminary flow reactions was run on mixed summerwood-springwood wafers in order to establish the reaction procedures and conditions necessary to bring about these objectives. Prior to reaction, the wafers were submerged under water and impregnated by repeated application and release of vacuum. The wafers thus treated no longer gave off air bubbles when submerged under vacuum and readily sank to the bottom of the beaker filled with dilute peracetic acid solution. A summary of the reaction conditions employed in the preliminary studies is summarized in Appendix III.

Of primary concern was the necessity to establish the fact that the wood wafers were thin enough that the impregnation and reaction procedures employed would result in uniform delignification across the thin radial dimension of the wafers. Therefore, color photomicrographs were obtained of lignin-stained, microtome cross sections of unreacted and partially delignified wood wafers from the preliminary flow reactions. The wafers were sectioned so that the centermost portion of the wafers was examined, or that part which would be least accessible to the peracetic acid solution during reaction. A sketch of a wood wafer and the cross section obtained from it are shown in Fig. 7.

Four stains – "C" stain, Jackson's crystal violet stain, iodine-malachite green stain, and phloroglucinol stain – were used successfully on the cross sections. In general, these stains all indicated that the peracetic acid solution completely penetrated the wood chips, and delignification proceeded uniformly across

the radial dimension of the wafers. A more detailed account of the embedding and staining methods is presented in Appendix IV, as well as example photomicrographs of cross sections stained with "C" stain and Jackson's crystal violet stain.

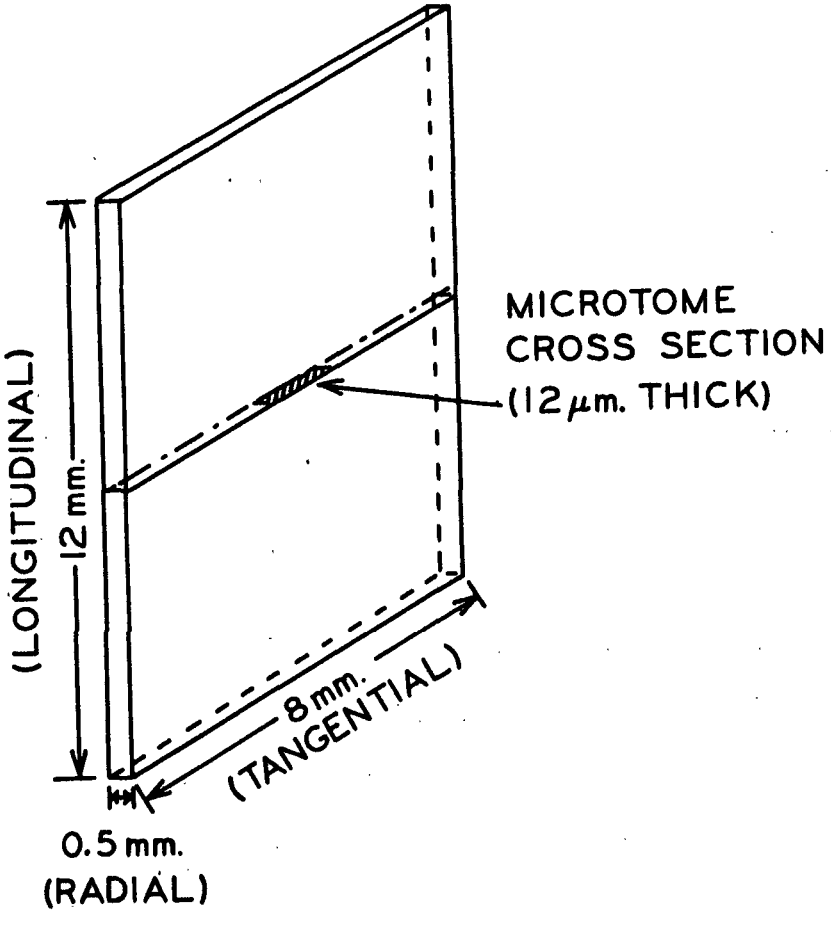

Figure 7. Sketch of Wood Wafer and Microtome Cross Section Stained and Photographed

Two additional observations were made as a result of this investigation. The first concerned the staining by phloroglucinol stain of wafers partially delignified with peracetic acid. Phloroglucinol in hydrochloric acid reacts with lignin in various plant materials to yield a purple, violet, or red-purple color (74). Adler, et al., (75-76) attributed the phloroglucinol color reaction to a condensation reaction with cinnamaldehyde-type carbonyl groups, which are present in 3% or less of the phenylpropane units of lignin.

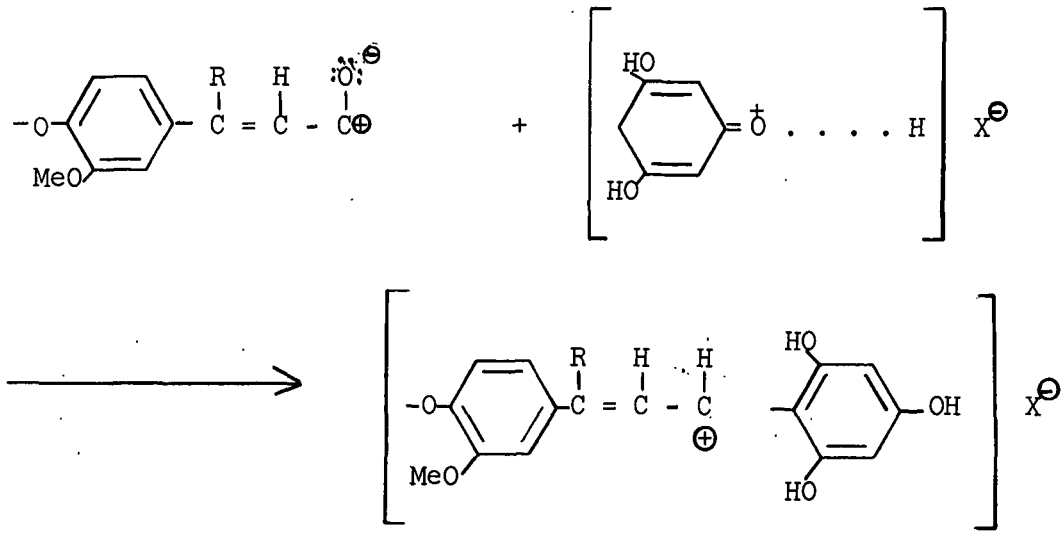

When sections of unreacted loblolly pinewood were stained with phloroglucinol, the expected color reaction occurred (Fig. 8a). However, no color reaction occurred when partially delignified wafers were treated with phloroglucinol. At 92.1% yield (Fig. 8b), approximately 75% of the original lignin is still present in the wood. The fact that no color reaction occurred with this lignin shows that all the structures responsible for reaction have been modified to some extent and dramatically verifies that uniform penetration throughout the wood wafers has been achieved.

The second additional observation made as a result of the lignin staining investigation concerns the possible topochemical effect occurring during the delignification of loblolly pine by peracetic acid. Certain sections, made from

wafers which were delignified to about 60% of their original lignin content and stained with either Jackson's crystal violet stain or iodine-malachite green stain, appeared to be more darkly stained in the middle lamella region than in the cell wall. This is well illustrated in Fig. 34 (Appendix IV) of sections colored with Jackson's crystal violet stain. Comparing photo 34a with 34d, color intensity decreased more significantly in the cell wall than in portions of the middle lamella completely surrounded by fibers. However, solubilization of the lignin in the middle lamella appeared to be quite complete in open areas of fracture between the fibers. Verification and quantitative measurement of possible topochemical effects would require sophisticated application of UV-microscopy techniques, such as those of Proctor, et al. (55).

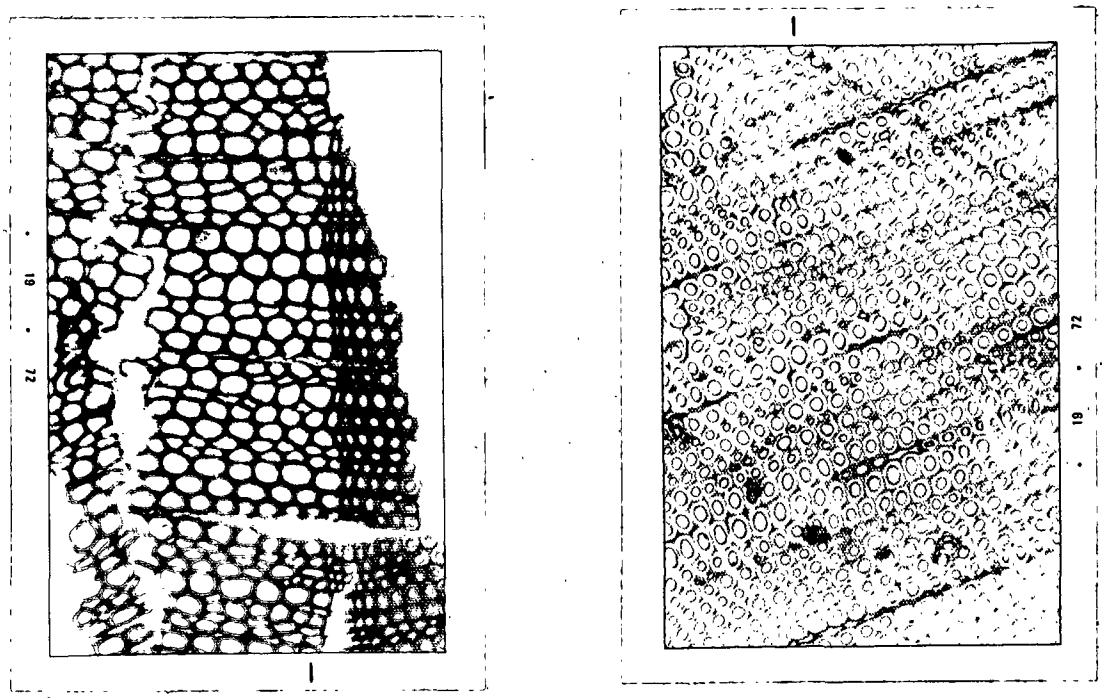

a) b)

Figure 8. Cross Sections Stained with Phloroglucinol Stain at a) 100.0% Yield and b) 92.1% Yield

In summary, studies of preliminary flow reactions on mixed summerwood-springwood wafers and lignin-staining of these wafers indicated that the following reaction conditions were suitable for bringing about the desired reaction characteristics:

Peracetic acid: 3.0% (pH = 3)

Temperature: 60°C.

Flow rate: 25 ml./min.

Wafer charge: 35.00 g. (ovendry)

Under these conditions, a yield of 80% was achieved in 7.0-7.5 hours. Peracetic acid concentration decreased to about 2.7% in passing through the flow apparatus and, therefore, was in excess during the time of exposure to the wood wafers. Thermal decomposition of the peracetic acid caused this decrease in concentration. No corrosion of the stainless steel was visible. The established reaction procedure is presented in detail in the experimental section.

SELECTIVITY IN PERACETIC ACID DELIGNIFICATION

The high selectivity of peracetic acid delignification of wood has been reviewed in the introduction (1-4). It is necessary here to establish just how selective peracetic acid delignification is under the continuous flow procedures employed and to determine if the lignin and carbohydrate materials made soluble can be accounted for in the solubilized reaction products. Therefore, lignin analyses of untreated and partially delignified loblolly wafers, and carbohydrate analyses both of the solubilized reaction products and of untreated and partially delignified loblolly wafers have been obtained. All analyses have shown that when loblolly pinewood is partially delignified to 80% yield by peracetic acid under the conditions employed, approximately 7% of the solubilized reaction products are derived from the carbohydrate portion of the wood. The rest of these products are partially degraded lignin fragments.

Lignin Analyses of Untreated and Partially Delignified Wood Wafers

Lignin content was determined for both mixed summerwood-springwood wafers at several yield levels and springwood wafers at about 80% yield. Carbohydrate loss was calculated by material balances. The results of a Klason, acid-soluble lignin analysis on mixed summerwood-springwood wafers at several yield levels are presented in Table VI, and the results of a modified lignin analysis (77) on springwood wafers are shown in Table VII. A modified lignin analysis differs from a Klason, acid-soluble lignin analysis in that the chips are first extracted with alkali. This alkali extraction is thought to result in detection of certain lignin-derived materials which are unrecognized by the Klason, acid-soluble method of analysis. At 80% yield, the apparent carbohydrate loss upon delignification of loblolly pine springwood wafers is 7.85% of the solubilized reaction products.

In addition to demonstrating that lignin fragments constitute over 90% of the solubilized reaction products, these analyses point out one other possibly significant fact. A significant portion of the lignin still present in the wood has been modified by the oxidative peracetic acid treatment. This is seen by the significant increases in alkali-extracted and acid-soluble lignins upon delignification of springwood to 80.9%. At this yield level, 42% of the original lignin is still present in the wood, but only 41% of this residual lignin is detectable as Klason lignin. In unreacted springwood, 95% of the ligninlike material present was insoluble in 72% sulfuric acid.

Carbohydrate Analyses of Solubilized Reaction Products

The carbohydrate content of the reaction products, made soluble by peracetic acid delignification of springwood wafers to about 80% yield, has been determined as alditol-acetates by gas chromatography according to the method of Borchardt and Piper (78). The purpose was to verify the results of the modified lignin analyses – that is, that carbohydrate solubilization during reaction is typically less than 10%.

TABLE VI

LIGNIN CONTENT OF PARTIALLY DELIGNIFIED LOBLOLLY SUMMERWOOD-SPRINGWOOD[a]

Yield, %	Klason[b] Lignin	Acid-Soluble[b] Lignin	Total Lignin[c] in Wafers	Lignin[d] Removed	Yield Plus Lignin Removed	Apparent Carbohydrate Loss
100.0	28.73	0.38	29.11	0.00	100.0	0.0
95.0	26.34	0.72	27.06	2.05	97.1	2.9
88.1	13.13	4.12	17.25	11.86	100.0	0.0
74.2	0.96	3.76	4.72	24.39	98.6	1.4

[a]All analyses are expressed on the basis of g./100 g. o.d. unreacted wood wafer.
[b]All values are the average of two individual determinations.
[c]Calculated by addition of two preceding columns.
[d]Calculated by difference in total lignin from 100% yield.

TABLE VII

LIGNIN CONTENT OF PARTIALLY DELIGNIFIED LOBLOLLY SPRINGWOOD[a]

Yield, %	Alkali-Extd.[b] Lignin	Klason[b] Lignin	Acid-Soluble[b] Lignin	Total Lignin[c] in Wafers	Lignin[d] Removed	Yield Plus Lignin Removed	Apparent Carbohydrate Loss
100.0	1.56	28.66	0.10	30.32	0.00	100.0	0.0
80.9	3.51	5.25	3.98	12.75	17.57	98.5	1.5

[a]All analyses are expressed on the basis of g./100 g. o.d. unreacted wood wafer.
[b]All values are the average of two individual determinations.
[c]Calculated by addition of three preceding columns.
[d]Calculated by difference in total lignin from 100% yield.

The results of the carbohydrate analysis are shown in Table VIII. By this analysis, the percent carbohydrate in the solubilized reaction products is 6.28%, as compared to.7.85% by modified lignin analysis.

TABLE VIII

SUGARS IN SPRINGWOOD PRODUCT LIQUOR AFTER HYDROLYSIS

	% of Total Solids[a]
Arabinose	1.91
Xylose	0.27
Mannose	2.32
Galactose	0.96
Glucose	0.82
	6.28

[a]Values represent single determinations.

Polysaccharide Analyses of Unreacted and Partially Delignified Springwood Wafers

Sugar analyses (78) were also performed on unreacted springwood wafers and on partially delignified springwood wafers at 80.9% yield. The results are summarized in Table IX. Carbohydrate loss is within the experimental error of the determination.

The values obtained in this polysaccharide analysis appear to be low in terms of total polysaccharide present. However, relative comparison is valid. Adding the polysaccharide content (57.3%) to the lignin content (30.3%) of unreacted loblolly pine springwood accounts for a total of only 87.6% of the material present. By comparison, the polysaccharide content of unreacted loblolly pine springwood as obtained by Leopold (3) by another method was 64.5%. The method of wood chip preparation employed by Leopold was very similar to that used in this study, with the exception that extraction was with 2:1 ethanol-benzene rather than acetone.

TABLE IX

POLYSACCHARIDES IN UNREACTED AND PARTIALLY DELIGNIFIED SPRINGWOOD[a]

Sugar Units	Unreacted Springwood[b]	Springwood at 80.9% Yield
Rhamnose	0.1	0.0
Xylose	6.7	7.0
Arabinose	1.4	0.7
Galactose	2.4	1.9
Glucose	37.4	39.0
Mannose	9.3	9.3
	57.3	57.9

[a]All analyses are expressed on the basis of g./100 g. o.d. unreacted wood wafers.

[b]Values represent single determinations.

POROSITY CHANGES IN WAFERS WITH DELIGNIFICATION

The application of the solute exclusion technique to the determination of cell wall pore volume and pore size distribution has been discussed in the literature review. In light of the basic differences between the conventional pulping processes and selective delignification of wood, an aspect of this study was to examine the changes in cell wall porosity of loblolly pine wafers with delignification by peracetic acid.

Solute exclusion experiments were carried out using a series of narrow molecular weight fractions of the anhydroglucose polymer dextran from Leuconostoc mesenteroides strain B512 as available from Pharmacia AB. Most of the glucosidic linkages are α-D-1→6, with branching introduced by 5-10% 1→3 and/or 1→4 linkages. Dextrans were selected as the solute molecule in these experiments for several reasons. They were readily available as narrow molecular weight fractions and

had been used successfully in previous solute exclusion studies (66-67). They would be expected to be essentially spherical in solution. Finally, dextran concentration in solution could be accurately determined by measuring the optical rotation. Because of their high specific rotation ($[\eta]^{20}_{546}$ = +235°), changes in concentration of a 2% dextran solution could be measured to ± 0.002%, when determined polarimetrically at 546 nm. The mercury green (546 nm.) wavelength was chosen because of the associated higher specific rotation and greater eye sensitivity as compared to the sodium D wavelength.

Inaccessible water δ, is that water within the cell walls which is not available for dilution of the stock polymer solution because it is enclosed in pores too small to be penetrated by the solute molecule. Inaccessible water was calculated from the following equation, given by Stone and Scallan (67).

$$\delta = \frac{w+q}{p}\left[1 - \frac{w}{w+q}(c_i/c_f)\right] \qquad (13)$$

where

δ = inaccessible water, g./g. wood

w = dextran solution added, g.

q = water associated with wood, g.

p = dry weight of wood, g.

c_i = initial dextran concentration

c_f = final dextran concentration

Hence, by measuring the change in concentration of a known weight of polymer solution brought about by a known weight of wood wafers of known moisture content, inaccessible water could be determined.

Diffusion Versus Sorption of Dextrans in Solute Exclusion Studies

Application of the solute exclusion technique to the determination of porosity of a wood sample requires that there be neither chemical nor physical interaction of the solute molecules with the wood samples. If no interaction occurs, the inaccessible water δ, calculated from Equation (13) should be independent of the initial concentration of the dextran polymer in solution. Stone and Scallan reported this to be the case when dextrans were used as the solute molecule (67). To verify this conclusion, two sets of solute exclusion experiments were run, using the procedure presented in the experimental section. Within each set of experiments, the initial dextran concentration was varied between 0.1 and 2.0%. In the first set, the wood sample was unreacted summerwood-springwood and the dextran used was T40 ($\bar{M}_w/\bar{M}_N$ = 1.5), whose diameter in solution was estimated to be 90 A. by Stone and Scallan (67). In the second set, the inaccessible water of a summerwood-springwood sample at 90.9% yield was determined with dextran T10 ($\bar{M}_w/\bar{M}_N$ = 2.0), which had an estimated diameter of 51 A. (67). On the basis of previous work (67), these molecules would be expected to be large enough that the inaccessible water calculated would be equal to the fiber saturation point, or total pore volume of the cell wall.

The results of these experiments are tabulated in Appendix VI. If sorption accounted for a substantial portion of the decrease in dextran concentration, this would be reflected in an increase in the value of inaccessible water as initial dextran concentration was increased from 0.5 to 2.0%. If, on the other hand, sorption accounted for only a small percentage of the decrease in dextran concentration, this would be detectable by an increase in δ at very low c_i. Neither of these effects can be seen in the data collected, although the precision in determining δ becomes poorer as c_i decreases, as discussed in Appendix VI. Despite the lack of precision, however, it was concluded that inaccessible water was independent of initial dextran concentration, and therefore sorption effects were negligible.

Application of the Porous Sphere Model to Solute Exclusion Studies in the Literature

In Table X, a summary is presented of the change in cell wall porosity of softwoods during peracetic acid delignification and kraft pulping. At high yields, a comparable change in both the fiber saturation point and cell wall volume appears to occur for all three delignification reactions. It would be expected, therefore, that the changes in pore size and pore size distribution during peracetic acid delignification would also closely parallel that reported for kraft and sulfite pulping in Table X (67) and sodium chlorite holopulping in Table V (72).

TABLE X

COMPARISON OF CELL WALL POROSITY AT HIGH YIELDS FOR SEVERAL DELIGNIFICATION PROCESSES

Process	Wood Species	Yield, %	Inaccessible Water,[a] g./g. wood	Cell Wall Volume, ml./g.
	Loblolly pine	100.0	0.31[b]	0.98
Peracetic acid	Loblolly pine	90.9	0.74[b]	1.28
(67)	Sitka spruce	100.0	0.42	1.09
Kraft (67)	Sitka spruce	89.3	0.80	1.31
Sulfite (67)	Sitka spruce	87.7	0.85	1.33

[a] Values given are equivalent to the fiber saturation point of the cell wall.

[b] These values are the average of duplicate determinations of δ at an initial dextran concentration of about 2.0% (Appendix VI).

After initiating this thesis work, it was learned that certain specially prepared Pharmacia dextrans of low molecular weight, used by Stone (66-67), were no longer commercially available. These dextrans, of molecular weight below 10,000, penetrate a fraction of the porous structure of wood, and therefore they yield pore size distribution data. Considering the approximate correspondence

of pore size data already collected with that in the literature, and the difficulty of obtaining sufficient narrow fractions of low molecular weight dextrans, it was decided not to pursue pore size distribution by further solute exclusion experiments.

Nevertheless, it has been possible to consider further the change in cell wall porosity of loblolly pinewood upon peracetic acid delignification. An analysis is presented in Appendix VII (p. 173) which shows that an improved, larger estimation of the size of dextran molecules in solution, over that used by Stone and Scallan (67), is achieved by the application of the porous sphere model of Seely (56), a theory already reviewed in the introduction. As a result of this analysis, it is possible to estimate the change in the median pore width of loblolly pine springwood wafers which occurred as delignification with peracetic acid proceeded. This relationship is presented in Fig. 9. Median pore width, as defined by Stone and Scallan (67) is the pore size at which one half of the pore volume is contained in larger pores and one half in smaller pores. The estimated median pore width of loblolly pine increased from 12 A. for unreacted wood to 35 A. at 75% yield.

PHYSICAL CHARACTERIZATION OF THE SOLUBILIZED LIGNIN

DELIGNIFICATION IN STAGES AND THE EFFECT UPON GPC ELUTION CURVES

On the basis of previous discussion it has been postulated that selective delignification of loblolly pine springwood wafers results in an increase in the pore volume of the wood, comparable to that measured for other delignification processes at high yield. The investigation now turned generally to consideration of the physical nature of the solubilized reaction products. To accomplish this, a reaction was run with loblolly pine springwood wafers in which the solubilized reaction products were collected in stages as the reaction proceeded and then were examined separately by gel permeation chromatography.

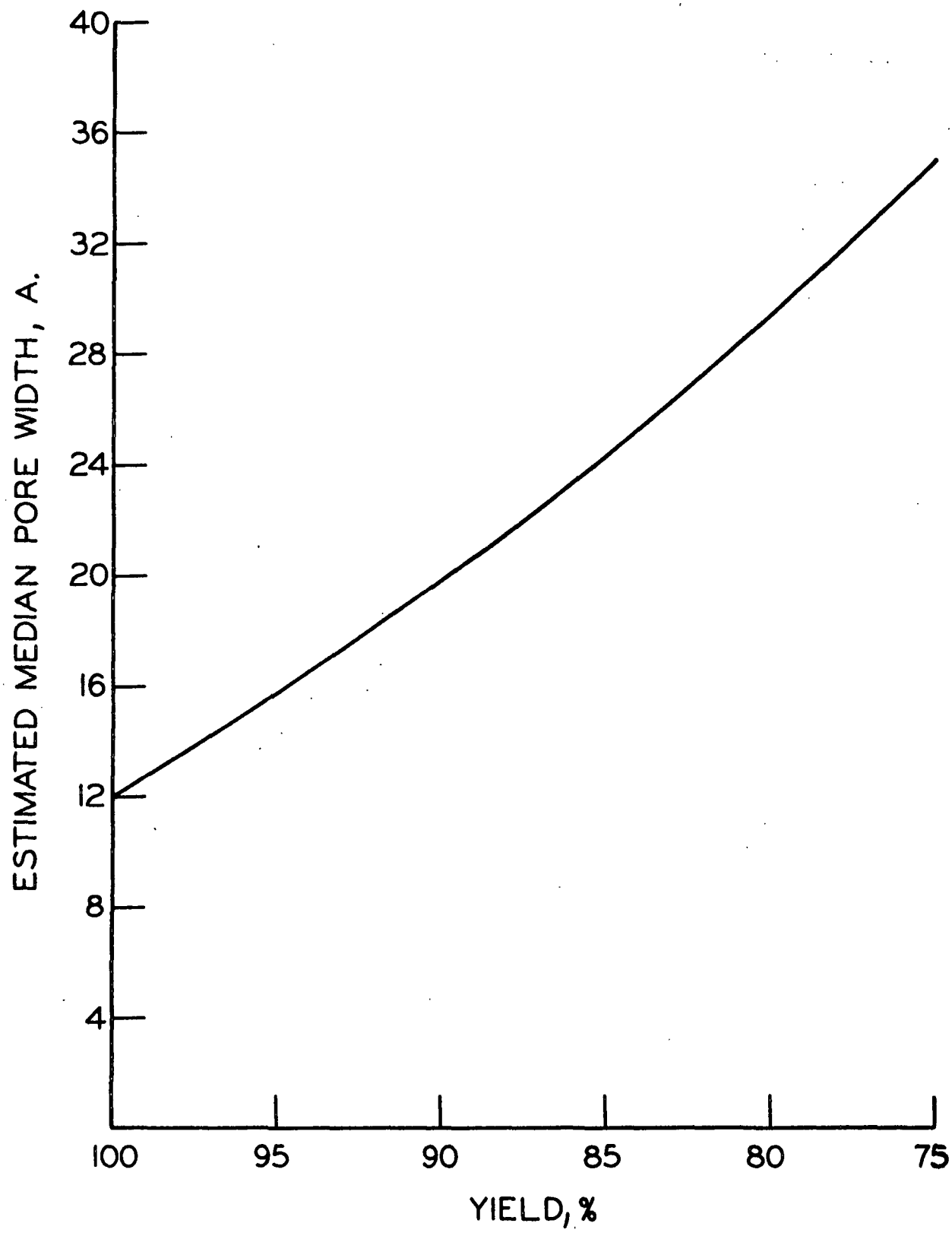

Figure 9. Estimated Change in Median Pore Width upon Progressive Delignification of Loblolly Pine Springwood by Peracetic Acid

The stagewise delignification procedure used was based on the established reaction procedure as discussed in the experimental section. The yield at the end of the last of seven successive reaction stages was determined to be 77.0%.

The use of gel permeation chromatography in the analysis of liquors from various delignification processes has been discussed in the literature review. In this investigation, a GPC column apparatus was designed and constructed to provide for the fractionation of the water-soluble reaction products of the delignification reaction. A photograph of GPC column apparatus is shown in Fig. 10, and a complete description of the entire GPC column setup is presented in Appendix V.

In order to provide a column which would be usable indefinitely, the column packing gel selected had to be insensitive to changes in pressure as the sample was placed on the column. Therefore, Porasil, a rigid packing material which does not swell in aqueous suspension, and thus is not a true gel, was selected for the GPC column. When packed in a GPC column, Porasil offers definite advantages over organic polymer gels, such as Sephadex (79-80a). Its rigidity allows fractionation to be performed in much simplified column setups – that is, sufficient rates of flow may be achieved by hydrostatic head alone. Pressure pumps are seldom required. The chemical inertness of Porasil to materials in this investigation minimized sorption problems in GPC. Finally, a Porasil-packed column, once constructed, is usable indefinitely. There is no possibility of sample contamination due to bacteriological or chemical degradation of the gel, and the column may be cleaned *in situ* with, for example, hot nitric acid. Once deaerated and packed, Porasil does not change its volume or porosity within the column. Material balances on preliminary runs on a small column packed with Porasil B showed that there was no permanent absorption of lignin materials within the column.

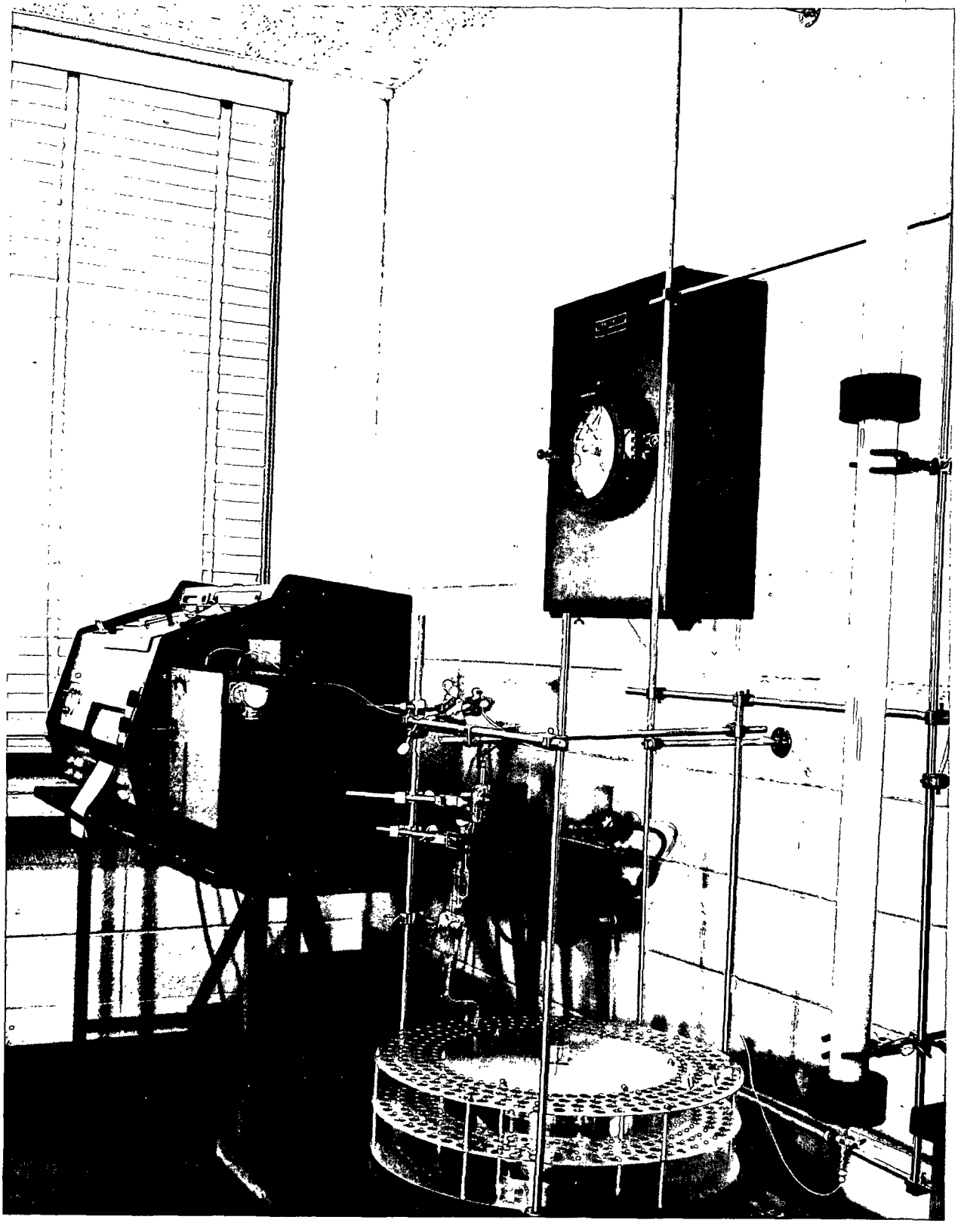

Figure 10. Gel Permeation Chromatography Column Apparatus

The void volume of the GPC column, $\underline{V_o}$, was determined to be 1290 ml. Total liquid volume in the column, $\underline{V_t}$, was calculated from the following formula, using the value of specific volume of Porasil B found by Swenson (81):

$$V_t = \pi R^2 h - g_m \cdot V' \qquad (14)$$

where

$\underline{R}$ = 2.5 cm.

$\underline{h}$ = 160.0 cm.

$\underline{g_m}$ = 1238.9 g. (dry weight of Porasil B)

$\underline{V'}$ = 0.448 ml./g. (specific volume of Porasil B)

$\underline{V_t}$ = 2567 ml.

Continuous quantitative detection of lignin materials in the solution eluting from the column was accomplished by monitoring the absorbance at 275 nm. The 275 nm. wavelength was chosen for column monitoring because direct ultraviolet curves of lignin solubilized by peracetic acid showed a slight maximum at 275 nm., rather than at 280 nm. Absorbance was monitored for elution volumes between 1290 ml. ($\underline{V_o}$) and 3350 ml. This range is equivalent to a total of 103 20-ml. fractions.

The solubilized reaction products of the stagewise delignification were investigated using GPC experimental procedures presented in the experimental section, p. 132. In order to examine the shapes of the GPC elution curves independent of any variation in rate of solubilization of lignin, the GPC curves of the successive reaction stages were each computed on a normalized basis. To do this it was necessary to calculate the sum of the absorbances of the 103 total fractions for each curve. These sums are presented as a function of time of flow in Fig. 11. In the first stage of the reaction, the solubilized reaction products were less concentrated than at later stages, due to dilution by liquor initially in the final sections of the flow apparatus. For the last six stages of the reaction,

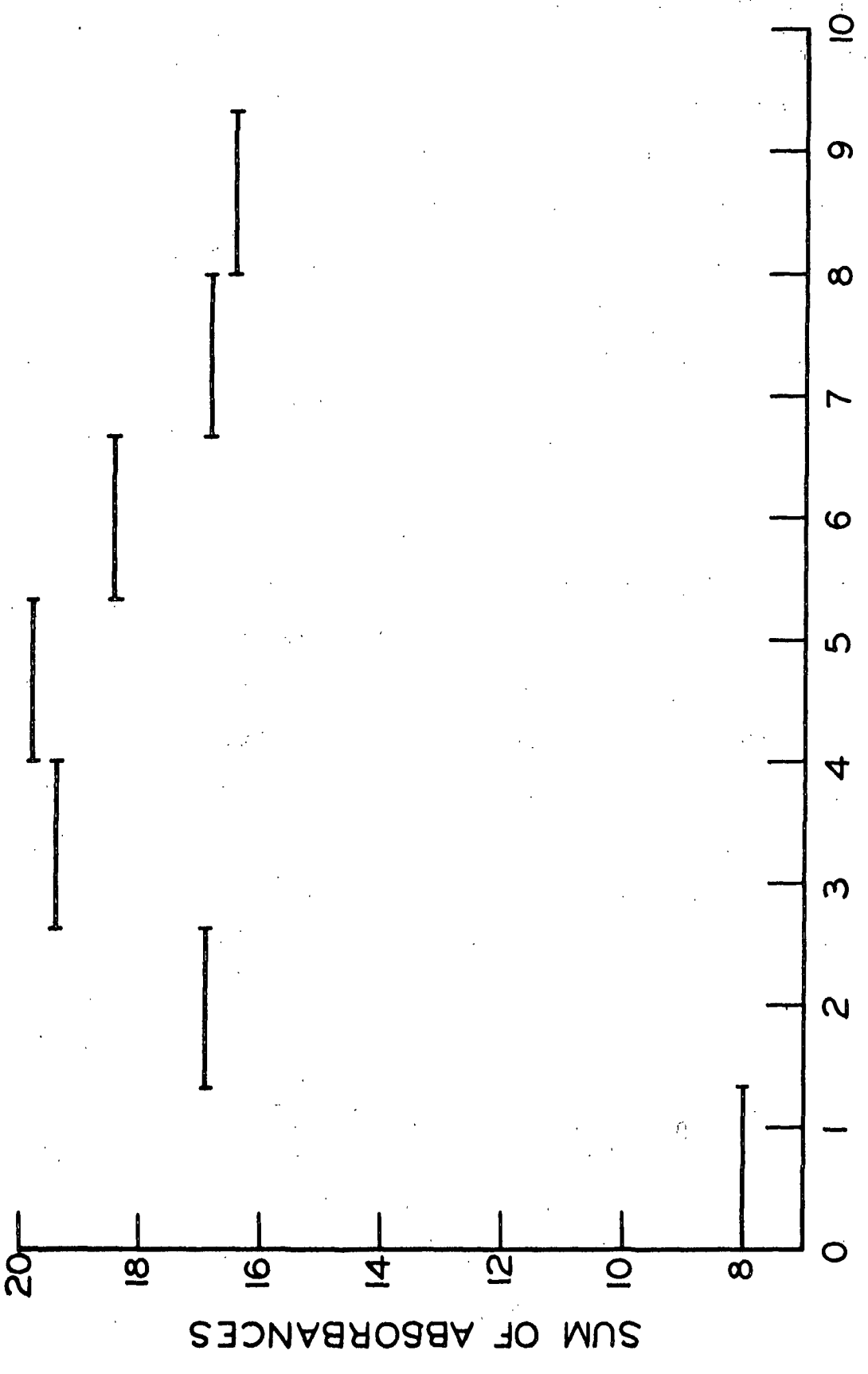

Figure 11. Sum of Absorbances at 275 mm. for Seven Successive Reaction Stages

the total absorbance of the solubilized reaction products was nearly constant. If total absorbance is directly related to total mass in solution, this would mean that the rate of lignin solubilization is independent of the amount of residual lignin in the wood. This observation is not in accord with exponential behavior found in other systems where the delignifying reagent was in excess and the behavior was attributable to apparent first-order kinetics (81a). In model compound studies, the consumption of peracetic acid has been found to conform to pseudo-second-order rate laws proportional to the multiplied product of the concentration of reactant by that of each substrate (12).

In Fig. 12, the normalized elution curves for the seven successive reaction stages are plotted. Yield at the end of each of the first six stages was estimated by direct proportion to the total absorbance between Fractions 1 and 103, assuming that total absorbance was directly related to total mass in solution. A marked trend is evident in the elution curves. As delignification proceeded, the relative abundance of larger lignin fragments increased, as was observed in other delignification studies (52-53). This increase in the size of lignin molecules solubilized seems to parallel the increase in pore size observed in solute exclusion experiments and lends support to the notion that pore size distribution may be at least correlated to the size of lignin macromolecules solubilized during peracetic acid delignification of wood. However, somewhat unexpectedly, the shapes of the elution curves do not have a simple slope that would reflect an evenly graduated distribution of molecular size. Rather, as reaction proceeded, the relative abundance of species eluting shortly after V_o, centering at about Fraction 10, increased substantially. This increase was at the expense of some material eluting later (approximately Fraction 50) within the included volume of the column and even more noticeably, material in those regions beyond the calculated total liquid column volume.

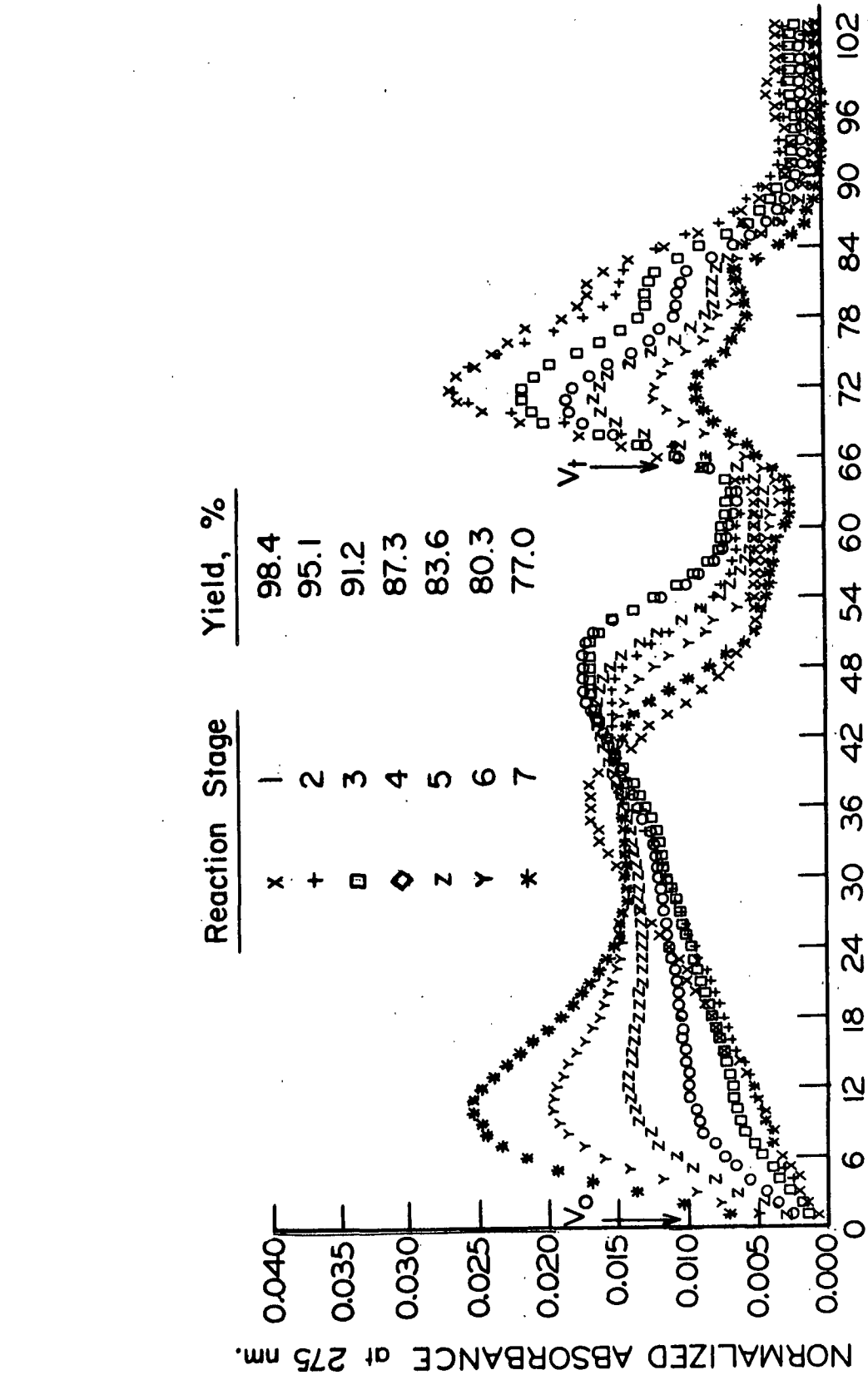

Figure 12. Normalized GPC Elution Curves of Product Liquors of Successive Reaction Stages

In order to assess quantitative significance to the changing elution curves with stagewise delignification, it was necessary to characterize the GPC column – that is, to determine the relationship between the molecular weight of the lignin polymer and its elution volume on the column. Cazes (27) reviewed the use of several direct and indirect techniques for column calibration, but none of these were adaptable to characterization of a polydisperse, water-soluble, naturally-occurring polymer, obtained in a partially degraded state. Rather, it was necessary first to fractionate the polymer into fractions of presumably narrow molecular weight range and then to measure the physical characteristics of the lignin fractions. Of particular interest in this investigation was the relationship between the size of lignin macromolecules in solution and elution volume. The review of the mechanism of GPC fractionation presented in the introduction showed that macromolecular size is expected to decrease continuously with increasing elution volume between V_o and V_t. The porous sphere model for cross-linked polymers in solution, proposed by Seely (56), was discussed in the literature as a possibly useful approach to estimating the molecular size of lignin solubilized by peracetic acid and fractionated by gel permeation chromatography. Application of this model requires that independent determinations of both molecular weight and intrinsic viscosity be made as a function of elution volume.

ELUTION AND FRACTIONATION OF COMPOSITE PRODUCT LIQUOR

The material used to characterize a GPC column should contain all the polymeric species in the system which are anticipated ever to be analyzed on the column. Therefore, a composite product liquor was prepared which contained all the solubilized reaction products down to about 80% yield. In order to provide sufficient material for later analysis, four replicate delignification

runs were made according to the established reaction procedure discussed in the experimental section. Yield data are presented in Table XI. All the concentrated product liquors were combined to yield 3800 ml. of 0.75% product liquor for further analysis. At this concentration, the product liquor was an intense yellow-gold color, giving indirect evidence for quinone structures in the solubilized reaction products.

TABLE XI

REACTIONS OF PERACETIC ACID WITH LOBLOLLY PINE SPRINGWOOD WAFERS TO PRODUCE COMPOSITE PRODUCT LIQUOR FOR COLUMN CHARACTERIZATION[a]

Run No.	Initial Concentration, % PAA	Initial Concentration, % H_2O_2	O.D. Wafer Wt., g.	Time of Flow, hr.:min.	Yield, %
I	2.94	0.040	39.31	7:00	80.4
II	3.13	0.067	35.00	7:20	80.9
III	3.02	0.045	35.00	6:50	80.6
IV	3.03	0.029	35.00	7:05	80.4

[a] Reaction temp. = 60.0°C., approximate flow rate = 25 cc./min.

A total of 12 replicate GPC fractionation runs were made using the standards procedure for a column run presented in the experimental section.. The elution curve of a typical fractionation run is reproduced in Fig. 13. Quite good duplication of the elution curves was achieved and, therefore, corresponding fractions of the twelve replicate runs could be combined for use in column characterization.

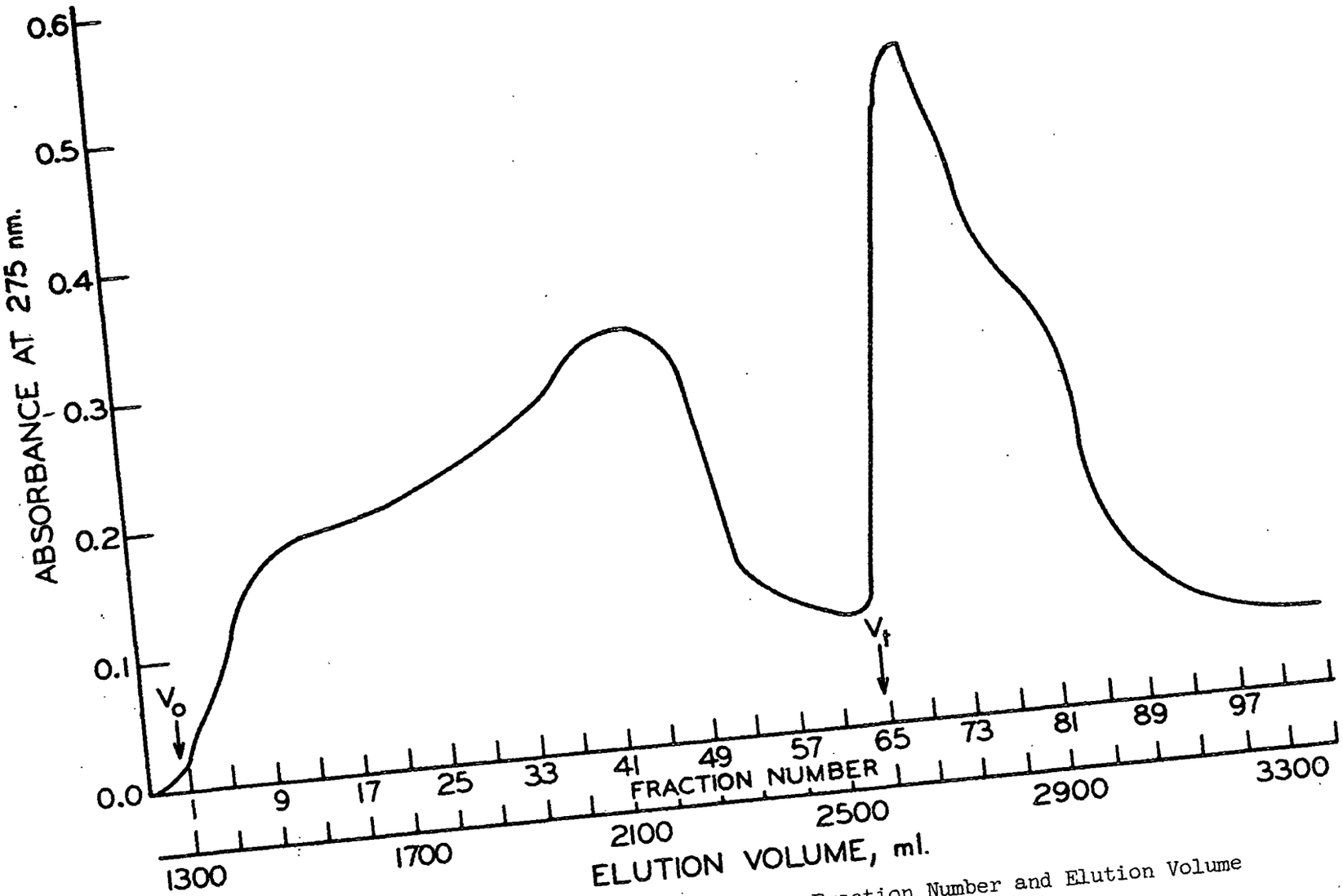

Figure 13. Absorbance at 275 nm. Versus Fraction Number and Elution Volume for Composite Springwood Product Liquor

Absorbance at 275 nm. was used to quantitatively monitor lignin materials in solution as they eluted from the GPC column. In order to relate absorbance to concentration, it was first necessary to demonstrate that Beer's law applies over the concentration range in consideration. In its simplest form, Beer's law states:

$$A = abc \qquad (15)$$

where A = absorbance at a given wavelength

a = absorptivity of a species at that wavelength, l./g.cm.

b = path length of absorbing solution, cm.

c = concentration of absorbing species, g./l.

Volumetric dilution of lignin solutions from several fractions demonstrated that Beer's law was obeyed both below and above V_t. Upon this observation, characterization of the fraction lignin in terms of absorptivity at 275 nm., intrinsic viscosity, and number-average molecular weight all followed.

ABSORPTIVITY AT 275 NM. OF THE FRACTIONATED LIGNIN

The first step in the characterization of softwood lignin solubilized by peracetic acid was the determination of the value of its absorptivity at 275 nm. A major consideration in the interpretation of the elution curves is whether or not this absorptivity value is constant, independent of elution volume. Gravimetric determinations of lignin concentration in solution were performed for an assortment of fractions, and the absorptivity values were calculated from Beer's law. The procedures used to measure absorbance at 275 nm. and to gravimetrically determine concentration are presented in the experimental section.

Attempts to determine the amount of material in solution were frustrated by the fact that those fractions above V_t could not be freeze dried to solids of low moisture content, as was possible for all fractions between V_o and V_t. Fractions above V_t freeze dried to heavy syrups of about 65% moisture content. The reason for this behavior is uncertain, but it is possible that extraneous molecules in solution, such as acetic acid, acetaldehyde, or hydrogen peroxide were responsible. The effect was to make less certain the calculated values of absorptivity for fractions above V_t.

The calculated values of absorptivity for representative fractions both below and above V_t showed that this quantity indeed does depend on elution volume. The values calculated fell into two distinct populations, with the dividing line at V_t. A best-fit polynomial solution was fitted separately to each population.

Between V_o and V_t, the data yielded a best-fit polynomial of degree six:

$$a_{275} = -0.1516337 + 1.462274x - 0.1274257x^2 + 0.005690033x^3 - 0.0001329335x^4 + 0.000001536025x^5 - 0.000000006945609x^6 \quad (16)$$

where x = fraction number ($1 \leq x \leq 64$).

The best-fit plot is shown in Fig. 14. Absorptivity is nearly constant at 6.5 to 7.3 l./g.cm. through the center of this range, between Fractions 12 and 48, dropping to lower values at the very early and very late fractions. These low absorptivity values are in agreement with literature values (13,20) and suggest substantial demethoxylation of the aromatic structure of lignin.

Above V_t, calculated absorptivity at 275 nm. averaged 2.8 l./g.cm. A first-degree fit satisfied the experimental observations:

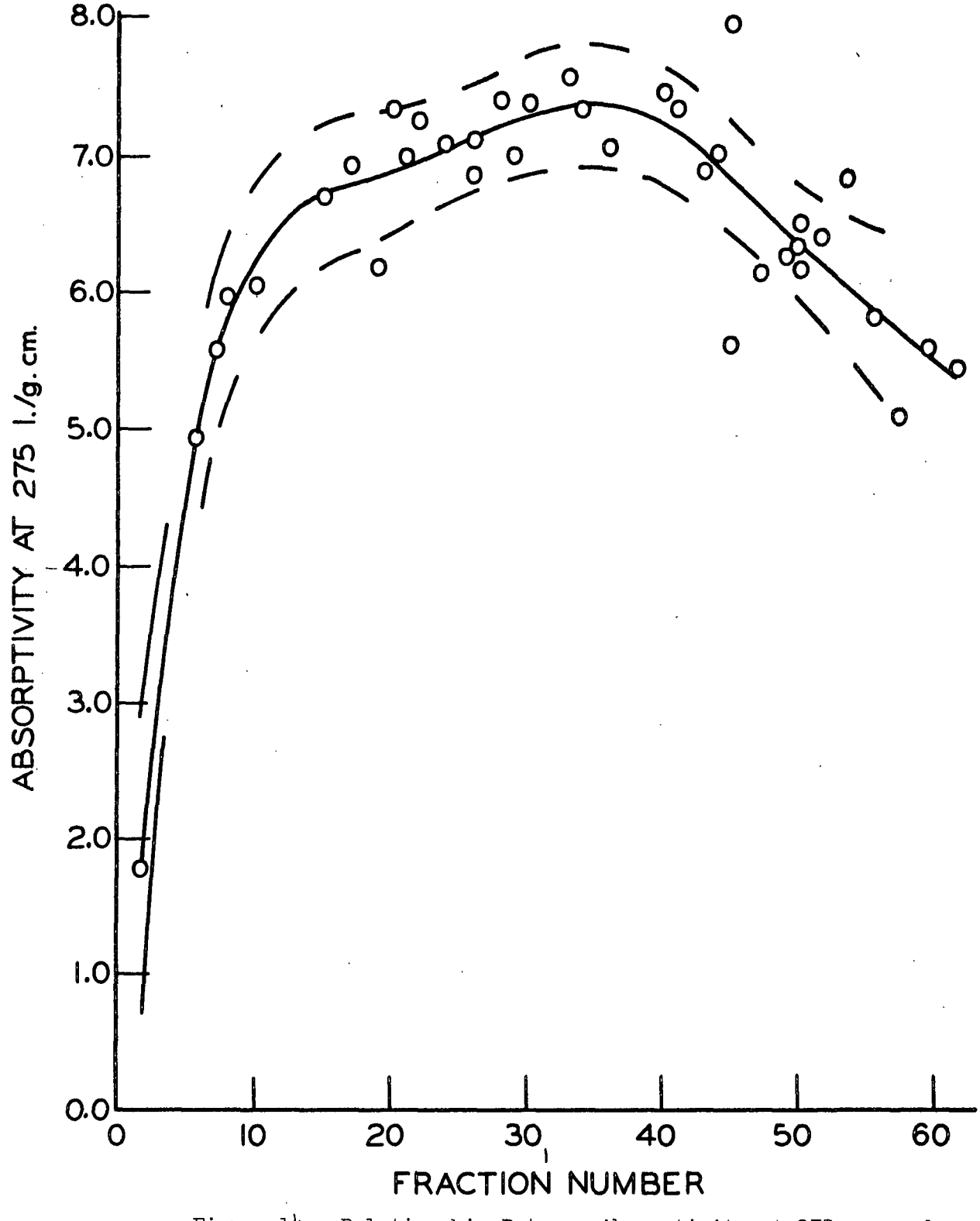

Figure 14. Relationship Between Absorptivity at 275 nm. and Fraction Number for Fractions Between $\underline{V}_o$ and $\underline{V}_t$

$$a_{275} = 1.521186 + 0.015931x \qquad (17)$$

where x = fraction number ($65 \leq x \leq 103$).

The values of the best-fit solutions of a_{275} *versus* fraction number are presented in Table XXIX, Appendix VIII.

The absorptivity relationships derived above demonstrate that there were significant between-fraction differences in the fractionated lignin fragments. Goring found that the overall absorptivity at 280 nm. of both unfractionated sulfite (52) and kraft (53) lignins made soluble in successive reaction stages was constant and concluded from this that both of these solubilized lignins were chemically uniform. However, it is only when determinations of absorptivity are made on a well-fractionated lignin that the more subtle differences in chemical structure may be realized.

INTRINSIC VISCOSITY OF THE FRACTIONATED LIGNIN

Intrinsic viscosities of the fractionated lignin were determined by capillary viscometry as described in the experimental section. The determinations were made in the absence of electrolytes in order to approximate the solution conditions during the delignification reaction. Intrinsic viscosity did not depend on whether the stock solution was made up from freeze-dried lignins or simply taken as concentrated fraction solutions. The intrinsic viscosities found for lignin solubilized by peracetic acid were typical of lignins in general – that is, for the most part, they were less than 0.05 dl./g., as compared to the intrinsic viscosities of hemicellulosic materials which are typically several times those of solubilized lignins.

The intrinsic viscosity values obtained experimentally were used to calculate the best-fit polynomial applying to intrinsic viscosity over the entire range of 103 fractions collected:

$$[\eta]_{30} = 0.1617671 - 0.02055135x + 0.00145923x^2 - 0.0000538546x^3 + 0.000001022896x^4 - 0.00000000917857x^5 + 0.0000000000307496x^6 \quad (18)$$

The intrinsic viscosity relationship is plotted in Fig. 15. As would be expected for GPC fractionation of a chemically uniform polymer differing only in molecular weight, the intrinsic viscosity dropped, at first sharply, then more gradually. The initial sharp descent was reasonable, as column fractionation is not as efficient immediately after $\underline{V}_o$ as it is for smaller molecules that more completely penetrate the internal volume of the gel. However, a rather sharp rise in intrinsic viscosity after the minimum at Fraction 36 was apparent. This behavior was incompatible with that expected for a chemically uniform polymer. Beyond $\underline{V}_t$, extraneous molecules in solution could decrease the rate of flow in the viscometer tube without being recognized in the concentration term. However, the rise in intrinsic viscosity between Fraction 36 and Fraction 64 suggested that the system being studied could not be considered a strictly chemically homogeneous polymer in solution. Differences in chemical species in solution are a reasonable possibility, considering the various reactions which may occur between peracetic acid and lignin in wood.

NUMBER-AVERAGE MOLECULAR WEIGHT OF THE FRACTIONATED LIGNIN

In spite of the complexity of the intrinsic viscosity relationship demonstrated above, an investigation of the molecular-weight relationship was undertaken. The number-average molecular weight of several lignin fractions was determined by membrane osmometry as presented in the experimental section.

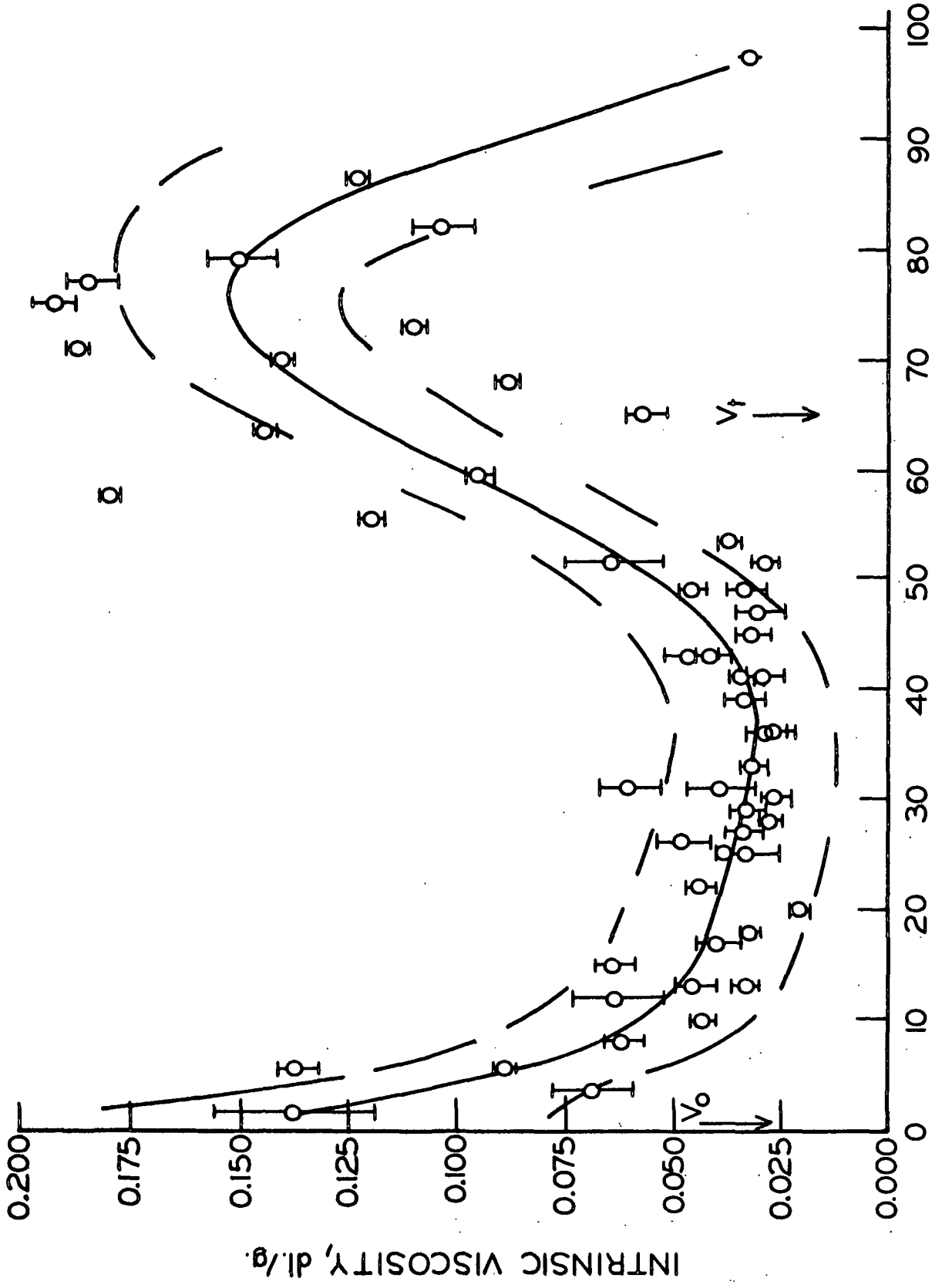

Figure 15. Relationship Between Intrinsic Viscosity at 30 °C. and Fraction Number

In membrane osmometry the number of particles of a polymer of known concentration in solution is determined from the resultant osmotic pressure across a semipermeable membrane. The number-average molecular weight is then calculated from van't Hoff's law:

$$\bar{M}_n = RT/(\pi/c)_o \qquad (19)$$

where R = gas constant

T = temperature

$(\pi/c)_o$ = ratio of osmotic pressure to concentration at zero concentration

To depress any polyelectrolyte effect, the solvent used to determine $\bar{M}_n$ for the lignin fractions was 1% NaCl in distilled water. Since only those fractions below V_t could be obtained in the absence of impurities, no determinations of $\bar{M}_n$ could be made for fractions above V_t. Osmometer operation and the analysis of data collected are presented in Appendix X.

The number-average molecular weights obtained are summarized in Table XII and plotted in Fig. 16. The $\bar{M}_n$ reported reflects only the degree of precision of the linear extrapolation applied but does not reflect the accuracy of the method in this application. In order to verify these values of molecular weight, a comparison to values obtained by another method, such as sedimentation equilibrium or light-scattering, would have to be made. Such a comparative determination was not practical in this investigation. However, the reproducibility of these runs was good enough to assure that relative comparisons could be made with a fair degree of confidence.

An attempt was made to obtain a value of $\bar{M}_n$ for Fraction 63-64, but the effects of polymer diffusion, discussed in Appendix X, were too great to yield a reliable figure. Molecules eluting in this fraction appeared to be too

TABLE XII

NUMBER-AVERAGE MOLECULAR WEIGHTS OF LIGNIN FRACTIONS

Fraction Number	$\bar{M}_n$	$\bar{M}_n$ Range
1-2	21,300	30,033-32,659
8	13,900	12,944-14,945
14	12,500	12,022-12,976
15	11,300	10,802-11,941
19	12,000	11,610-12,436
21	11,000	10,657-11,209
22	18,100	15,822-21,053
26	16,900	16,107-17,821
26	19,300	17,892-20,834
30	18,200	16,535-20,333
33	17,200	16,417-17,964
35	15,900	14,782-17,152
38	13,200	12,475-14,117
40	10,600	10,073-11,111
44	9,200	8,768- 9,703
44	12,600	11,868-13,384
48	10,800	10,197-11,430
50	12,100	11,184-13,280
53-54	10,600	9,945-11,272
57-58	10,500	11,148-14,199
57-58	9,800	8,630-11,213

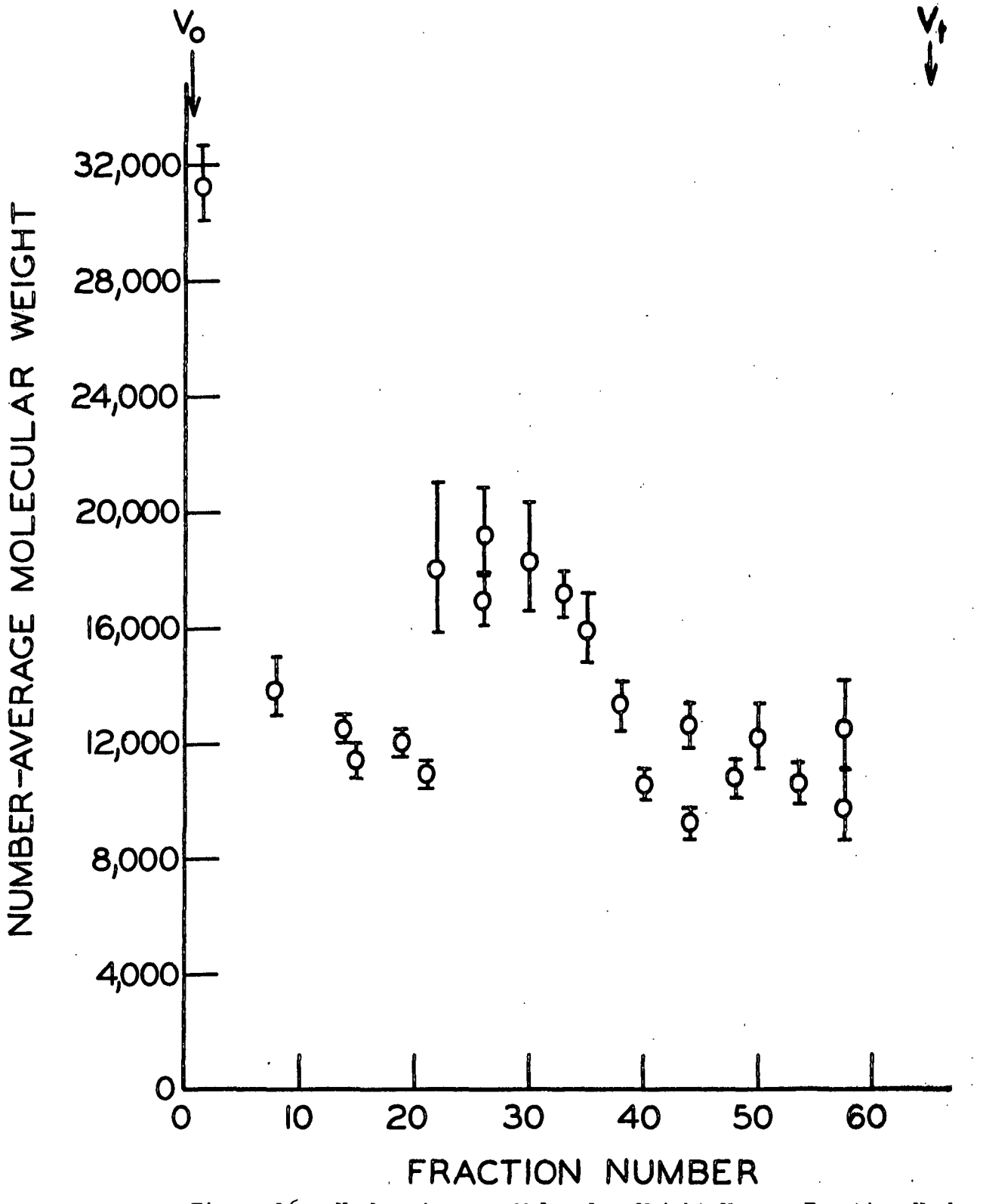

Figure 16. Number-Average Molecular Weight Versus Fraction Number

small to be counted accurately by membrane osmometry. Those lignin fragments which eluted above $\underline{V}_t$ would be expected to be of even smaller molecular size and lower molecular weight than those in Fraction 63-64. Thus, the molecular size fractionation by the GPC column seems generally to be reflected by the $\underline{\bar{M}}_n$ data collected, but a direct relationship between $\underline{\bar{M}}_n$ and fraction number could not be realized. As was the case for intrinsic viscosity measurements, the molecular weight data collected suggest that the lignin solubilized by peracetic acid cannot be considered a chemically uniform polymer in solution – that is, one consisting of a homologous series of macromolecules.

APPLICATION OF THE POROUS SPHERE MODEL TO THE LIGNIN POLYMER IN SOLUTION

At an earlier date, it was believed that the porous sphere model of Seely (56), presented in the introduction, could be applied to the intrinsic viscosity-molecular weight data over the entire lignin fractionation range to yield a unique relationship between hydrodynamic radius and molecular weight. The complexity of the $[\eta]$ and $\underline{\bar{M}}_n$ data collected has rendered this approach impossible. However, since the delignification of wood by mild peracetic acid oxidation does not appear to completely destroy the cross-linked structure of the lignin, an attempt was made to apply the porous sphere model to a limited range of fractions. If successful, this would yield a relationship between molecular radius and fraction number which could be roughly extrapolated to cover the entire fractionation range. Comparison of the elution curves of the successive reaction stages could then be made in terms of lignin size in solution.

Consideration of several types of data collected, including some analytically determined chemical determinations and some trial applications, has led to a successful solution of the porous sphere model using physical data obtained for Fractions 22 through 48. Linear regression was applied to both intrinsic viscosity and number-average molecular weight data to yield the following relations, where $\underline{x}$ is fraction number:

$$\bar{M}_n = 27{,}875.79 - 374.9734x \tag{20}$$

$$[\eta] = 0.04262141 - 0.0002095992x \tag{21}$$

where $22 \leq \underline{x} \leq 48$.

Solutions to Equations (20) and (21) for Fractions 22 through 48 were used to calculate the functions $1/[\eta]$ and $\bar{M}_{\underline{n}}^{-2/3}$, and linear regression was applied to these functions in the form of Equation (9), page 26. From the intercept and slope of the straight line obtained, the values of $\underline{A}$ and $\underline{B}$ were calculated:

$$\underline{A} = 5.2949 \text{ cm.}^3/\text{g.}$$

$$\underline{B} = 297.38$$

The permeability, $\underline{K}$, and the hydrodynamic radius, $\underline{a}$, were then arrived at using Equations (10) and (11), respectively:

$$K = 12.283 \times 10^{-16} \text{ cm.}^2$$

$$a = 0.643 \times 10^{-8} \bar{M}_n^{1/3} \text{ cm.} \tag{22}$$

This result compares fairly reasonably to that obtained by Seely using lignosulfonate data abstracted from the literature: $\underline{a} = 1.02 \times 10^{-8} \bar{M}_{\underline{n}}^{1/3}$ cm.

Using Equations (20) and (22), the hydrodynamic radius of the solubilized lignin may be calculated as a function of fraction number between Fractions 22

and 48. The results are plotted in Fig. 17. This calculated radius function is valid to the degree of certainty of the intrinsic viscosity-molecular weight data from which it was derived. For comparison, the same physical data used to obtain the relationship between the porous sphere hydrodynamic radius and fraction number may be substituted into the Einstein viscosity relation to yield the value of the equivalent solid hydrodynamic sphere, R_e, (82):

$$[\eta] = 0.025 \frac{N}{M} (4/3\pi R_e^3) \tag{23}$$

$$R_e = \left(\frac{30[\eta]M}{\pi N} \right)^{1/3} \tag{24}$$

where N = Avogadro's number

$[\eta]$ = intrinsic viscosity, dl./g.

M = molecular weight

R_e decreases from 14.4 A. for Fraction 22 to 8.0 A. for Fraction 48. Brown, et al. (45) obtained estimates of molecular radii of enzymatically liberated lignins which were larger and more comparable to those of the porous sphere model derived above than to those calculated for the solid hydrodynamic sphere.

It is interesting to compare the hydrodynamic radii, a, of these solubilized lignins with the radii of cross-linked dextrans of corresponding molecular weight from Table XXVII, Appendix VII. This comparison is summarized in Table XIII. It can be seen that the lignin solubilized by peracetic acid delignification of loblolly pinewood is only a fraction of the size in solution that the dextrans are. This statement applies whichever model is used for hydrodynamic radius, and the difference would be even greater if the same averages of molecular weight were applied in each case. This significant size difference accounts for an observation made both in this study and in the comparison of work by Stone (67) and Goring (53). Lignin macromolecules of

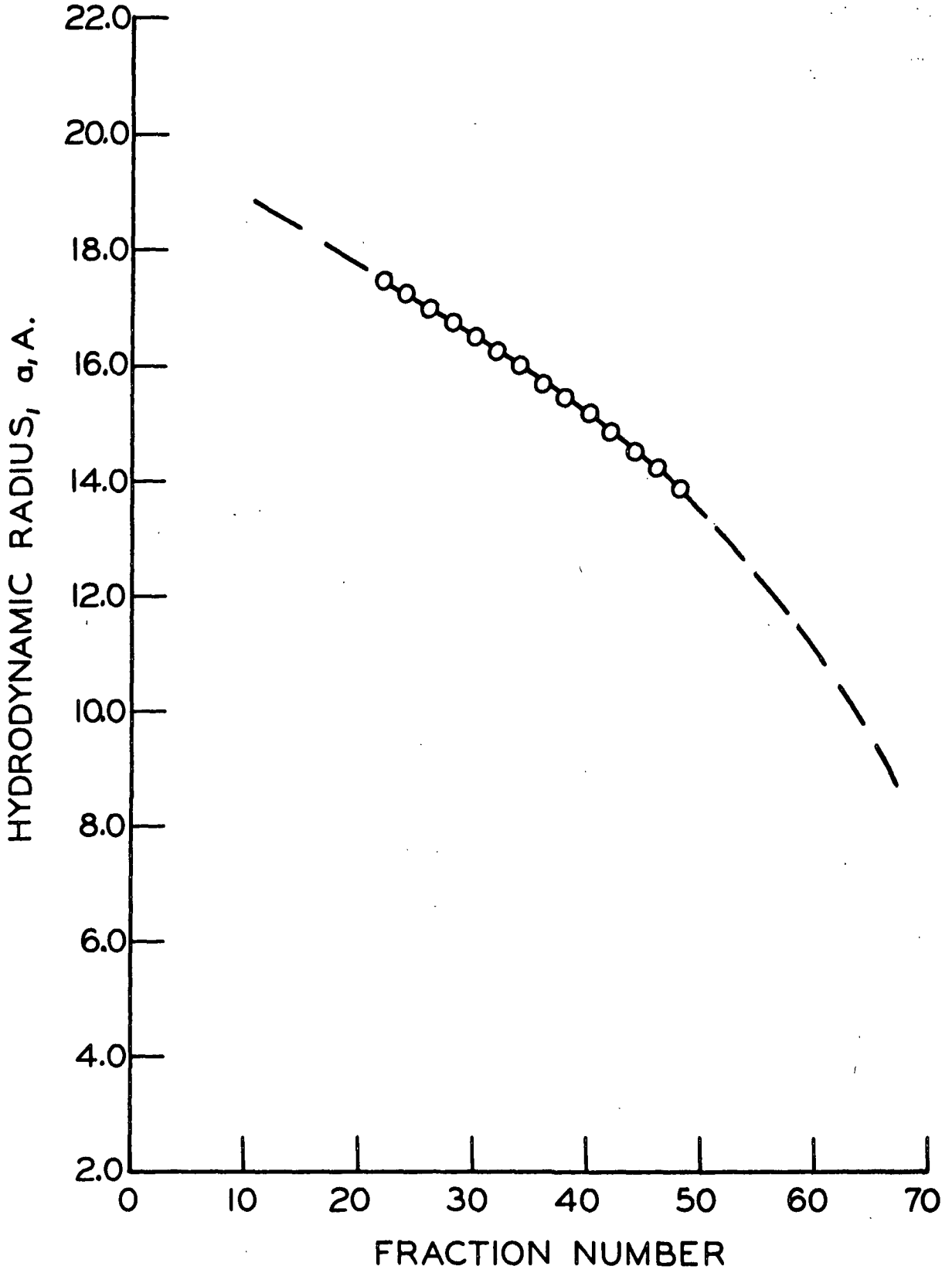

Figure 17. Hydrodynamic Radius of Solubilized Lignins, Calculated from the Porous Sphere Model Applied Between Fractions 22 and 48

quite high molecular weight (>20,000) diffused out of the porous cell wall of wood while dextran molecules of much lower molecular weight were excluded from the same porous structure.

TABLE XIII

COMPARISON OF HYDRODYNAMIC RADII

Molecular Weight[a]	Solubilized Lignin		Dextrans	
	$\underline{a}$, A.[d]	R_e, A.[b]	$\underline{a}$, A.[d]	R_e, A.[c]
10,000	13.9	8.1	52	24
15,000	16.0	9.4	74	38
20,000	18.0	14.5	80	42

[a] Molecular weights of solubilized lignins are number-average; those of dextrans are weight-average.

[b] Calculated by Equation (24), Einstein-Stokes model.

[c] Calculated by Stone (67) using Equation (12), Einstein-Stokes model

[d] Calculated by Equation (22), Seely model.

EVALUATION OF PORE SIZE AS A RESTRICTING MECHANISM IN THE DELIGNIFICATION OF LOBLOLLY PINE BY PERACETIC ACID

The increase in porosity of loblolly pine wafers with progressive delignification has been demonstrated, and the effect upon median pore width has been estimated in Fig. 9. In addition, it has been shown that as delignification proceeded, the distribution of the solubilized lignin fragments shifted in favor of presumably larger molecular size (Fig. 12). The determination of the relationship between hydrodynamic radius and fraction number, shown in Fig. 17, demonstrates that the elution curves in Fig. 12 indeed do reflect an increasing av. diameter of lignin macromolecules solubilized as delignification proceeded, as was previously inferred from knowledge of GPC principles. In

addition, the relationship in Fig. 17 makes possible a more quantitative comparison between these two size changes, median pore width and distribution of macromolecular diameter.

Thus, the elution curves in Fig. 12 represent a distribution of absorbance with respect to molecular size in solution, where absorbance is related to mass of solubilized lignin. For each elution curve there would therefore be a midpoint in terms of mass distribution. Expressed in another way, each elution curve would have a median fraction number which would correspond to this midpoint of mass distribution. Like the elution curves, the median fraction numbers shift toward lower fraction number with stagewise delignification. If pore size serves as a restricting mechanism in this delignification reaction, the estimated median pore width at a given yield should correspond approximately to the median fraction number of the elution curve at that reaction stage – that is, the estimated median pore width should be approximately equal to the diameter of the lignin macromolecule at the midpoint of the mass distribution. This comparison is presented in Table XIV. From Fig. 9, the estimated median pore width was read as a function of yield. Then from Fig. 17 the fraction number was read which corresponded to a lignin macromolecule having a diameter which was equal to the estimated median pore width at that yield. For this purpose the relationship in Fig. 17 was extrapolated to larger molecular radii at earlier fraction numbers and to smaller molecular radii at later fraction numbers. The fraction numbers in Table XIV can be seen to be approximately midway in their corresponding elution curves in Fig. 12, and it is postulated, therefore, that the development of cell wall porosity during the delignification of loblolly pine is one of the controlling factors in the removal of lignin by peracetic acid.

TABLE XIV

COMPARISON OF ESTIMATED MEDIAN PORE WIDTH AND LIGNIN FRACTION NUMBER HAVING EQUAL MACROMOLECULAR DIAMETER

Reaction Stage	Yield, %	Estimated Median Pore Width, A.[a]	Fraction Number Having Equal Molecular Diameter[b]
	100.0	12.0	>65
1	98.4	12.8	>65
2	95.1	15.6	>65
3	91.2	18.8	65
4	87.3	22.2	60
5	83.6	25.8	53
6	80.3	29.1	44
7	77.0	32.6	32

[a] From Fig. 9.
[b] From Fig. 17.

CHEMICAL CHARACTERIZATION OF THE SOLUBILIZED LIGNIN

In the preceding section, gel permeation chromatography has been shown to be a useful tool in the separation of the solubilized reaction products of the delignification of loblolly pine by peracetic acid. Differences in the GPC elution curves have been found with stagewise delignification which demonstrated that the proportion of the larger-sized lignin fragments made soluble increased as the yield decreased. This observation was then correlated to the increasing porosity of the cell wall which also occurred with decreasing yield.

Examination of the fractionated materials has revealed a changing absorptivity value and intrinsic viscosity and molecular weight relationships

which were more complex than that expected for fractionation of a chemically uniform polymer. These observations all pointed to the possibility of there being appreciable diversity in the chemical composition of the fractionated lignin material. Realization that the peracetic acid delignification of loblolly pine involved a mechanism of degradation, which was more complex than simple lignin fragmentation, led to further activity being focused on studying the chemical composition of the material obtained by GPC fractionation. Additionally, research was concentrated on the 64 fractions between V_o and V_t, since these could be freeze dried and were better suited to quantitative study.

PHENOLIC HYDROXYL, CARBOXYL, AND METHOXYL ANALYSES

To learn more about the chemical composition of the solubilized lignin, analytical data were obtained on the phenolic hydroxyl, carboxyl, and methoxyl contents of various fractions.

Approximately one-fourth of the guaiacyl units of softwood lignin have a free phenolic group on the 4-position of the aromatic ring (83,84). The remaining units are linked to another guaiacyl unit by some type of ether bond at the 4-position. The free phenolic group is known to be an important factor in the delignification reactions of certain conventional pulping processes (85), and model compound studies (8) suggested that it is likewise important to the mechanism of delignification of wood by peracetic acid.

Numerous literature sources (8,10,13-16,19) reported that oxidation of lignin and lignin model compounds by peracetic acid results in carboxyl groups by both ring cleavage and side chain oxidation. Therefore, the carboxyl group was also a logical functional group to attempt to measure quantitatively for the fractionated lignin.

The methoxyl content of the guaiacyl nucleus of softwood lignin is typically 15-16% (86). The low values of absorptivity at 275 nm. measured in this study and in several previous studies (8,10,12-16,18,19) on peracetic acid oxidation of lignin and model compounds all have suggested that substantial demethoxylation of the aromatic ring occurred prior to lignin solubilization.

Phenolic Hydroxyl Content

By Reaction with 1-Nitroso-2-Naphthol

Olcay (87,88) has developed a method for the determination of free phenolic groups in softwood lignin which is based on the color reaction occurring between 1-nitroso-2-naphthol and eugenol. Olcay studied the color reaction occurring with several model compounds having one or two para-substituted guaiacyl nuclei. Under the conditions employed, the color reaction did not take place unless the one ortho- and both meta-positions to the free phenolic hydroxyl were unsubstituted. In addition, compounds containing a carbonyl group in the α-position of the side chain did not react with 1-nitroso-2-naphthol. Applying the color reaction to spruce milled-wood lignin, a value of 0.255 phenolic hydroxyl per methoxyl group was obtained.

The 1-nitroso-2-naphthol color reaction was applied to two model compounds, conidendrin and ferulic acid, and to twenty of the lignin fractions. The experimental procedure employed is detailed in Appendix XII.

A satisfactory color reaction was achieved in the reaction of 1-nitroso-2-naphthol with the model compounds. The reagents and reaction procedure were, therefore, of acceptable quality. However, no color reaction occurred between 1-nitroso-2-naphthol and any of the lignin fractions tested. It can, therefore, be concluded that either there are no free phenolic hydroxyl groups in softwood lignin solubilized by peracetic acid or the lignin has been modified by peracetic

acid in such a way that this specific color reaction can no longer occur with any free phenolic groups still present.

By Ultraviolet Difference Spectra

The ultraviolet absorption curve of native lignin, certain modified lignins, and many lignin model compounds is considerably different when obtained in alkali media as compared to neutral or acidic media. Aulin-Erdtman (89) was a pioneer in the development of the $\Delta\varepsilon$-method – that is, subtraction of the absorbance curve obtained in neutral solvent from the more intense absorbance curve obtained in alkali. In general, the $\Delta\varepsilon$-method in ultraviolet spectroscopy serves to differentiate those chromophoric groups whose absorbance is dependent on the pH of the solvent from those chromophoric groups which are not. The UV absorption bands of free phenolic groups in aromatic compounds, including lignin, undergo a bathochromic shift (shift to longer wavelength) upon ionization in alkali, and therefore the $\Delta\varepsilon$-method can be used to quantitatively measure the phenolic hydroxyl content of these compounds.

Wexler (90) developed a technique to relate the peak height of the UV difference maximum at 250 nm. quantitatively to the phenolic hydroxyl content of softwood lignosulfonates, and the technique was applied with apparent success to spruce dioxane lignin by Arseneau and Pepper (91). This technique, with modification as presented in the experimental section, was applied to a number of freeze-dried lignin fractions.

A typical difference spectrum is shown in Fig. 18. A large maximum in the UV difference spectra occurred between 250 and 253 nm. for all fractions runs. The band at 300 nm. has been attributed to phenolic hydroxyl groups conjugated to chromophoric groups on the side chain (90,91). The phenolic hydroxyl contents calculated from the 250 nm. band are presented in Table XV. The average phenolic

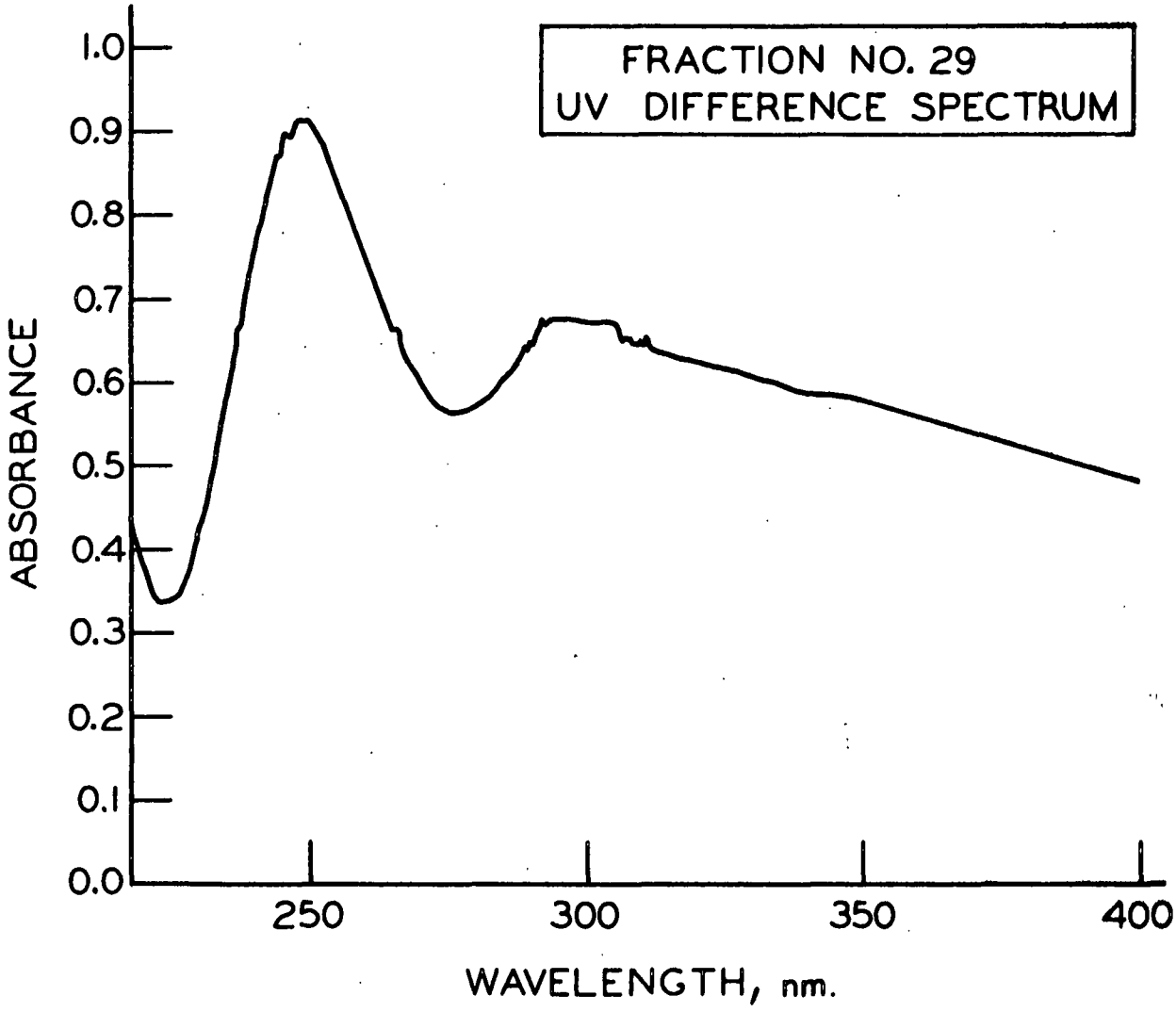

SAMPLE BEAM	REF. BEAM	CONCN.	λ_{MAX}	ΔA_{MAX}
BASIC	ACIDIC	0.1248	252	.480

Figure 18. UV Difference Spectrum of Fraction 29

TABLE XV

PHENOLIC HYDROXYL, CARBOXYL, AND METHOXYL CONTENTS OF FRACTIONATED LIGNIN

Fraction Number	Phenolic Hydroxyl,[a]		Carboxyl,[a]		Methoxyl,[a]	
	%	meq./100 mg.	%	meq./100 mg.	%	meq./100 mg.
3-4			7.20	0.160		
8					4.13	0.128
9	0.50	0.030				
11			9.23	0.205		
16	0.56	0.033			4.32	0.134
18					4.16	0.129
23	0.72	0.042				
27			11.93	0.265		
29	0.74	0.043				
31					4.01	0.124
33	0.77	0.045				
34			13.28	0.295		
35	0.73	0.043				
39			12.83	0.285		
40					4.38	0.136
42	0.93	0.055				
44			12.60	0.280		
48	0.99	0.058			3.92	0.122
53-54			12.60	0.280		
55-56	0.82	0.048				
57-58					3.78	0.117
59-60			9.00	0.200		
61-62	0.47	0.028				
63-64					1.46	0.045

[a] All analyses are on the basis of ovendry sample.

hydroxyl content of these fractions is about one-third that of unmodified softwood lignin. The phenolic hydroxyl content first increased, then decreased, with increasing fraction number.

The acidic solutions of all the fractions were colorless at these concentrations, as expected. However, immediately upon addition of alkali, the same lignin solutions became noticeably yellow in color. This color change is typical of the conversion of phenolic hydroxyl groups from nonionized to ionized form. In order to check whether this color change was reversible, the alkaline solutions of lignin were reacidified. The color disappeared immediately. Direct UV spectra were obtained of the lignin solutions in all three solvents – acidic, alkaline, and reacidified, as shown in Fig. 19. The spectrum of the reacidified solution (Curve 3) was the same, except for dilution, as the spectrum of the acidic solution (Curve 1) for all fractions measured. Therefore, ultraviolet and visible absorption both indicated that what was being observed upon conversion of the lignin solutions to alkaline solvent was the reversible ionization of ionizable groups, such as phenolic hydroxyl groups.

Carboxyl Content

The carboxyl content of a number of freeze-dried lignin fractions was determined by potentiometric titration, using the procedure presented in the experimental section. This procedure would be expected to neutralize free carboxylic acid groups but would not detect lactone or ester groups in the sample.

All fractions titrated as typical weak carboxylic acids with equivalence occurring at about pH 7.5. The potentiometric titration curve of Fraction 34, for example, is shown in Fig. 20.

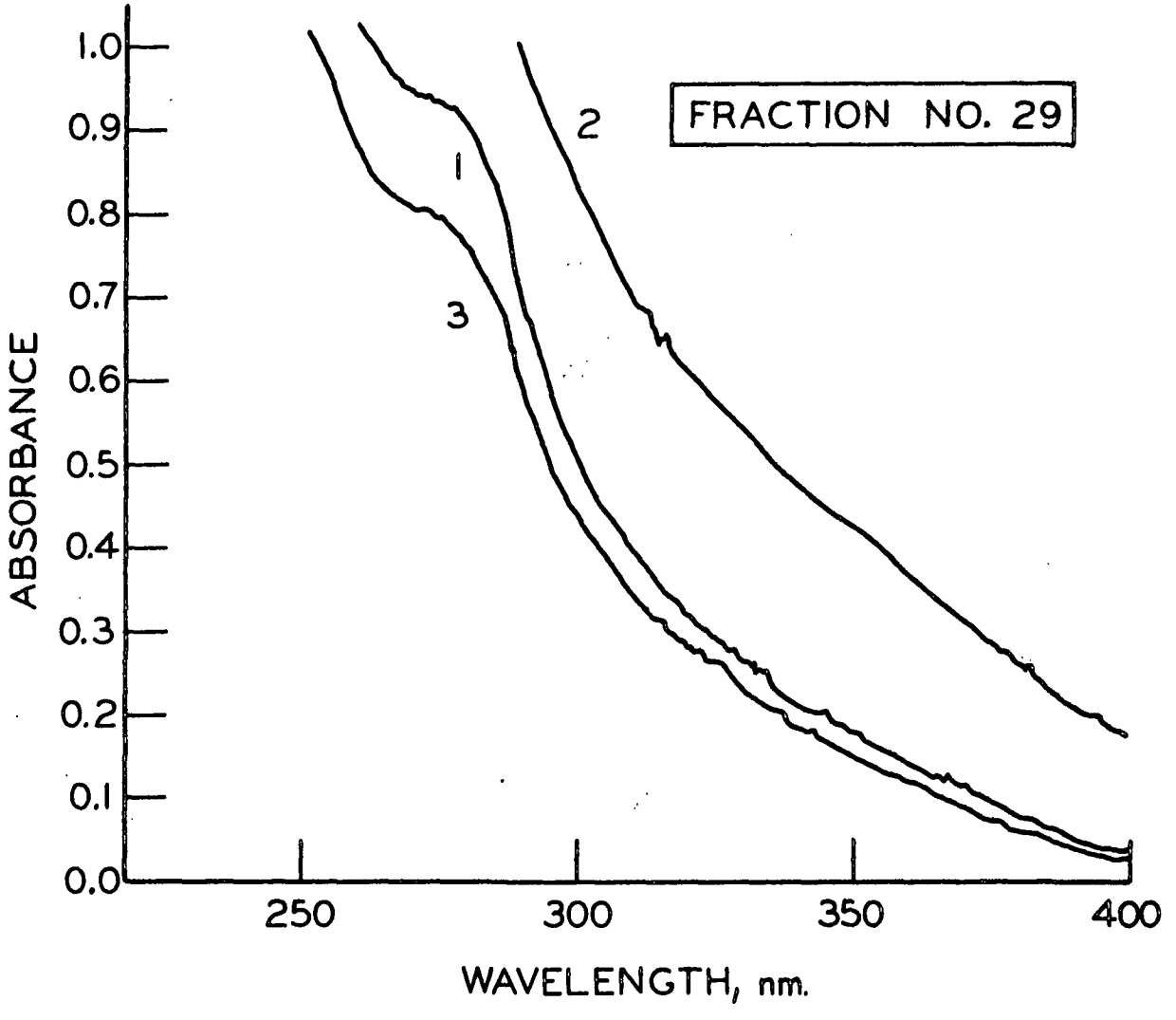

CURVE NO.	SOLVENT	CONCN.
1	0.1N HCl	0.1248
2	0.1N NaOH	0.1248
3	REACIDIFIED ALKALI	

Figure 19. Direct UV Spectra of Fraction 29 in Acidic, Alkaline, and Reacidified Solvents

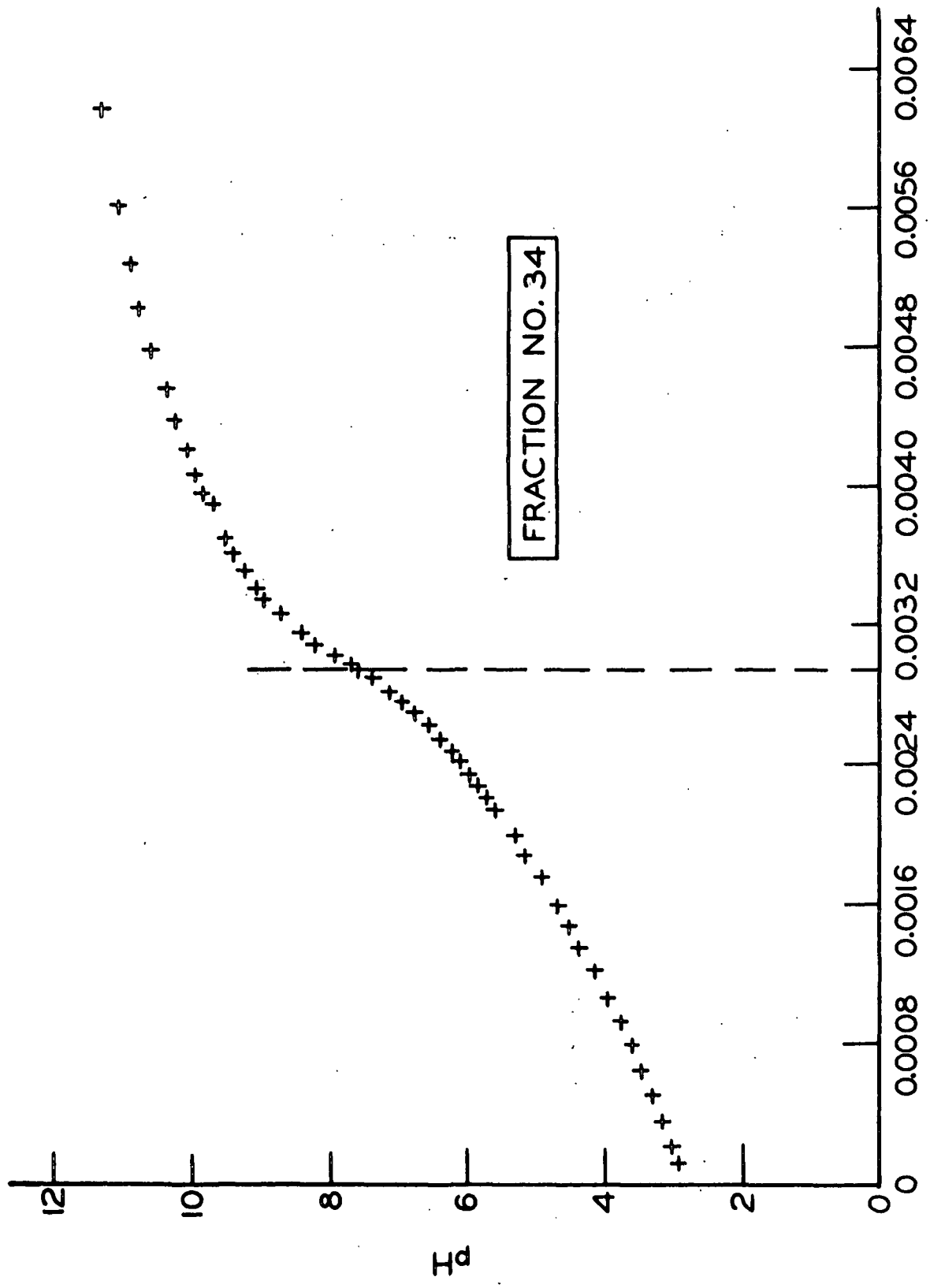

Figure 20. Potentiometric Titration Curve of Fraction 34

The results of the carboxyl group determination are presented in Table XV. Much like the phenolic hydroxyl content, the carboxyl group content first increased, then decreased, with increasing fraction number. However, the number of carboxyl groups was consistently 5-7 times the number of phenolic hydroxyl groups present.

One fraction above V_t, Number 77, was also titrated. The carboxyl group content of this fraction was found to be 0.077 meq./mg. This fraction contained a large amount of background absorbance from quenched peracetic acid, and therefore acetic acid in solution was probably responsible for this large titer.

Methoxyl Content

The methoxyl content of a number of freeze-dried lignin fractions was determined according to Institute Method 18 (92).

The results of the methoxyl analyses are presented in Table XV. The observed methoxyl content of about 4% is only about one-fourth as great as the methoxyl of an unmodified softwood lignin. The methoxyl content is quite stable at this value until late in the fractionation range, where there is a sharp decrease. The methoxyl content, therefore, points out a certain structural consistency for all ligninseluting below about Fraction 60, as compared to the phenolic hydroxyl and carboxyl contents which demonstrated that the amounts of hydrophilic groups present in these lignins varied with fraction number. Thus, a certain amount of chemical nonuniformity has been shown to exist between the lignin fractions. This nonuniformity undoubtedly contributed to the changing absorptivity value and to the complexity of the intrinsic viscosity and molecular weight relationships discussed previously.

ULTRAVIOLET ABSORPTION CHARACTERISTICS OF LIGNIN SOLUBILIZED BY PERACETIC ACID

Ultraviolet absorption of organic molecules in the near UV is generally associated with the electronic transitions of unbonded and π-bonded electrons. However, the location and intensity of these bands may be influenced by other functional groups on the molecule. In studies of various lignins, comparison of the ultraviolet spectra to that of various model compounds has been used as evidence for the presence of certain chemical structures (23,89,90,93-98). Although this approach, used independently, may lead to erroneous conclusions, ultraviolet spectra of lignins can be used to complement information gained from IR spectra and other chemical evidence to suggest more reliably the probable changes occurring during the degradation of lignin.

Certain applications of ultraviolet spectroscopy in this investigation have already been discussed. Fractionated lignins have been shown to obey Beer's law at a wavelength of 275 nm. Absorbance at 275 nm. has been used to monitor lignin materials in solution eluting from the GPC column. Finally, ultraviolet difference spectroscopy has been successfully employed to determine the free phenolic hydroxyl content of the fractionated lignin. Additional information about the chemical structure of the lignin solubilized by peracetic acid delignification of loblolly pine can be expected to be realized from more complete examination of the ultraviolet absorption characteristics of this lignin.

Ultraviolet absorption spectra of a number of representative lignin fractions had previously been obtained at several concentrations. In Fig. 21, the complete UV absorption spectra (200-400 nm.) of four lignin fractions below V_t are presented. Several observations may be made upon examining these spectra. All the spectra have the same general shape. Three major

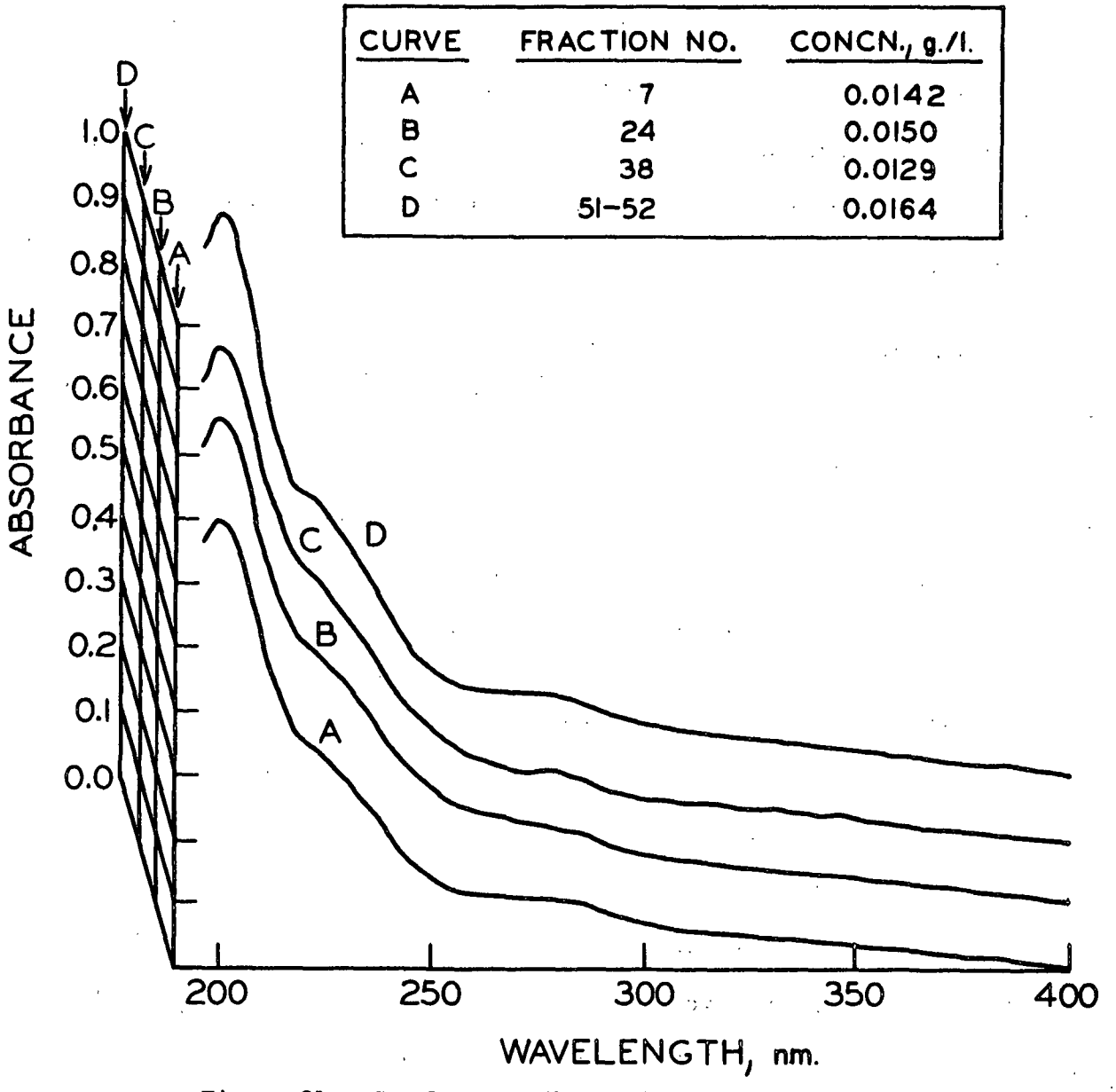

Figure 21. Complete UV Absorption Spectra of Lignin Fractions

absorption bands can be seen in these spectra, centering around 200, 220, and 275 nm., respectively. The positions of these three absorption bands are the same throughout all the spectra, but their relative intensities change.

In order to more rigorously examine the UV absorption of these lignin fractions in the longer wavelength region, spectra of the same four fractions were obtained at higher concentration. These spectra are presented in Fig. 22. Differences in the shape of the spectra in the 275 nm. region are apparent. In addition, a fourth band at about 340-350 nm. can be seen in the spectrum of Fraction 38. This band is very weak or absent in the spectra of the earlier and later fractions.

The low wavelength absorption maximum which appears at 200 nm. in all lignin fractions is the major band present in all lignin preparations (91,93). The major contribution to it arises from electronic transitions of the π-electrons of the benzene nucleus and is insensitive to the various functional group difference between the fractions. The intensity of the 200 nm. maximum is 6 to 8 times that of the 275 nm. absorption.

The spectra of all the lignin fractions contained a distinct shoulder at 220 nm. This absorption might be assignable to chromophoric groups conjugated with the benzene ring, such as α-carbonyl or α-ethylenic structures. Another type of structure which might be responsible for this absorption is muconic acid-type degradation products. α,β-Unsaturated carboxylic acids give rise to strong absorption in this region (99). The intensity of absorption and the degree of bathochromic shift of these carboxylic acids are known to be increased by alkyl substitution and by extended conjugation through ethylenic groups, as is the case in muconic acid structures.

CURVE	FRACTION NO.	CONCN., g./l.
A	7	0.1136
B	24	0.1200
C	38	0.1034
D	51-52	0.1315

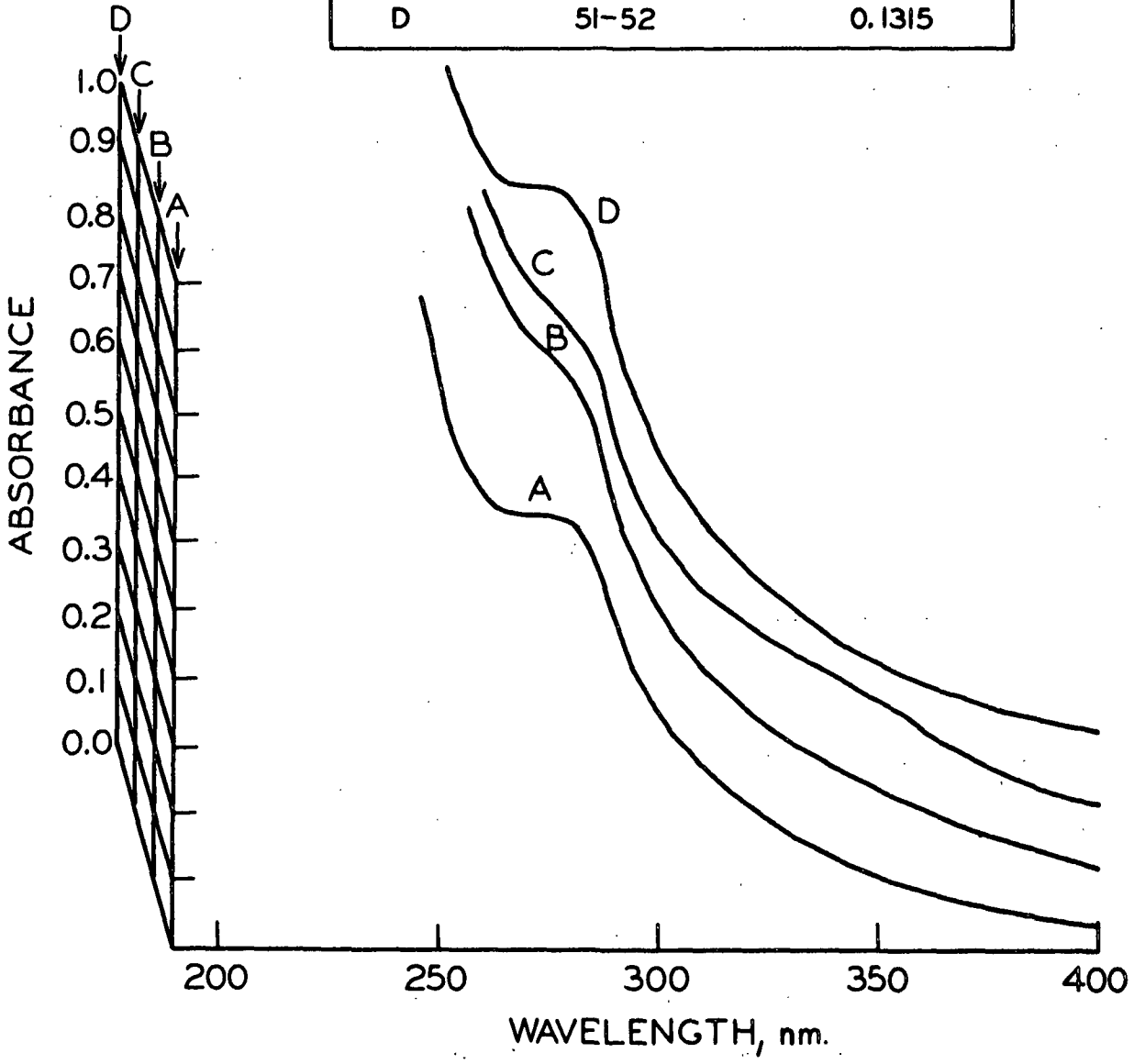

Figure 22. UV Absorption Spectra of Lignin Fractions Above 250 nm.

The intensity of absorption in the 275-285 nm. region is related to the degree of oxygen substitution upon the aromatic ring of lignin (90,91,93). Typically for softwood lignin, this band is located at 280-282 nm. (91). Demethoxylation shifts this band to shorter wavelength and decreases the intensity of absorption. The low values of absorptivity at 275 nm., discussed previously and presented in Fig. 14, suggested that substantial demethoxylation of the aromatic structure of lignin occurred during the delignification reaction, and this interpretation proved to be verified by the methoxyl contents obtained analytically (Table XV). If absorptivity in this region of the UV is calculated from the product of the average methoxyl content, 0.0013 mole OMe/g., times the molar absorptivity of lignin on a methoxyl basis, 3160 l./g. mole (22,100), a value of 4.0 is arrived at. This value is generally lower than that presented in Fig. 14. This intensified absorption at 275 nm. of lignins solubilized by peracetic acid is due to the overlapping of the stronger band at 220 nm. and appears to correlate well with the carboxyl group content of the lignin fractions (Table XV). Therefore, the assignment of absorption in the 220 nm. region to α,β-unsaturated carboxylic acids seems to be consistent with analytical data.

A fourth region of ultraviolet absorption, at 340-350 nm., can be seen in the spectrum of Fraction 38 in Fig. 22. Absorption in this region of the ultraviolet spectra of lignins has generally been assigned carbonyl groups at the carbon atom of the side chain alpha to the aromatic ring (91,95,100). At most, only very weak absorption in this region was detectable for lignin solubilized by peracetic acid. Of the fractions presented in Fig. 22, the most intense absorption in this region can be seen in the spectrum of Fraction 38. The presence of small amounts of absorption could be more readily detected in the UV difference spectra of the fractions at about Δ345 nm.

(Fig. 18). However, when the direct spectra in Fig. 22 are compared to spectra of enzymatically-liberated lignin by Pew and Conners (95), it becomes apparent that most of the alpha-carbonyl functions of the lignin have been destroyed by peracetic acid oxidation.

INFRARED ABSORPTION CHARACTERISTICS OF LIGNIN SOLUBILIZED BY PERACETIC ACID

Infrared spectroscopy has proven to be a valuable tool in the interpretation of functional group changes which occur during the chemical modification of lignin (22,23,91,101-110). It is particularly useful in the investigation of functional groups which cannot be measured analytically. A summary from the literature of infrared band assignments of lignin and carbohydrate materials is presented in Appendix XIII.

Infrared spectra of lignins isolated in the dry state may be conveniently obtained by making use of the pressed disk technique (102-105). A particular advantage of the technique is the small sample size required. The IR spectra of a number of freeze-dried lignin fractions were thus obtained, using potassium chloride pellets made up according to the procedure presented in the experimental section. Potassium chloride rather than potassium bromide was used in making up the pellets in order to decrease absorption due to moisture present. Since the pellets were made up at constant concentration, they could be used in pairs, with one pellet in the sample beam and the other in the reference beam, to directly compare any functional group differences between the fractions. Spectra obtained in this manner will be termed "differential spectra" in this discussion.

The infrared spectrum of a typical groundwood pulp as it appears in untreated wood is presented in Fig. 23 (111). Other good examples of untreated lignin spectra may be found in the work by Kolboe and Ellefsen (105). The infrared spectra of a number of representative lignin fractions obtained by the peracetic acid delignification of loblolly pine are shown in Fig. 24.

There are a number of notable differences between the spectrum of the unreacted lignin in wood and the spectra of lignins solubilized by peracetic acid. Significant intensification of the absorption in the carbonyl region, 1800-1600 $cm.^{-1}$, is most apparent in the spectra of the solubilized lignins. However, there is no longer a well-defined band at 1660 $cm.^{-1}$, present in the spectrum of unreacted wood and generally assigned to α-carbonyl structures (102,104). There is a moderate increase in absorption around 3400 $cm.^{-1}$, attributable to hydroxyl groups (102,104), and also around 2600 $cm.^{-1}$, attributable to hydrogen-bonded hydroxyl absorption of carboxyl groups (8). Aromaticity in lignin is best indicated by a band at 1515 $cm.^{-1}$. This band is present in the spectra of the solubilized lignins but relative to background absorption, it is less distinct than in the spectrum of unreacted wood. The significant demethoxylation of lignin by peracetic acid was verified by the decreased absorption in regions characteristic of methoxyl groups in unreacted wood, i.e., at 1465, 1430, and 1270 $cm.^{-1}$. In addition, there is decreased differentiation in the spectra of solubilized lignins of the band at 1220 $cm.^{-1}$ which is assignable to phenolic hydroxyl groups. This also is in agreement with analytical data presented previously. Finally, general absorption in the 1300-1100 $cm.^{-1}$ region is much stronger for the solubilized lignins than for untreated wood lignin (105). Farrand's model compound studies (8) suggest that the C-O stretching vibrations of lactone ring structures would be responsible for this general absorption. In addition,

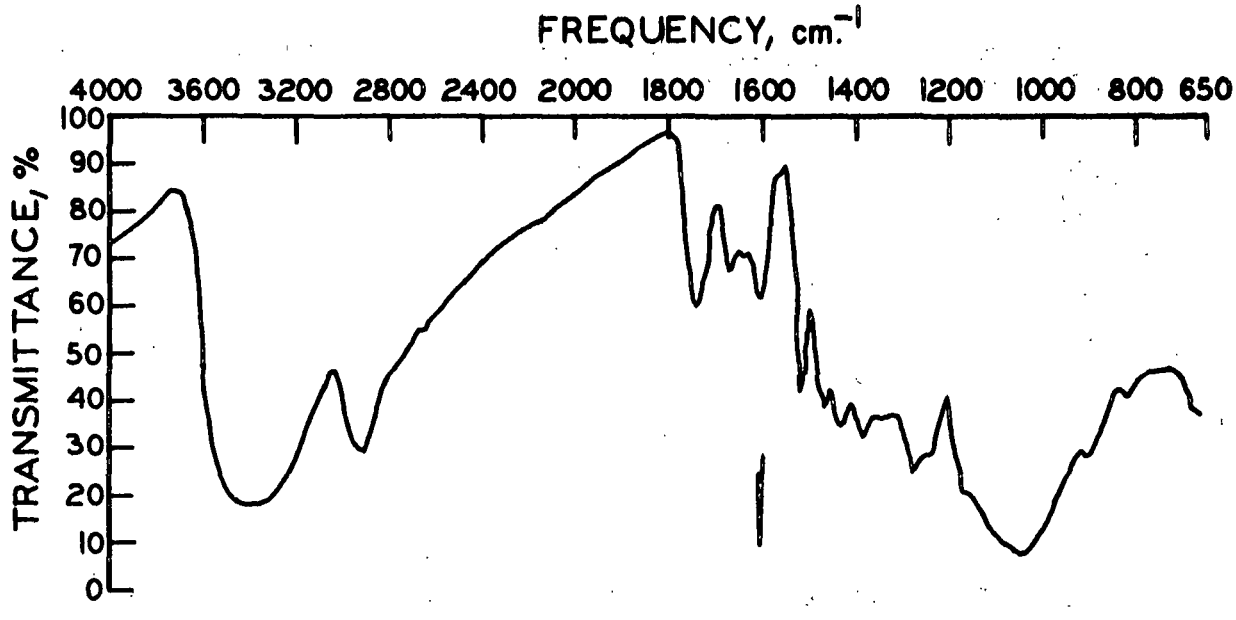

Figure 23. IR Spectrum of Groundwood Pulp from a Softwood Species (111)

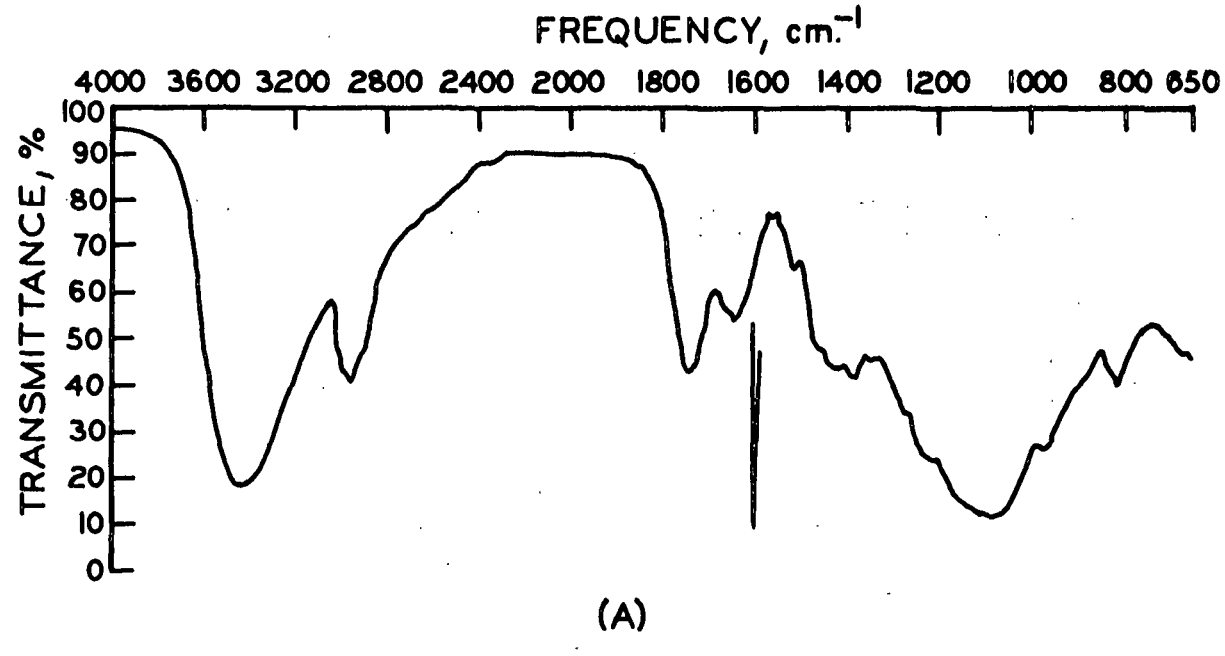

Figure 24. IR Spectra of Lignin Solubilized by Peracetic Acid: (A) Fraction 1-2

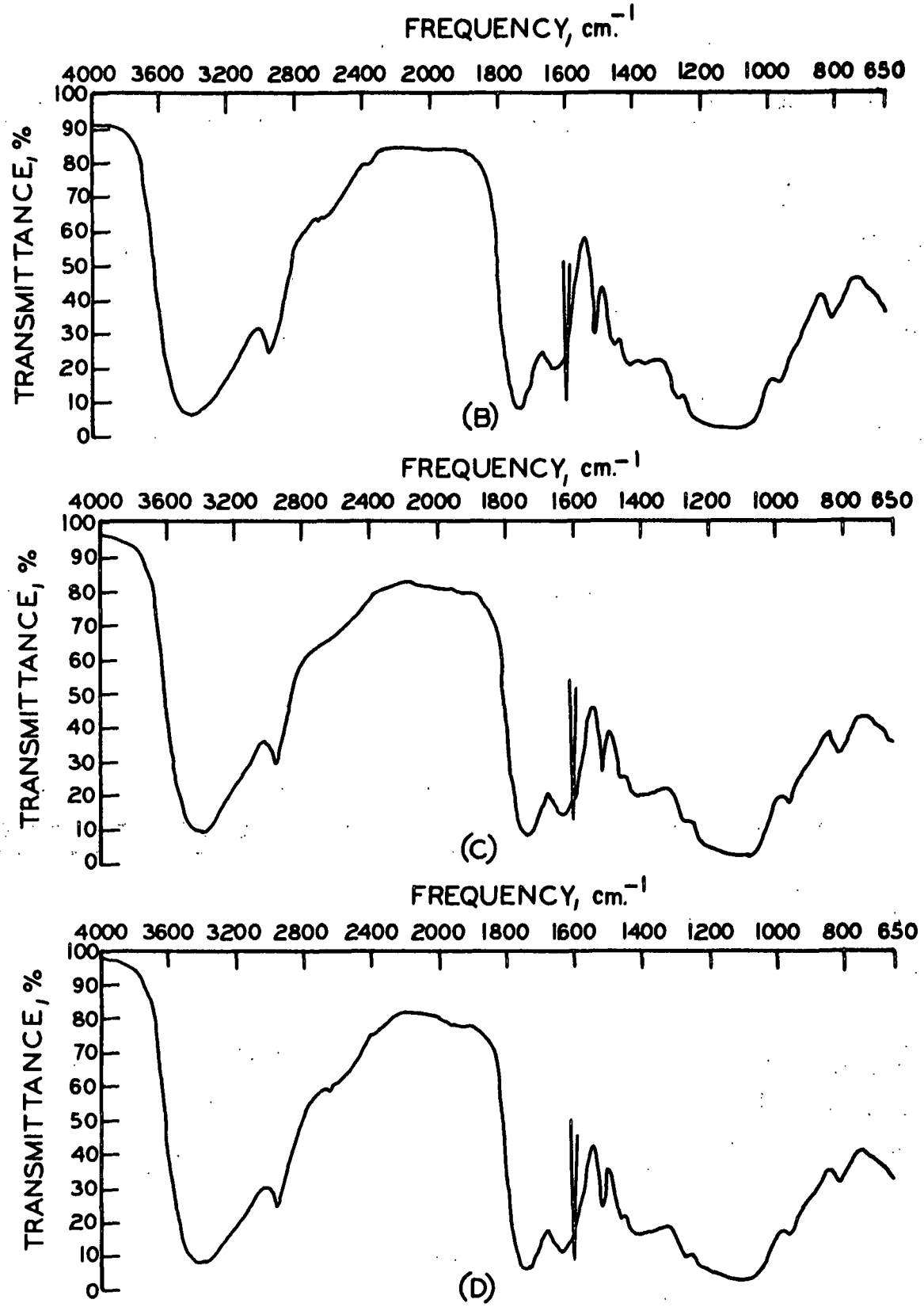

Figure 24 (Cont'd). IR Spectra of Lignin Solubilized by Peracetic Acid: (B) Fraction 11, (C) Fraction 25, (D) Fraction 40

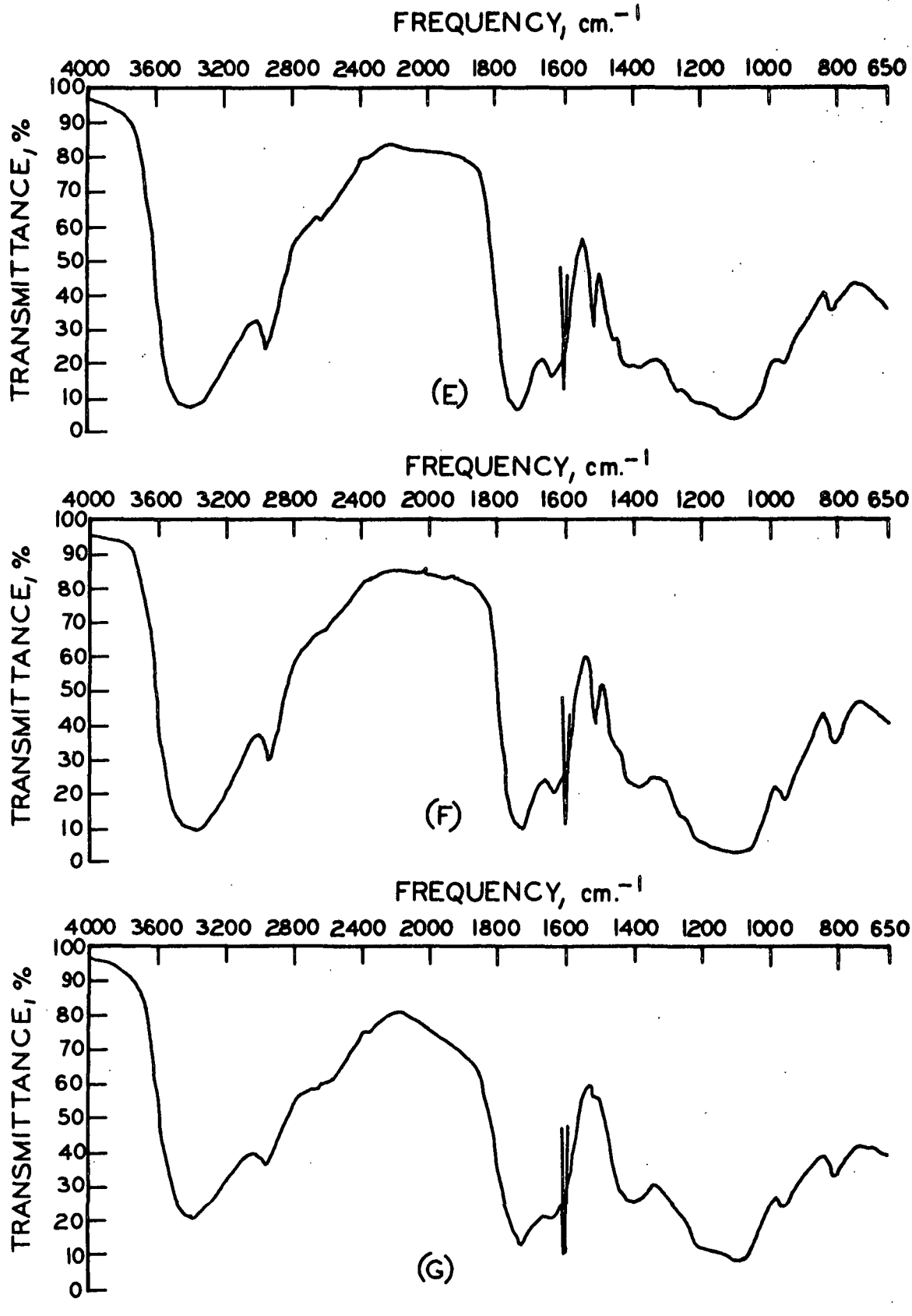

Figure 24 (Cont'd). IR Spectra of Lignin Solubilized by Peracetic Acid: (E) Fraction 48, (F) Fraction 55-56, (G) Fraction 63-64

absorption near 1640 cm.$^{-1}$ may be assigned in part to carbon-carbon double-bond stretching of these lactones (8).

A distinct band appears at 1513-1511 cm.$^{-1}$ in the spectra of all the lignin fractions in Fig. 24. This band is characteristic of the C=C symmetrical stretching vibration of the benzene nuclei of lignin and has been shown to be a reliable measure of bulk lignin content (108). It therefore appears to be a suitable reference peak for the estimation of the relative aromaticity of the lignin fractions and the consideration of destruction of this aromaticity during peracetic acid delignification.

As discussed in the literature review, the principal functional group produced by peracetic acid oxidation of lignin is the carboxyl group. The abundance of this group in the fractionated lignin in this study has been shown to vary between about 0.3 and 0.6 equivalent per C_9 unit. Of the various differences between the spectra of solubilized lignin in Fig. 24 and the spectrum of untreated softwood lignin in Fig. 23, the much stronger absorption in the carbonyl region, 1800-1600 cm.$^{-1}$, would appear to reflect best this oxidation by peracetic acid.

One major peak dominates the carbonyl region in all the IR spectra in Fig. 24. With the exception of Fraction 63-64 where the peak is located at 1725 cm.$^{-1}$, this carbonyl band is found within a rather narrow range, 1740-1735 cm.$^{-1}$, for all the fractions. However, when spectra were obtained of the fractions freeze-dried out of alkaline solution (pH >11), it became apparent that this absorption is actually the result of two individual peaks very closely spaced. Half or more of the peak shifted to the 1600-1580 cm.$^{-1}$ region, as shown in Fig. 25. This behavior is typical of the shift which the carboxylic acid group undergoes when converted to the ionized form, and

therefore this band can be confidently assigned to the carbonyl groups of carboxylic acid structures. In addition, a very strong band can be seen in the 1410-1400 cm.$^{-1}$ region of Fig. 25 which is not present in the spectra in Fig. 24. This band can be identified as the symmetric stretching vibration of the carboxylate anion (112). In the basic spectrum of Fraction 44 it is only slightly weaker than the asymmetric vibration of 1590 cm.$^{-1}$.

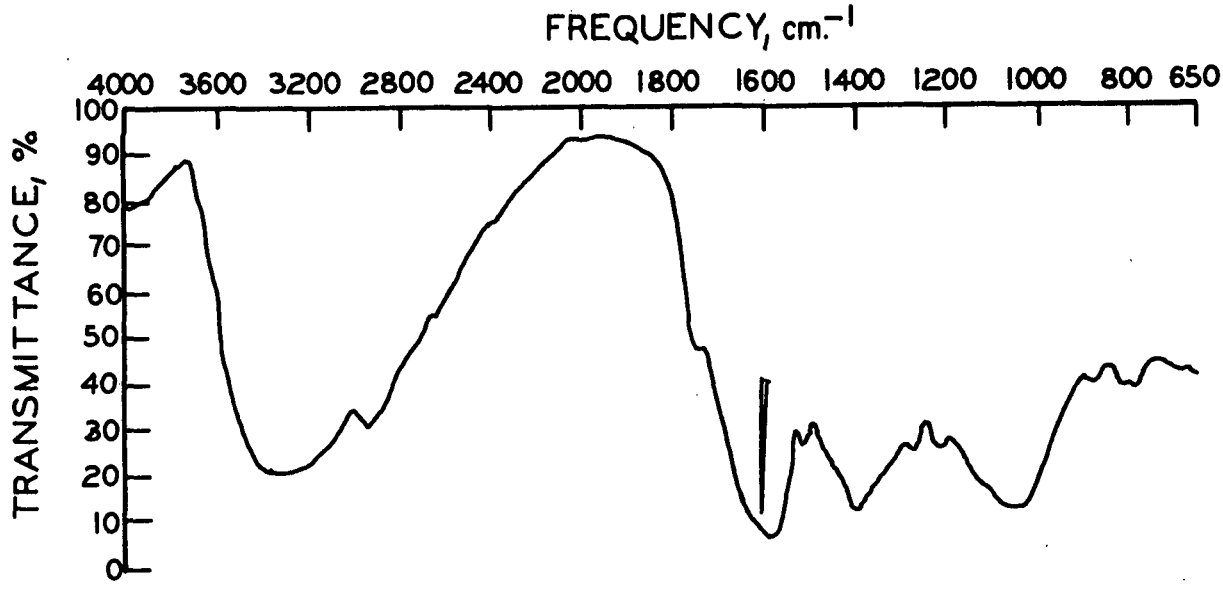

Figure 25. IR Spectra of Lignin Fraction 44 Obtained at pH >11

Further identification of the double peak at 1740-1735 cm.$^{-1}$ can be found by comparison to IR frequencies observed in peracetic acid model compound studies by Farrand (Table XVI). The monomers of saturated aliphatic acids absorb near 1760 cm.$^{-1}$ (112), and in Farrand's studies, the carboxyl group of the free acid in the γ-alkyl-γ-lactones (XV,XVI) absorbed at 1775-1770 cm.$^{-1}$. Several factors can result in shifts of this absorption to lower frequency (111) – that is, to the 1740-1735 cm.$^{-1}$ region observed for lignin solubilized by peracetic acid. Remote unsaturation decreases the frequency slightly, but the effect is greater for α,β-unsaturation. Internal hydrogen bonding reduces the frequency of the carbonyl

stretching absorption to a greater degree than does intermolecular hydrogen bonding. From Farrand's studies, the carbonyl stretching frequency for β-alkyl-muconic acids (XIII) and the free acid in β-alkyl-γ-lactones (XIV) would be expected to be 1688-1687 cm.$^{-1}$ ..

TABLE XVI

CARBONYL AND HYDROXYL IR FREQUENCIES OF LIGNIN OXIDATION PRODUCTS SUGGESTED FROM MODEL COMPOUND STUDIES (8)

Structure	Type of Carbonyl			H-Bonded Carboxylic Acid OH
	COOH	Lactone	Cyclic Ketone	
β-alkyl-muconic acids (XVIII)	1688 (vs) H-bonded	--	--	2680 (m) 2590 (m)
β-alkyl-γ-lactones (XIV)	1687 (vs) H-bonded	1730 (vs)	--	2580 (broad)
γ-alkyl-γ-lactones (XV)	1775 (vs)	1740 (vs)	--	--
γ-hydroxy-γ-lactones (XVI)	--	1740 (s)	--	--
4-hydroxy-4-alkyl-2,5-cyclohexadienone	--	--	1660 (s)	--

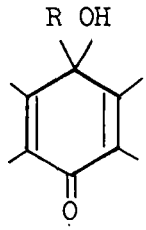

Approximately one-third of the 1740-1735 cm.$^{-1}$ peak was unaffected by base. Model compound studies by Farrand (8) showed that absorption in this area can be attributed to the carbonyl group of lactone structures (XIV,XV,XVI). Room temperature titration with alkali would not be expected to open these ring structures. However, determination of the saponification equivalent by hot alkali hydrolysis (14) did result in the ring opening. Normally, γ-lactones

absorb in the 1760-1795 cm.$^{-1}$ region (111). Unsaturation alpha to the carbonyl group reduces the frequency of the absorption band, as in the structures isolated by Farrand, where lactone absorption may be identified consistently with absorption in the 1740-1730 cm.$^{-1}$ region (Table XVI).

In general, the intensity pattern of the 1740-1735 cm.$^{-1}$ peak in the spectra in Fig. 24 parallels the carboxyl contents of the lignin fractions (Table XV), with maximum response at Fraction 40. Considering what has just been discussed about the reactions of peracetic acid with model compounds, it seems that this peak should serve as a suitable reference peak for comparison of the degree of oxidation of the lignin fractions. Comparison of the spectra in Fig. 24 with respect to two internal reference peaks, that at 1513-1511 cm.$^{-1}$ denoting aromaticity and that at 1740-1735 cm.$^{-1}$ representing oxidation, is expected to serve as a suitable basis for comparing further the similarities and differences in chemical structure between the fractions.

It can be readily seen that there are structural differences between the lignin in Fraction 1-2 and in Fraction 11 (Fig. 24). Both the 1740 cm.$^{-1}$ and the 1513 cm.$^{-1}$ bands increased substantially in intensity with increased fraction number. Spectra of Fractions 11 and 16 were virtually superimposable. In going from Fraction 16 to Fraction 25, there was a small increase in the intensity of the 1740 cm.$^{-1}$ band relative to the 1513 cm.$^{-1}$ band. This increase can be more readily seen in the differential spectra of these fractions presented in Fig. 26. The spectra of Fractions 25, 32, and 40 were nearly identical, suggesting that lignin fractions in this range were chemically very similar. The next evidence for change in the structure occurred between Fractions 40 and 48. There was a slight decrease in aromatic absorption

relative to carbonyl absorption between these fractions. This trend continued in later fractions. By Fraction 55-56 there was a very small decrease in intensity of the 1740 cm.$^{-1}$ peak but a much more apparent decrease in the 1513 cm.$^{-1}$ band. The change between Fractions 55-56 and 63-64 was even more apparent. Carbonyl absorption decreased moderately, and the absorption most characteristic of aromatic structures in lignin almost disappeared completely.

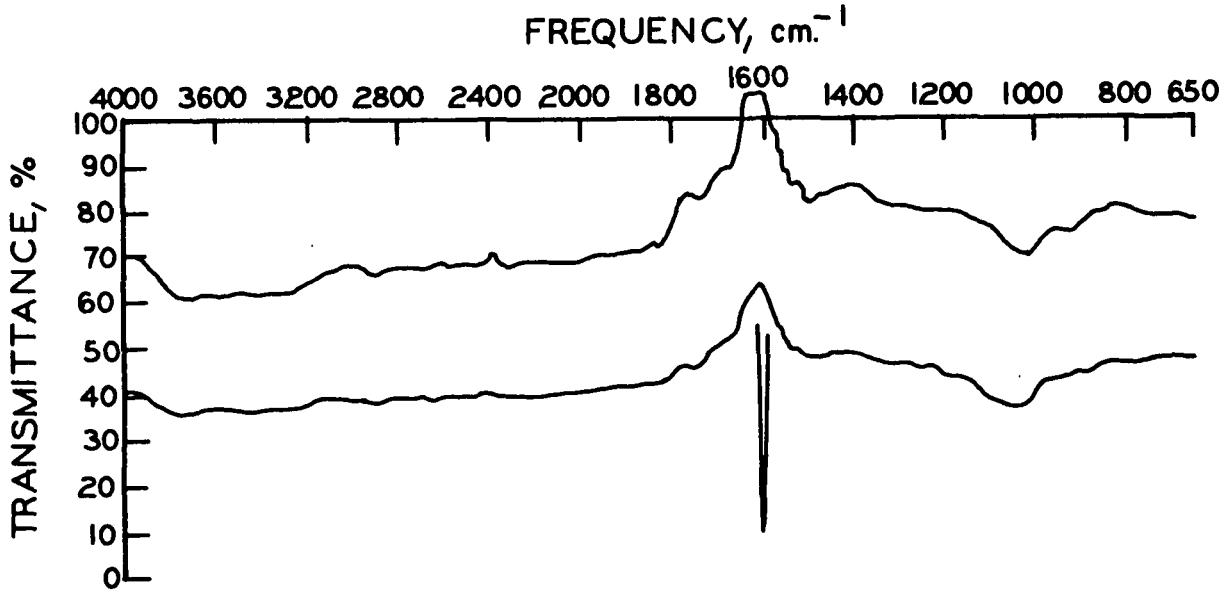

Figure 26. Differential IR Spectra: Sample = Fraction 16, Reference = Fraction 25

Thus, examination of the lignin fractions with respect to changes in aromaticity and the degree of oxidation has verified evidence presented previously which indicated that the lignin fractions were not chemically uniform over the entire range between $\underline{V}_o$ and $\underline{V}_t$. However, infrared evidence does suggest that there are certain ranges of fractions which are very nearly identical in chemical structure, and therefore the molecules eluting in these fractions apparently behaved on the GPC column as polymers which differed in molecular weight only. The first of these groups of fractions

extends between at least Fractions 11 and 16, and the second ranges between at least Fractions 25 and 40. There are definitely chemical differences between these groups of fractions, however, and these differences can explain the breaks observed in the molecular weight data.

In Fig. 27, a comparison is made between the molecular weight data and the carboxyl and phenolic hydroxyl data as a function of fraction number between $\underline{V}_o$ and $\underline{V}_t$. Number-average molecular weights were previously reported in Table XII and Fig. 16, and carboxyl and phenolic hydroxyl contents were presented in Table XV. The relationship between molecular weight and fraction number can now be better understood in terms of the changing chemical structure of the solubilized lignin fractions.

One region of chemically uniform lignin has been shown by IR spectroscopy to range over at least Fractions 11 through 16. A second region of chemically uniform lignin, more highly oxidized than lignin in the earlier fractions, was found to extend over at least Fractions 25 through 40. These observations can be seen to be compatible with the data presented in Fig. 27. Number-average molecular weight decreased between Fractions 8 and 21 as expected from the principles of gel permeation chromatography. Lignin which eluted within this range of fractions may be characterized as having a carboxyl content of about 0.20 meq./100 mg. and a phenolic hydroxyl content of about 0.03 meq./100 mg.

Number-average molecular weight increased sharply between Fractions 21 and 22. Then, over the range between Fractions 22 and about 48, the molecular weight again decreased in a manner compatible with that expected for molecular size fractionation of a structurally uniform polymer. Accordingly, the porous sphere model for a cross-linked polymer in solution was applied over this range of fractions, as discussed previously. Lignin which eluted within this range of

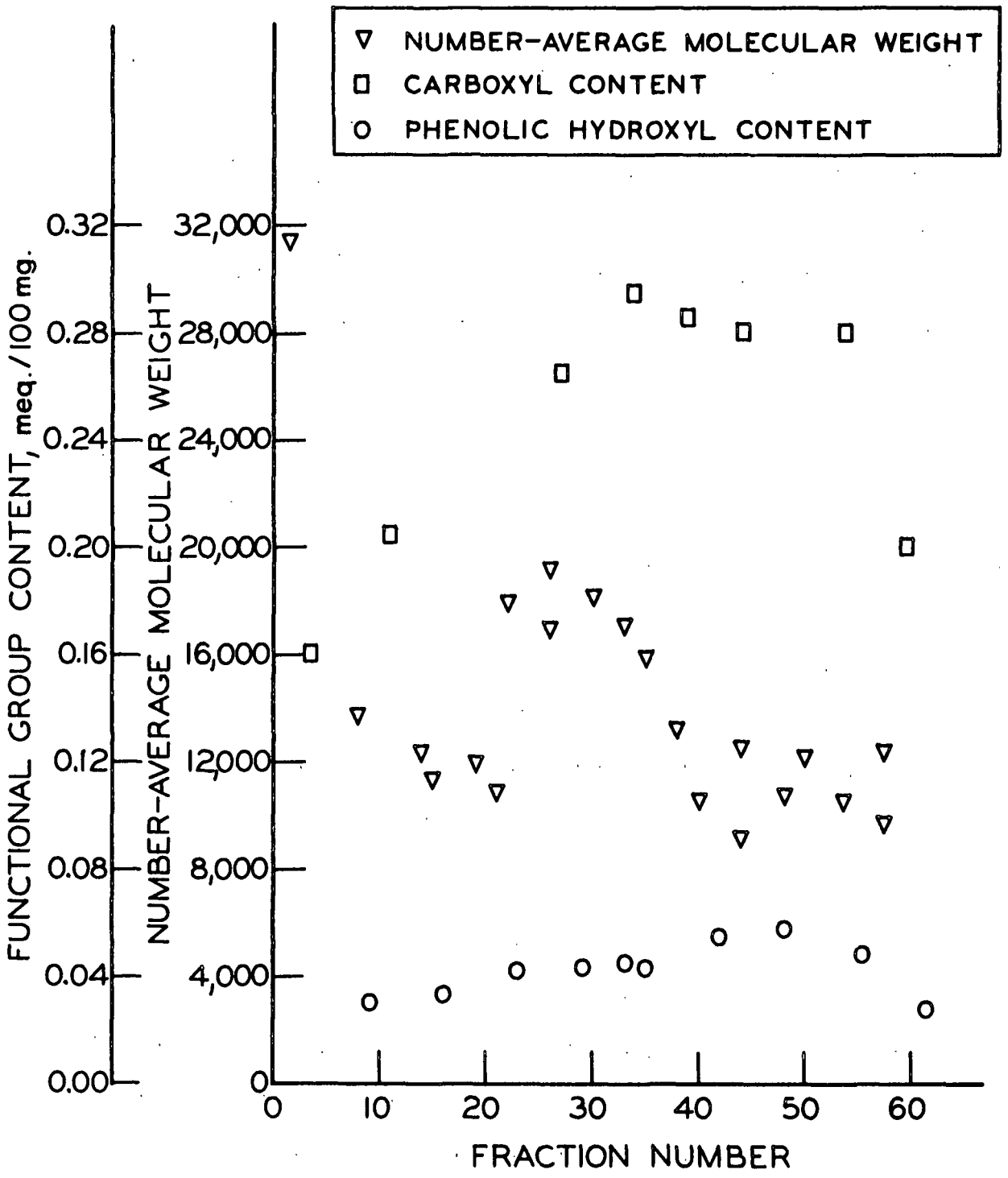

Figure 27. Comparison of Number-Average Molecular Weight, Carboxyl Content, and Phenolic Hydroxyl Content of Lignin Fractions Between V_o and V_t

fractions had a carboxyl content of about 0.28 meq./100 mg. and a phenolic hydroxyl content of about 0.04 meq./100 mg. IR spectra suggested that near the end of this region, changes in structure of the polymer were again becoming evident. This trend became more pronounced in the later fractions prior to V_t and is also reflected in the data presented in Fig. 27. The phenolic hydroxyl content of the lignin began to vary to a significant extent beyond Fraction 40, and in the same region the molecular weight became a steady function. The carboxyl content of the lignin decreased significantly beyond Fraction 54.

CARBOHYDRATE ANALYSES OF THE SOLUBILIZED REACTION PRODUCTS

Carbohydrate Materials Present in the Lignin Fractions

Approximately seven percent of the total solubilized reaction products upon peracetic acid delignification of loblolly pine springwood to 80% yield has been shown to be unoxidized carbohydrate materials. Broad infrared absorption in the 1350-1200 $cm.^{-1}$ region of the infrared spectra may be due in part to carbohydrates present in the fractions (103). Norrstrom and Teder (97) observed that a small percentage of carbohydrate was inseparable from lignosulfonates by GPC fractionation. If carbohydrate materials were present in all the lignin fractions, these would be expected to have a significant influence on the physical-chemical data collected for the lignin fractions. Therefore, analysis of a number of freeze-dried lignins for individual sugars present was undertaken, using the same procedure reported for previous determinations (78).

The results of the carbohydrate analyses are presented as percent by weight of total solid material in each fraction in Table XVII. At these low carbohydrate contents, the accuracy is $\pm$0.2% of the total material. Total carbohydrate was calculated by summing the individual determinations, and uncertainty of the total is thus $\pm$1.2%. There seems to be a systematic error in this determination

between those fractions analyzed in the first set, marked *, and those fractions analyzed at a later date.

TABLE XVII

POLYSACCHARIDE CONTENT (AS SUGAR UNITS) OF FRACTIONATED LIGNIN AS PERCENT OF TOTAL MATERIAL IN FRACTION[a]

Fraction Number	Rhamnose	Xylose	Arabinose	Galactose	Glucose	Mannose	Total, %
* 3-4	0.5	0.9	2.0	3.0	2.2	0.8	9.4
10	0.1	0.8	1.3	1.7	5.5	2.4	12.2
* 12	0.1	1.4	1.4	1.5	0.6	2.1	7.1
13	0.03	0.8	0.9	0.6	0.4	1.8	4.53
* 18	0.03	0.8	0.1	0.9	0.6	2.2	5.63
23	--	0.4	0.8	0.6	0.4	1.8	4.0
* 31	--	0.6	1.1	0.7	1.0	2.5	5.9
40	--	0.3	1.2	0.4	0.2	1.9	4.0
* 48	--	0.5	2.6	0.8	0.7	3.2	7.8
* 57-58	--	0.2	1.8	1.4	1.6	5.4	10.4
63-64	--	0.2	1.5	0.7	0.3	2.3	5.0

[a] All values represent single determinations.

It is apparent that some carbohydrate material is present in all the lignin fractions below V_{-t}. This carbohydrate material might be bound to the lignin present as a lignin-carbohydrate complex or it might be present as free hemicelluloses. Total carbohydrate present was near 10% for the earliest fractions, decreasing to a rather moderate plateau of approximately 5% for fractions between about 13 and 45. Then total carbohydrate rose to 7-10% for the remaining fractions eluting below V_{-t}. This decreasing, then increasing, total carbohydrate content would be expected to be reflected in the physical-chemical data and in the quantitative infrared spectra presented earlier. The intrinsic viscosity of hemicellulosic materials is typically 5-10 times that of lignins [see, for example, Ref. (50)]. The presence of higher concentrations of carbohydrate in the fractions

eluting from the column just after $\underline{V_o}$ (1-10) and just prior to $\underline{V_t}$ (49-62) would therefore result in unexpectedly high intrinsic viscosities for these fractions, as was observed. Thus, the successful application of Seely's porous sphere model (56) to $[\eta]$-$\underline{\bar{M}_n}$ data collected over Fractions 22 through 48 appear to be largely due to the fact that total carbohydrate present was relatively stable.

The relative percentage of the various sugars is presented in Table XVIII. The most notable trend in these figures is the rise in relative mannan content from less than 10% in the earliest fractions to nearly 50% of the total carbohydrate present in the later fractions.

TABLE XVIII

POLYSACCHARIDE CONTENT (AS SUGAR UNITS) OF FRACTIONATED LIGNIN AS RELATIVE PERCENT OF TOTAL CARBOHYDRATE IN FRACTION

Fraction Number	Rhamnose	Xylose	Arabinose	Galactose	Glucose	Mannose	Relative Basis Total, %
* 3-4	5.3	9.6	21.3	31.9	23.4	8.5	100.0
10	0.8	9.9	10.6	13.9	45.1	19.7	100.0
* 12	1.4	19.7	19.7	21.1	8.5	29.6	100.0
13	0.7	17.6	19.9	13.3	8.8	39.7	100.0
* 18	0.5	14.2	19.5	16.0	10.7	39.1	100.0
23	0.0	10.0	20.0	15.0	10.0	45.0	100.0
* 31	0.0	10.2	18.6	11.9	16.9	42.4	100.0
40	0.0	7.5	30.0	10.0	5.0	47.5	100.0
* 48	0.0	6.4	33.3	10.3	9.0	41.0	100.0
* 57-58	0.0	1.9	17.3	13.5	15.4	51.9	100.0
63-64	0.0	4.0	30.0	14.0	6.0	46.0	100.0

Lignin and Carbohydrate Materials Solubilized Upon Stagewise Delignification

The chemical characterization of the fractionated lignin polymer which has been discussed in the preceding pages was based on fractions of a composite product liquor obtained upon delignification to 80% yield. It has been assumed that the fractions obtained were made up of narrow molecular weight

distribution polymers which did not vary greatly in chemical structure within each fraction. In addition, it has been shown that there was approximately 5-10% carbohydrate material universally present in the fractions between $\underline{V}_o$ and $\underline{V}_t$. However, it has not been shown whether or not, for a given fraction number, the chemical composition of the lignin and/or the carbohydrate materials present are independent of yield. In order to determine if both the chemical composition of the lignin and the amount of carbohydrate present in a given fraction is independent of the reaction stage at which the reaction products became soluble, the lignin and carbohydrate portions of the reaction products have been investigated independently as a function of reaction stage. The procedures used to study the lignin and carbohydrate materials solubilized upon stagewise delignification are presented in the experimental section (p. 125).

The evidence for a lignin-carbohydrate linkage in wood has been reviewed earlier. The presence of 5 to 10% unoxidized carbohydrate in all lignin fractions brings up the question as to whether these carbohydrates are chemically bonded to the lignin or merely present as a physical mixture. It has been shown that the fractions could be freeze-dried and then redissolved in water to obtain viscosity data consistent with that obtained for never-dried fractions. This observation tends to suggest that the lignin and carbohydrate materials are chemically bonded. The question of a possible lignin-carbohydrate linkage in the solubilized reaction products provides a second reason for investigating the lignin and carbohydrate material within a fraction at different yields. If it is found that the carbohydrate content of a given fraction, both as total percent present and as relative abundance of the various sugars, is independent of the reaction stage, this will provide strong circumstantial evidence for an actual link between the lignin and carbohydrate materials. Since delignification was accomplished under relatively mild conditions, any lignin-carbohydrate linkage found in the solubilized reaction products can be assumed to have been present in the wood itself.

Ultraviolet absorption spectra have been shown to be sensitive to the degree of oxidation of the lignin portion of the solubilized reaction products. Direct UV spectra were therefore obtained as discussed in the experimental section in order to determine if the lignin eluting at a given fraction number was independent of the reaction stage at which it was extracted from the wafers. This was found to be the case. Therefore, ultraviolet evidence indicated that the chemical structure of the lignin portion of the solubilized reaction products exiting the GPC column at a given elution volume was not dependent upon the extent of delignification.

A gross measure of the total carbohydrate material in a lignin fraction can be had by measuring the total optical rotation of the fraction. With the differing amounts of sugars present, the direction and degree of rotation might be expected to change to some extent with fraction number. Within a fraction, if carbohydrate content is independent of the reaction stage, the direction of rotation would be expected to be the same for early, mid, and late reaction stages. The degree of rotation would then be proportional to the concentration, within experimental limits.

Optical rotation was examined as a function of fraction number and reaction stage, as discussed in the experimental section. The results are presented in Table XIX. The optical rotation is expressed simply as the observed rotation (corrected for solvent) in a two-decimeter polarimeter tube divided by the concentration in mg./ml. The 95% confidence limits apply only to the precision in reading the optical rotation of the solutions.

TABLE XIX

OPTICAL ROTATION OF GROUPS OF LIGNIN FRACTIONS

Fractions	Reaction Stage	Concentration, mg./ml.		Optical Rotation at 546 nm., (°/2 dm.mg./ml.)
4-8	2,3 (early)	2.09		+0.026 ± 0.006
	4,5 (middle)	2.89		+0.036 ± 0.007
	6,7 (late)	2.46		+0.019 ± 0.007
			Mean	+0.027 ± 0.004
19-23	2,3 (early)	2.22		-0.035 ± 0.006
	4,5 (middle)	2.88		-0.033 ± 0.006
	6,7 (late)	3.76		-0.031 ± 0.006
			Mean	-0.033 ± 0.004
28-32	2,3 (early)	3.07		-0.042 ± 0.005
	4,5 (middle)	4.16		-0.033 ± 0.007
	6,7 (late)	4.54		-0.029 ± 0.006
			Mean	-0.035 ± 0.004
38-42	2,3 (early)	4.48		-0.037 ± 0.003
	4,5 (middle)	5.00		-0.035 ± 0.003
	6,7 (late)	4.70		-0.030 ± 0.004
			Mean	-0.034 ± 0.002
52-56	2,3 (early)	3.97		-0.042 ± 0.005
	4,5 (middle)	5.89		-0.038 ± 0.003
	6,7 (late)	3.81		-0.046 ± 0.005
			Mean	-0.042 ± 0.003

The mean specific rotation of Fractions 4-8 was positive and differed from the other groups of fractions to a very high degree of significance. The mean specific rotation of Fractions 19-23, 28-32, and 38-42 were not significantly different. This is in general agreement with results presented earlier (Tables XVII and XVIII) which showed that the carbohydrate composition of these fractions was quite stable. The mean specific rotation of Fractions 52-56 was significantly more negative than the other groups of fractions. The increasingly negative specific rotation with increasing fraction number reflects the increasing mannan content. Most of the mannose found in wood is present as relatively low molecular-weight glucomannan (113). Since the linkage is known to be β-1-4, and the

specific rotation of β-D-mannose is negative (-17.0°), these results are reasonable.

In four out of five groups of fractions, there appeared to be a trend toward lower magnitudes of optical rotation in the later reaction stages. However, this variation in specific rotation was not quite statistically significant at the 95% confidence level. Polarimetry results are thus inconclusive with respect to the question of whether the carbohydrate content of the fractions varies as a function of incremental delignification.

A more rigorous investigation of the carbohydrate content of lignin samples requires that they be analyzed quantitatively for the various sugars present. Therefore, carbohydrate content was measured as a function of fraction number and reaction stage, as discussed in the experimental section.

The results of the carbohydrate analyses are presented in Tables XX and XXI. In general, the carbohydrate content of the fractions increased as delignification proceeded. The carbohydrate analyses of the lignin fractions, presented in Tables XVII and XVIII, were thus an expression of average carbohydrate solubilized as reaction proceeded, and a certain amount of correspondence may be seen between those data and the averages of the data presented in Tables XX and XXI.

Now considering the change in carbohydrate composition in terms of individual sugars present, it can be seen that for all three groups of fractions, the xylan, galactan, glucan, and mannan contents of the freeze-dried lignins increased significantly as reaction proceeded. However, the araban associated with each of the groups of lignin fractions remained constant through these yields. Thus, circumstantial evidence for the chemical linkage of lignin with all carbohydrates present in the fractions has not been found. Xylan, glucan, mannan, and some

TABLE XX

PERCENT OF POLYSACCHARIDES CALCULATED AS SUGAR UNITS[a]
IN SOLUBILIZED PRODUCTS UPON STAGEWISE DELIGNIFICATION

Fraction Number	Reaction Stage	Rhamnose	Xylose	Arabinose	Galactose	Glucose	Mannose	Total, %
9-13	2,3	0.08	0.1	1.0	0.7	0.06	0.5	2.44
	4,5	0.04	0.6	1.3	0.4	0.04	1.3	3.68
	6,7	0.04	2.4	1.3	1.8	0.8	3.7	10.04
33-37	2,3	--	0.02	1.7	0.05	--	0.5	2.27
	4,5	--	0.5	1.5	0.7	0.4	2.1	5.20
	6,7	--	1.4	1.0	1.4	1.2	4.7	9.70
47-51	2,3	--	0.2	2.6	0.6	0.2	1.4	5.00
	4,5	--	0.5	2.5	1.2	1.0	3.6	8.80
	6,7	0.08	1.2	2.1	2.0	2.1	7.9	15.38

[a] All values represent single determinations. However, unlike the values presented in Table XVII, all these determinations were made in a single batch of analyses.

TABLE XXI

RELATIVE PERCENT OF POLYSACCHARIDES CALCULATED AS SUGAR UNITS
IN SOLUBILIZED PRODUCTS UPON STAGEWISE DELIGNIFICATION

Fraction Number	Reaction Stage	Rhamnose	Xylose	Arabinose	Galactose	Glucose	Mannose	Relative Basis Total, %
9-13	2,3	3.2	4.1	40.1	28.7	2.4	20.5	100.0
	4,5	1.1	16.3	35.3	10.9	1.1	35.3	100.0
	6,7	0.4	23.9	13.0	17.9	8.0	36.8	100.0
33-37	2,3	--	0.9	74.9	2.2	--	22.0	100.0
	4,5	--	9.6	28.8	13.5	7.7	40.4	100.0
	6,7	--	14.4	10.3	14.4	12.4	48.5	100.0
47-51	2,3	--	4.0	52.0	12.0	4.0	28.0	100.0
	4,5	--	5.7	28.4	13.6	11.4	40.9	100.0
	6,7	0.5	7.8	13.7	13.0	13.7	51.3	100.0

galactan in the fractions may be present as free hemicelluloses of varying molecular weight. The amounts of these sugars solubilized increased as delignification proceeded. However, circumstantial evidence for the existence of a lignin carbohydrate bond has been found, where the carbohydrate involved is araban and possibly galactan. The preferred retention of glucan, mannan, and xylan as compared to galactan and araban in peracetic acid holocelluloses prepared from loblolly pinewood has been reported previously by Leopold (3) and is summarized in the literature review (Table IV). The same observation can be made by reviewing the data presented in Tables VIII and IX. The relative abundance of araban and galactan in unreacted springwood wafers was found to be 2.4 and 4.2%, respectively, of the total carbohydrate. However, in the composite springwood product liquor, 30.4% of the carbohydrate present was arabinose, and 15.3% was galactose.

This brief study has not offered clear evidence for a lignin-carbohydrate bond in wood which can be removed intact by mild delignification. Yet, certain observations have suggested that this, in fact, is the case. First, the presence of a small percentage of carbohydrate was found in all fractions, at all yield levels. Second, intrinsic viscosity data could be reproduced after drying and redissolving the fractions. Third, one particular sugar, arabinose, was present in a given fraction at a constant amount, whether solubilized early or late in the delignification reaction. And finally, no apparent solubility separation of the freeze-dried fractions could be achieved. The fractions could be redissolved in water or dioxane to about 1% concentration. However, none of the freeze-dried material appeared to be soluble in less polar solvents, such as ether, ethyl alcohol, or acetone.

THE PHYSICAL-CHEMICAL MECHANISM OF SELECTIVE DELIGNIFICATION OF WOOD BY PERACETIC ACID

PHYSICAL ASPECTS OF THE DELIGNIFICATION REACTION

When loblolly pine springwood wafers were delignified by aqueous peracetic acid treatment, two effects were observed. First, a substantial increase in the porosity of the cell walls occurred. Secondly, the molecular size distribution of the solubilized lignin fragments shifted in favor of larger molecules as delignification proceeded to lower yield. An approximate correspondence has been noted between the median pore size at a given yield and the average molecular diameter of the lignin solubilized at that same yield level. Pore size refers to the minimum dimension of a void in the cell wall, but it does not specify any overall shape to the pore. It has been concluded from these observations that pore size serves as at least a contributing factor in determining the size distribution of the solubilized reaction products. The influence of a physical factor would also explain why the rate of lignin extraction from the wood deviated from that predicted by apparent first-order kinetics.

In attempting to understand how pore size change serves as a restricting factor during delignification, and thereby in part controls the transport of macromolecules out of the wood wafer, two concepts of pore development need to be envisioned. In the simplest model, pore development can be envisioned as a mere simultaneous displacement of a solubilized lignin fragment by water, leaving a pore of equal size to the original encrusted lignin. This simple view may well occur for lignin fragments having direct access to the lumen. However, Stone and Scallan (67), Feist and Tarkow (72), and Lapinoja (114) all showed that the cell wall actually swells during delignification and, therefore, lignin is not simply displaced by water of equal volume.

The second concept of pore development during pulping arises when one considers the fate of a large lignin fragment, no longer chemically bonded to the rest of the material in the wood wafer. If this lignin fragment does not have direct access to the lumen, it must diffuse through the cell wall of the fiber until it encounters the lumen, or some other site of free passage out of the wafer. If, however, this diffusion cannot occur because all the pores through which the fragment has access to the lumen is too small to allow passage of the fragment, the large lignin fragment will not reach the lumen and be transported out of the wafer. Then, if this trapped fragment is to be released from the wafer, the restricting pore dimension must first be enlarged by either further chemical delignification or swelling of the cell wall.

Lignin staining reactions, particularly that with phloroglucinol, showed that all the lignin, both that in the cell wall and that in the middle lamella, was accessible to peracetic acid under the conditions employed. Lignin in the middle lamella would be expected to become soluble quite readily if fracture of the wafer between cell walls occurred. However, this did not appear to occur to a significant extent, as the wafers were still intact, although softened, at 77.0% yield. Therefore, for the most part, lignin in the middle lamella would have to diffuse through pores in the cell wall in order to reach the lumen and be released into solution. The observation, made at intermediate yields, that lignin appeared to be preferentially solubilized from the cell wall is compatible with a pore size restriction mechanism. Lignin originally present in the middle lamella must diffuse all the way through the cell wall before reaching the lumen, and therefore the probability of encountering a narrow pore constriction is greater than for lignin originally present in the cell wall.

SOLUBILITY ASPECTS OF THE DELIGNIFICATION REACTION

The lignin solubilized by peracetic acid delignification of wood has been characterized by infrared and ultraviolet spectroscopy and by quantitative measurement of various functional groups present. The results of these analyses have indicated that many chemical similarities can be found which apply to all the solubilized lignin. Although some of the functional group contents were not constant for all fractions between $\underline{V}_o$ and $\underline{V}_t$, the same groups were found to always be present. Basically, peracetic acid delignification of a softwood species resulted in significant demethoxylation, destruction of some of the aromatic rings and free phenolic hydroxyl groups, and oxidation of aromatic rings and side chains to yield substantial amounts of carboxyl groups. These carboxyl groups are responsible for the water solubility of the degraded lignin fragments.

The phenolic hydroxyl, carboxyl, and methoxyl contents of the fractionated lignin have been expressed in two ways in Table XV – as percent by weight and as milliequivalents per 100 milligrams. The predominance of the carboxyl group is evident in these data. The lignin solubilized by peracetic acid may be characterized as having 5-7 carboxyl groups and 2-4 methoxyl groups per phenolic hydroxyl present. Assuming an equivalent molecular weight of 200, the carboxyl content of these lignins ranged from 0.32 to 0.59 equiv./equiv. mol. wt., as compared to 0.25 equiv./equiv. mol. wt. for the water-soluble, peracetic acid oxidation products of dioxane lignin (19). Then, when loblolly pinewood is delignified by peracetic acid, the solubilized lignin appears to be oxidized to a greater extent than necessary to merely become water-soluble, since pine dioxane lignin is chemically rather closely related to lignin as it exists in untreated pinewood.

Based on these studies, a reasonable explanation for the extensive oxidation of lignin in wood by peracetic acid is related to the porosity observations made earlier. If indeed a large lignin fragment becomes water-soluble at about 0.25 meq. COOH meq. per C_9 unit but is trapped within the cell wall by pore size restriction, then more extended contact with peracetic acid would likely lead to more highly oxidized lignin fragments of smaller molecular size. This suggestion is compatible with the molecular weights obtained for lignins solubilized by peracetic acid. These molecular weights were significantly lower than those reported for lignin solubilized during stagewise sulfite (52) and kraft (53) cooks, discussed in the literature review. Thus, when a large lignin fragment is trapped within the cell wall, it can apparently become free by the simultaneous operation of two mechanisms: (1) the continued erosion and/or swelling of the cell wall, resulting in increased pore size; and (2) the continued oxidation of the lignin fragments to yield smaller, more highly oxidized structures.

Now consider how these two mechanisms can explain the changing elution curves of the successive reaction stages in Fig. 12. Uniform penetration of the wood has been achieved – that is, all lignin which is accessible to peracetic acid through the porous structure of the untreated wood has been reached. By the time delignification has attained 92% yield, it is certain that all the lignin in the wood has been exposed to peracetic acid. Both this study and the literature indicate that the lignin in loblolly pine becomes water-soluble at a carboxyl content of 0.25-0.30 equiv. per C_9 unit. In addition, this degree of oxidation appears to be extensive enough to free lignin fragments from the rest of the lignin network.

Early in the reaction (Stages 1, 2, and 3), a high proportion of the lignin solubilized is expected to be of very low molecular weight. This was shown by Szabo and Goring (54) in their theoretical considerations of the delignification of wood, in which the Flory theory of trifunctional polymerization was applied in reverse to the degradation of a three-dimensional gel. Indeed, about half of the lignin solubilized in these early reaction stages eluted through the column at elution volumes beyond $\underline{V}_t$. Large lignin fragments which became water-soluble early in the reaction are likely to be trapped within restricting pore dimensions at these high yields. Further oxidative degradation would then be required before these fragments would pass out of the wafer. In accord with this, the absorption of the GPC elution curves of the early stages increased steadily from Fraction 1 to about Fraction 50. Only a very small portion of the lignin solubilized early in the reaction was high molecular weight material which had a carboxyl content only slightly greater than the minimum value for solubilization. Nearly half of the lignin solubilized early in the reaction (Fractions 30 through 53) was of moderate molecular size and contained about twice the amount of carboxyl apparently required for solubilization.

As delignification proceeds further (Stages 4 and 5), the proportion of larger molecular size, less oxidized lignin increased at the expense, principally, of very small molecular size material. More than half of the solubilized lignin eluted between $\underline{V}_o$ and $\underline{V}_t$. Pore size increased, favoring the release of a distribution of larger lignin fragments out of the wafer.

In the final stages of the reaction studied (6 and 7), nearly half of the solubilized lignin fragments eluted before Fraction 30. Beyond Fraction 40, the region of common intersection of all the elution curves, the elution curves of these stages fell significantly below those of the earlier reaction stages. Yet

there were low molecular weight materials present in even the latest reaction stage.

This observation corresponds to the theoretical and experimental findings of Szabo and Goring (54), which were presented in the literature review (p. 29). Their statistical treatment of the degradation of the lignin gel seems to find some qualitative verification in the peracetic acid delignification of wood. However, certain complicating factors, such as the porous structure of the cell wall and the role of hemicelluloses, were ignored in the theoretical treatment of Szabo and Goring. Considering the significance of a pore size mechanism in the delignification of wood by peracetic acid, these simplifications seem poorly chosen. It is felt that the two-gel concept of lignin is not necessary to explain either any topochemical effects or the molecular weight distribution observed in this system. Rather, the changing porosity of the cell wall is suggested as the restricting mechanism in the delignification of wood by peracetic acid.

CHEMICAL ASPECTS OF THE DELIGNIFICATION REACTION

Chemical characterization of the lignin solubilized by peracetic acid delignification of loblolly pine suggested that the reactions occurring during delignification involved both side-chain and ring oxidation. The principal functional group produced by the reaction was the carboxyl group, but other oxidized structures, in particular lactones, were also present in abundance in the solubilized lignins.

Both ultraviolet and infrared spectroscopy and also phloroglucinol lignin staining suggested that a principal point of attack upon the lignin by peracetic acid is the unsaturated structures on the side-chain of the C_9 unit which are conjugated to aromatic rings. α-Carbonyl structures may be completely destroyed by peracetic acid. Evidence from the literature (10) has suggested that such

oxidation may proceed to the formation of carboxyl groups on the side-chain of lignin. α-Ethylenic structures would also be expected to undergo oxidation by peracetic acid. These probable points of initial attack by peracetic acid upon conjugated structures in the lignin are shown in the Freudenberg lignin structure (115) presented in Fig. 28. Conjugated structures number about 1.3 of the 18 total C_9 units in the Freudenberg structure, and therefore by themselves can account for only a small fraction of the overall oxidation occurring upon delignification.

β-Carbonyl structures are present in two of the C_9 units in the Freudenberg lignin structure. These electron-rich sites would also be expected to be attacked by the peracetic acid molecule. β-Carbonyl groups in lignin absorb in the 1735-1710 $cm.^{-1}$ region of the infrared spectrum (22,23,102,103) as in Fig. 23. In this region of the spectra of solubilized lignins (Fig. 24), absorption due to carboxylic acid-type carbonyl groups was very strong, and therefore conclusive evidence for the attack by peracetic acid upon β-carbonyl structures was not demonstrated.

Other sites on the side-chain of lignin, such as hydroxyl groups or ether linkages, would not be expected to be as reactive to peracetic acid as the unsaturated sites discussed above, because they are much lower in electron density.

The side-chain oxidation of unsaturated sites alone cannot account for the observed 0.3 to 0.6 carboxyl group per C_9 unit in the lignin solubilized by peracetic acid. The remainder of the oxidized structures were due to the attack by peracetic acid upon the aromatic portion of the lignin. This resulted in significant demethoxylation and also in destruction of the aromatic rings to yield both carboxylic acid and lactone groups. Not all of the aromatic rings were destroyed under the conditions employed. At least one-fourth, and possibly as

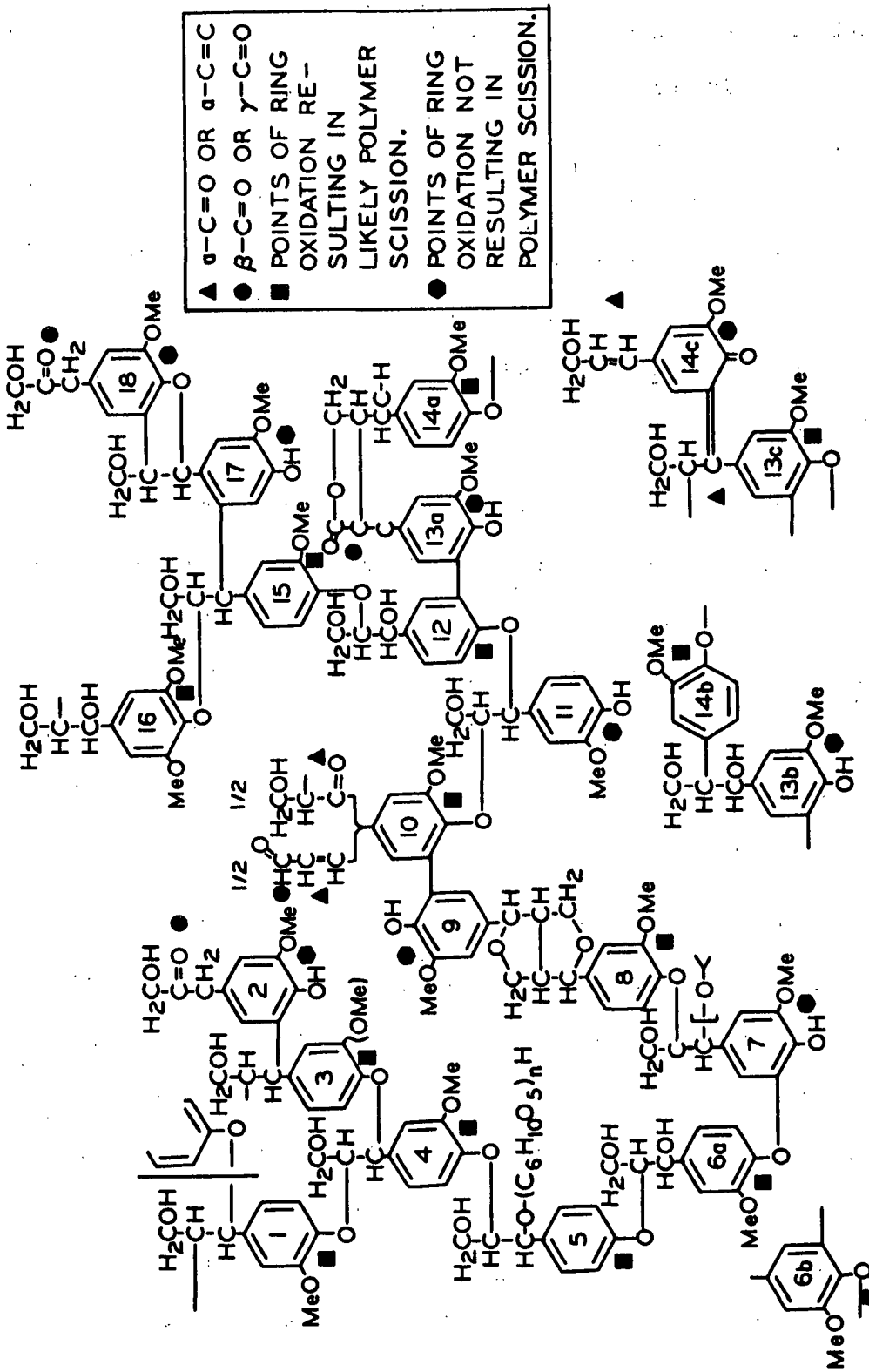

Figure 28. Freudenberg Lignin Structure (115) Showing Likely Points of Attack by Peracetic Acid

many as three-fourths in some fractions, were left unoxidized by peracetic acid. Approximately 0.7 methoxyl group per C_9 unit was removed during the delignification reaction. Since only 0.3-0.6 carboxyl group per C_9 unit was produced, other less highly oxidized structures were apparently present in the solubilized lignin. Previously reported evidence for quinone structures as semistable reaction products in peracetic acid model compound studies (16) was discussed in the literature review. Strong absorption in the 1640 $cm.^{-1}$ region of the infrared spectra of the lignin fractions could include the contribution of quinone structures, if present (112), although the freeze-dried lignin fractions were very pale in color.

Model compound studies (8) have shown that guaiacyl units in softwood lignin with a free phenolic hydroxyl group at C-4 would be expected to react more rapidly, by a fraction of about 1.25, with peracetic acid than those which are etherified. In lignin solubilized by peracetic acid, there was found an average of about 0.09 phenolic hydroxyl group per C_9 unit. However, it is not known if these phenolic hydroxyl groups were initially present in the untreated wood or were formed during the reaction itself.

Bolker and Brenner (116) neatly related the degradation of softwood lignin by certain acidic reagents, such as in sulfite pulping, to the breaking of benzyl ether linkages. This approach was an improvement over that of Szabo and Goring (54), who considered all linkages between phenylpropane units in lignin to be equally susceptible to cleavage. In Freudenberg's picture of the average 18-unit segment of the softwood lignin macromolecule (Fig. 28), only five of the units have a benzyl ether linkage (115). Using this model for lignin degradation and using model compound data to estimate the reactivity of phenylpropane units having a benzyl ether linkage, Bolker and Brenner were able to predict the increase in molecular weight of solubilized lignin observed during delignification.

If an approach similar to that of Bolker and Brenner were to be applied to the degradation of softwood lignin by peracetic acid, more complete information about the relative reactivities of the various sites on lignin to peracetic acid would first have to be gained through more extensive model compound studies. What is known now is that unsaturated sites at the alpha carbon of the side chain are particularly reactive, and oxidation of the aromatic ring also occurs. The reactivity of unsaturated sites at the beta carbon of the side chain is not well-defined. Oxidation of these unsaturated side-chain groups to carboxylic acid groups would increase the water-solubility of the lignin but would not result in polymer cleavage. The attack of peracetic acid upon the aromatic nucleus of lignin appears to result in carboxylic acid and lactone structures. If the mechanisms involved were analogous to those proposed by Farrand (8) and summarized in Fig. 1, cleavage of the lignin polymer would result at those guaiacylpropane units which are etherified at C-4 to another lignin polymer unit. In the Freudenberg lignin structure (Fig. 28), twelve of the eighteen units are etherified at C-4 and are therefore likely points of polymer scission. Attack would be favored at those units where the electron density of the ring is greatest. Oxidation of the aromatic rings of guaiacylpropane units which have a free phenolic hydroxyl group at C-4 by the same mechanism would not result in the cleavage of the polymer network at that point, but it would result in increased water-solubility of the lignin by formation of carboxyl groups.

In order to apply an approach similar to that of Bolker and Brenner to the degradation of softwood lignin by peracetic acid, the sites of polymer cleavage must first be established. As presented in the foregoing paragraph, these sites appear to be the ether linkages of guaiacylpropane units etherified at C-4. Since a majority of the C_9 units are chemically bonded to another unit through this linkage, the relative effects of both various side-chain and ring substituents

must be evaluated in order to assign relative reactivities to the etherified aromatic nuclei in the Freudenberg lignin structure. Model compound studies involving various ligninlike dimers need to be undertaken to measure these reactivities. If the rate of peracetic acid oxidation proves to depend significantly on structure, the number of reactive sites for polymer cleavage may be reduced, and a treatment such as that of Bolker and Brenner (116) might then be applied to predict the molecular weight of solubilized lignin to be expected in the absence of pore size restriction.

EXPERIMENTAL PROCEDURES

PREPARATION OF WOOD WAFERS FOR DELIGNIFICATION REACTION

A six-foot log of nineteen-year-old loblolly pine (Pinus taeda L.) which appeared to be particularly well formed was selected as the raw material from which to obtain the wood substrate for all subsequent work. The heartwood in the central region of the log was located by noting the point of change in the appearance of the inner and outer growth rings, and the number of rings from the bark to this point was counted. The log was sectioned lengthwise into boards at the Forest Products Lab in Madison, Wisconsin, according to the cross-sectional pattern shown in Fig. 29. The boards were then cut into blocks of approximately two-inch length. These blocks, which included only the sapwood region of the original log, were obtained from the shaded area of the cross section in Fig. 29. Finally, the tangential faces of the blocks were shaved into thin wafers on a metal shaper at the Fox River Tool Company, using a special wood cutting tool, shown in Fig. 30, borrowed from the Forest Products Lab. The approximate radial thickness of the shavings was 0.5 mm. or 10-15 fiber diameters.

The freshly shaved wafers (approx. 24 pounds, 44.4% moisture content) were extracted with acetone for seven hours in a large Soxhlet extractor, supplied with acetone from a twelve-liter round bottom flask. Extra thick shavings were discarded and the remainder broken by hand and separated into pure springwood and mixed summerwood-springwood wafers. Yield was 3.2 pounds of springwood and 6.0 pounds of mixed summerwood-springwood. Stored in polyethylene bags, away from light and at room temperature, the wafers remained stable at 6.50% (summerwood) and 6.85% (springwood) moisture content. The mixed summerwood-springwood wafers were used for all preliminary experiments to establish various reaction procedures. The final dimensions of the wafers were approximately 12 mm. (longitudinal) x 8 mm. (tangential) x 0.5 mm. (radial).

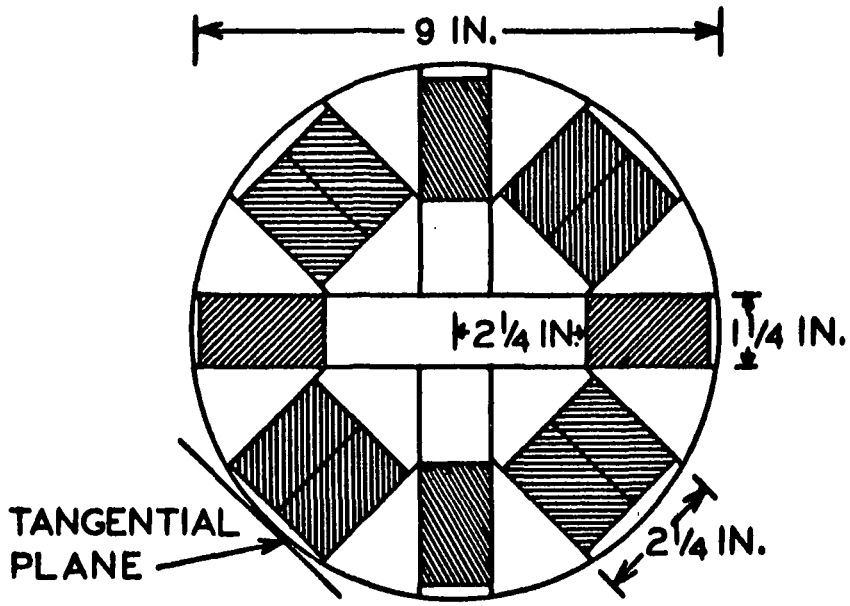

Figure 29. Cross-Sectional Cutting Pattern of Loblolly Pine Log

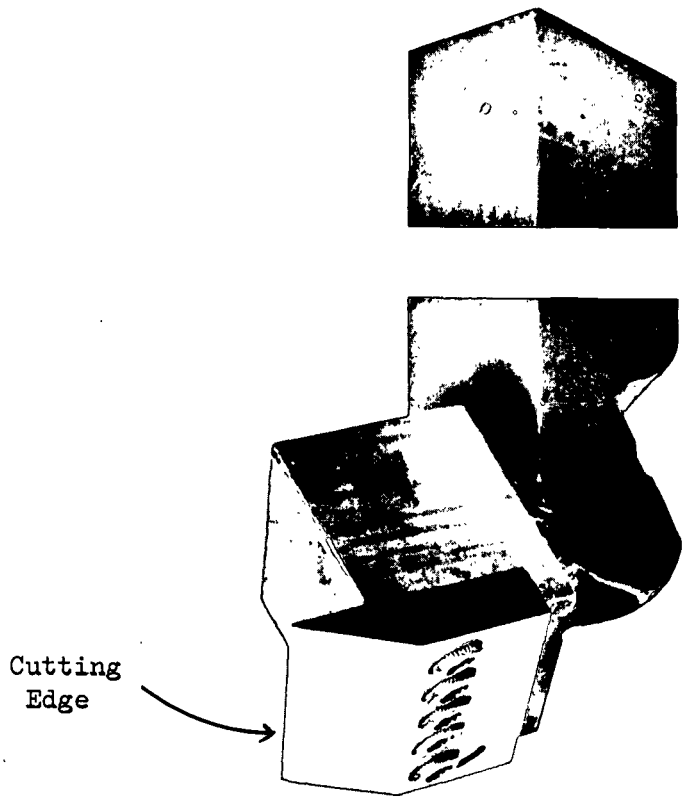

Figure 30. Cutting Tool Used to Obtain Thin Wood Wafers (See p. 125)

CONTINUOUS FLOW REACTION METHODS

GENERATION OF PERACETIC ACID

Peracetic acid was prepared by the hydrogen peroxide oxidation of acetic acid according to the method described by FMC Corporation (73). The method of preparation and generator used are discussed in Appendix I.

The composition of the solution collected from the generator was analyzed as described below and found to contain approximately 35% peracetic acid in water, with about 0.2% hydrogen peroxide and 4% acetic acid also present.

PERACETIC ACID AND HYDROGEN PEROXIDE ANALYSIS

Peracetic acid and hydrogen peroxide concentrations were determined in the presence of each other by modification of the procedure of Sully and Williams (117). The method is based on the potassium iodide reduction of peracetic acid, followed by the titration of the liberated iodine with sodium thiosulfate. Hydrogen peroxide is also reduced by potassium iodide, but at a much slower rate than peracetic acid, and on this basis the individual concentrations may be determined. Two modifications to the procedure of Sully and Williams were made. First, the starch indicator solution was replaced by thyodene which, in dry form, could be added directly to the titration solution. Second, titrations of reaction liquors at 3.0% peracetic acid were performed at room temperature, due to the very low hydrogen peroxide content. Details of the analytical procedure may be found in Appendix I.

REACTION PROCEDURE FOR DELIGNIFICATION

The following established reaction procedure was based on the results of preliminary reactions summarized in Appendix III.

Prior to reaction, 37.57 g. (35.00 g. ovendry) of loblolly pine springwood wafers were submerged in 350 ml. of distilled water in a six-inch vacuum desiccator and held in place by a porous, Plexiglas plate. Vacuum was applied, with occasional releases, for a period of 24 hours. The thin wafers readily degassed under vacuum, the air being replaced by water when vacuum was momentarily released. Then, one hour prior to packing the reaction vessel, 35 g. of generator peracetic acid were added, and vacuum was again applied.

Generator peracetic acid was diluted with distilled water to 3.0% by weight. The wet, impregnated wafers were packed between the perforated plates of the reaction vessel, and the entire assembly was sealed into the flow apparatus. The flow apparatus was filled with peracetic acid feed liquor through the constant head device, forcing all air out of the flow line. The bath was filled with hot tap water and the reaction vessel brought to 60°C. as quickly as possible.

When the desired temperature had been reached, flow was started, and the rate was controlled by manipulating a needle valve just prior to the collection vessel. The flowmeter indicated that a constant flow rate could be maintained indefinitely once any air bubbles were cleared out of the system. Temperature fluctuation was no more than 0.1°C. The product liquor was cooled and collected, and then residual peracetic acid was quenched by manual addition of excess acetaldehyde solution (52.0 g./1000 ml. product liquor). Samples of unquenched and quenched reaction liquor were collected and analyzed for peracetic acid and hydrogen peroxide according to the procedure of Sully and Williams (117), in order to assure that peracetic acid quenching was complete and the reaction liquor was safe for further handling. The quenched liquor was collected in batches and then stored at 5°C. in polyethylene bottles.

After the desired amount of feed liquor had been put through the reaction vessel, the water bath was lowered and the reaction apparatus drained. The partially delignified wafers (still intact) were removed from the reaction vessel and submerged in distilled water. Excess acetaldehyde was added to quench the small amount of peracetic acid remaining in the wafers. After thorough washing, the percent yield was determined (118).

Determination of yield for wafers which were to be examined by the solute exclusion technique was by an aliquot-drying procedure. The wafers were air dried on a fine sintered glass filter until all excess water had been removed from their outside surfaces. At this point the ovendry weight of the wafers was about 40% of the weight of the wet wafers. The total wet yield was measured, and then six aliquots of the wet wafers were immediately weighed out and oven dried (118) to obtain the dry fraction of the wet wafers. The total dry yield and the percentage yield were then calculated.

In the stagewise delignification reaction, the established reaction procedure was employed as detailed above. The reaction was allowed to proceed continuously for 9 hours and 20 minutes, with immediate reaction quenching. After completion of the run, the wood wafers, still intact but softened, were washed and oven dried to constant weight. The product liquor was collected in a series of batches as the reaction proceeded. A total of seven 2000-ml. batches was collected. The solubilized reaction products in these batches are referred to in the discussion section by denoting the batches as successive reaction stages. The solubilized reaction products were analyzed both for lignin distribution by gel permeation chromatography and also for lignin and carbohydrate composition. One thousand ml. of each successive reaction stage were analyzed by GPC as discussed below. For the analysis of lignin and carbohydrates present as a function of reaction

stage, adjacent pairs of the product liquors were combined (2 plus 3, 4 plus 5, and 6 plus 7) before column fractionation and analysis.

In the generation of composite product liquor from the delignification of springwood wafers, four replicate reactions were run according to the established reaction procedure. All the product liquor from these reactions was quenched and combined to yield the composite product liquor. Prior to fractionation by gel permeation chromatography, the composite product liquor was concentrated by a factor of 10, according to the procedure discussed in the experimental section on GPC.

SOLUTE EXCLUSION STUDIES

Diffusion to Equilibrium

The procedure followed in the solute exclusion experiments was essentially that of Stone and Scallan (66,67). A series of dextrans was obtained from Pharmacia Fine Chemicals of Uppsala, Sweden and two were used as received.

Unreacted wafers were thoroughly impregnated with distilled water prior to the experiment, according to the procedure discussed previously. Partially delignified wafers were never dried after removal from the reaction vessel. They were left submerged in distilled water, stored in the water-swollen state prior to solute exclusion experiments.

Samples of the wet wafers (p + q) were weighed into two-ounce, wide-mouth bottles. The samples contained about two grams of ovendry wood (p). Then about 25 ml. of dextran stock solution were weighed (w) into the jars. The wafers and solution were sealed inside the jars, mixed by shaking, and then set aside for three days with intermittent agitation. This time interval was shown to be

sufficient for equilibrium diffusion of dextrans into wood (66,67). After equilibrium had been reached, the wafers were gently removed from the dextran solution by filtration through fine sintered glass. The wafers were washed and soaked in distilled water and then oven dried at 105°C. to determine the dry weight of the sample. The initial concentration of the stock dextran solution (c_i) and the final concentration of the diluted dextran solution (c_f) were determined by polarimetry, as described below. Inaccessible water, in grams per gram of dry wood, was calculated from Equation (13), page 49.

Dextran Concentration by Precision Polarimetry

The Zeiss precision polarimeter, reading to ± 0.01°, was used at 546 nm. in determining the ratio of initial to final dextran concentration in solute exclusion experiments. The light source was a mercury lamp coupled with a green filter. A jacketed, two-decimeter polarimeter tube with side filling cup provided ease of filling without removing the end caps of the tube. Tube capacity was about twelve milliliters. All readings were made at 20.0°C., maintained by circulation of constant temperature water through the water-jacket of the polarimeter tube. Due to heat transfer from the air through the polarimeter and caps, water bath temperature had to be adjusted slightly according to the formula (119):

$$t_w = \frac{t_t - 0.026t_a}{0.974} \qquad (25)$$

where t_w = water temperature in jacket; equals the average of inlet and outlet temperatures
t_t = solution temperature in polarimeter tube, 20.0°C.
t_a = air temperature

Observed optical rotations were corrected for solvent and tube rotation by obtaining a zero reading for pure distilled water and subtracting this value from the observed rotations.

GEL PERMEATION CHROMATOGRAPHY OF SOLUBILIZED REACTION PRODUCTS

The void volume of the GPC column, V_o, was determined by the elution of very high molecular weight blue dextran. A 50-ml. solution at 0.2% concentration of the blue-dyed material was used in the determination.

Under the reaction conditions used, the concentration of the product liquor from the continuous flow reactor was about 0.7 g./liter. One thousand milliliter batches of product liquor were concentrated to 100 ml. in about two hours using a 125-ml. cyclone evaporator. Operated at 22-30°C. and 28.5-29.5 inches vacuum (Hg), the product liquor was concentrated with no apparent further lignin degradation, as evidenced by the unchanged ultraviolet spectra.

The standard procedure adopted for a column run was as follows. One-hundred milliliters of concentrated liquor were first filtered through coarse sintered glass and then through a fiberglass filter to prevent plugging of the fiberglass filter at the top of the column. The sample was then deaerated under vacuum for four hours at 72°F.

The column was drained until the head level just disappeared into the fiberglass filter on top of the column. Flow was stopped, and the sample was poured through a funnel onto the top of the column. The stopcock was opened immediately, and the eluting solution was collected in a graduated cylinder. The last traces of sample were carefully washed into the gel with a minimum of water before the full, constant head was applied. The flow rate was maintained at about 75 ml./hr. by manipulating the needle valve as necessary. After 1290

ml. (void volume) had eluted from the column, the flow was directed to the siphon, and 20.0-ml. fractions were collected. The eluting solution was monitored continuously by absorbance at 275 nm., with the chart drive mechanism of the Cary Model 15 spectrophotometer set for synchronous operation at X1, using gears A7 and B8. The chart paper was marked intermittently in terms of fraction number. Complete return to base line, absorbance = 0.0, occurred at about 4000 ml.

The product liquors of the seven successive reaction stages were eluted through the column according to the standard procedure presented above. Correction was made for the background absorbance of quenched peracetic acid which eluted beyond $\underline{V}_t$. A computer program was written to normalize the absorbance curves – that is, to adjust them all to the same area under the curve. Yield was estimated at the six intermediate reaction stages by direct proportion to the total absorbance recorded for elution volumes between 1290 ml. ($\underline{V}_o$) and 3350 ml.

The composite product liquor was concentrated by a factor of 10, as above, and fractionated in 100-ml. aliquots on the GPC column. A total of 103 20-ml. fractions were collected, beginning at 1290 ml. ($\underline{V}_o$) and extending to 3350 ml. Twelve replicate column runs were performed and the corresponding fractions of these runs combined. Then, certain of the adjacent fractions of low concentration were also combined. Finally, all were concentrated by evaporation, first using a cyclone evaporator and then a rotary evaporator with a directly attached condensor, to about 1% concentration for use as described below. These concentrated fractions were stored at 5°C. At a later date, these fractions between $\underline{V}_o$ and $\underline{V}_t$ were freeze dried to fluffy solids of low moisture content, using a New Brunswick Freeze Dryer.

ULTRAVIOLET ABSORPTION MEASUREMENTS

The Cary Model 15 spectrophotometer was used to obtain the direct absorption spectra of solutions of the lignin fractions. Spectra were obtained on the 0-1.0 absorbance scale, using matched silica cells having a path length of 1.0 cm. The lignin solution was placed in the sample beam and distilled water in the reference beam. Compensation for slight differences in the optical properties of the cells was made by recording the spectrum with distilled water in both the sample and reference cells. Absorbance at 275 nm. was taken to be the difference between the absorbance of the solution and the base-line absorbance of water.

GRAVIMETRIC DETERMINATION FOR THE CALCULATION OF ABSORPTIVITY AT 275 NM.

Samples of concentrated lignin fractions, in approximately 1% aqueous solution, were diluted by a factor of 1/100, and absorbance at 275 nm. was determined as above. Aliquots of the same concentrated fractions were added volumetrically to tared 250-ml. round-bottom flasks. The samples were then evaporated to about 100 ml. and frozen in a dry ice-acetone bath. Drying for 24 hours on a New Brunswick Freeze Dryer was followed by vacuum oven drying at 60°C. for 12 hours and 110°C. for 12 hours. Twenty fractions below $\underline{V}_t$ and seven fractions above $\underline{V}_t$ were dried to constant weight according to this procedure. Absorptivity values at 275 nm. were calculated from Beer's law, Equation (15).

Freeze-dried samples of lignin fractions below $\underline{V}_t$ were used in seventeen additional determinations of $\underline{a}_{275}$. The absorbance of solutions made up quantitatively from these samples was determined as above. The concentration of the solutions was based on the weight of the sample, multiplied by the factor 0.97, to take into account the approximately 3% moisture content of the

freeze-dried lignin, as indicated by Karl Fischer titration. These 17 absorptivity data points were combined with the 20 data points obtained from concentrated lignin solutions to make a total of 37 points from which the best fit polynomial of $\underline{a}_{275}$ versus fraction number was obtained, for the fractionation range between $\underline{V}_o$ and $\underline{V}_t$.

The individual gravimetric determinations by both above methods are presented in Appendix VIII along with the solutions to the best fit polynomial.

INTRINSIC VISCOSITY AT 30°C.

Intrinsic viscosities of the fractionated lignins were determined in aqueous solution. In making up the stock solutions at about 1% for intrinsic viscosity determinations, two procedures were used. A majority of the stock solutions were samples of the concentrated lignin fractions. The concentration of these stock solutions was determined by taking an aliquot, diluting it by a factor of 1/100, and measuring the absorbance at 275 nm., using the appropriate value of $\underline{a}_{275}$. On the other hand, since those fractions below $\underline{V}_t$ could be obtained in the freeze-dried state, a number of the stock solutions were also made up quantitatively in distilled water from these materials.

A Cannon-Ubbelohde viscometer, of capillary size 50, was suspended in a water bath maintained at 30.0°C. Exactly 1 ml. of stock solution was added into the viscometer using a 1.0-ml. syringe equipped with a long needle. The solution was allowed to rise to temperature, and then was drawn up through the viscometer until the miniscus was above the upper scribe line. The stopcock was opened, allowing the solution to drain through the capillary under gravity flow alone. A stopwatch was used to measure the time which it took the solution to pass between the upper and lower scribe lines. The procedure was replicated

until five close readings were obtained, indicating thermal equilibrium. The highest and lowest were dropped, and the middle three were averaged to yield the time, $\underline{t}$, for that concentration, $\underline{C}$. Then the product $(\underline{t} - \underline{t}_o/\underline{t}_o)/\underline{C}$ was calculated, where $\underline{t}_o$ is the time of flow of solvent in the viscometer.

Four successive dilutions of 0.25 ml. each were added to the solution, and the product, $(\underline{t} - \underline{t}_o/\underline{t}_o)/\underline{C}$, was obtained for these concentrations in the same manner as above. Linear regression analysis (Rax Q911A) was applied to a five-point plot of $(\underline{t} - \underline{t}_o/\underline{t}_o)/\underline{C}$ versus concentration. The intercept of this plot was intrinsic viscosity. Confidence limits were also obtained. The data collected for this determination are presented in Appendix IX.

NUMBER-AVERAGE MOLECULAR WEIGHT BY DYNAMIC MEMBRANE OSMOMETRY

The Mechrolab 501 High Speed Membrane Osmometer was used to obtain the number-average molecular weights of lignin fractions between $\underline{V}_o$ and $\underline{V}_t$. A 7.0-ml. stock solution was made up quantitatively from the freeze-dried lignins to about 1.5 g./liter in 1% NaCl in distilled water. This in turn was used to make up four additional solutions which were 80, 60, 40, and 20% of the concentration of the stock solution.

Two solution additions were made for each concentration level. Between each solution addition, fresh solvent was added to determine the appropriate solvent value, $\underline{P}_o$. Thus, a total of 20 additions was required to determine the molecular weight of a given lignin sample. Total experimental time required for each molecular weight determination was about four hours.

The operation of the osmometer and analysis of the osmotic pressure data are discussed in Appendix X.

PHENOLIC HYDROXYL CONTENT BY ULTRAVIOLET DIFFERENCE SPECTRA

The technique used to obtain the UV difference spectra of freeze-dried lignin fractions was as described by Wexler (90), except that solutions of smaller volume were made up. Solutions at 0.03% or less concentration were made up in distilled water in 25-ml. volumetric flasks. The solutions were agitated until completely clear, then 10.0 ml. of solution was pipetted into each of two 25-ml. volumetric flasks. The first solution was made basic by adding 2.5 ml. of 1.0N NaOH, and the second was made acidic by adding the same volume of 1.0N HCl. The solutions were diluted to volume to yield two samples of the same fractions at identical concentration, one in 0.1N alkali, the other in 0.1N acid.

Difference spectra were obtained in 1.0-cm. silica cells, using the Cary spectrophotometer. The alkaline solution was placed in the sample beam and the acidic solution in the reference beam. Wexler's base-line Method B (a straight line drawn tangent to the two minima on either side of 250 nm.) and the factor 0.192 for softwood lignins (90) were used to calculate the phenolic hydroxyl contents of the samples from their difference curves. Phenolic hydroxyl content, in percent, was related to the measured absorbance maximum at 250 nm. by the following equation (where cell path length is 1.0 cm.):

$$\% \text{ phenolic hydroxyl} = (0.192) \times \frac{A_{\Delta 250}}{\text{Concn. (g./l.)}} \qquad (26)$$

where $A_{\Delta 250}$ = the absorbance maximum at 250 nm., using Wexler's base-line Method B

CARBOXYL GROUP CONTENT BY POTENTIOMETRIC TITRATION

Approximately 70-mg. samples of freeze-dried lignin fractions were weighed out into a 43-mm. porcelain crucible and dissolved in 4.0 ml. of distilled water.

The samples were titrated with 0.100N NaOH, added from a 5-ml. buret that could be read to 0.001 ml. The solution pH was followed to 0.01 pH unit by using a combination glass-KCl/AgCl electrode, coupled to a Corning Model 12 pH meter. A first derivative of the titration curve was obtained to aid in picking off the equivalence point.

MAKEUP OF POTASSIUM CHLORIDE PELLETS FOR INFRARED SPECTRA

Nine freeze-dried lignin fractions (Numbers 1-2, 11, 16, 25, 32, 40, 48, 55-56, and 63-64) were placed in a vacuum desiccator and dried over P_2O_5 for two days. Exactly 2.50-mg. lignin and 500.00 mg. pure KCl were weighed out and mixed for one minute in a capsule vibrator. The mixed samples were dried over P_2O_5 under vacuum for five days. At this time, 402.0 mg. of each mixture were weighed out. In addition, 400.0 mg. of pure KCl were weighed out for the reference pellet when obtaining regular IR spectra. The mixtures were dried as above for nine days. Then, a pellet was made from each fraction, quantitatively transferring each mixture into the barrel chamber of the pellet dye. In the press, each pellet was evacuated for four minutes, then pressed to 22,000 p.s.i. for two minutes.

All regular and differential spectra were obtained within two days of when the pellets were made, using a Perkin-Elmer model 700 infrared spectrophotometer. Regular IR spectra were obtained with a pure KCl pellet in the reference beam to compensate for disk absorption and scattering. Differential spectra were obtained by placing one pellet in the sample beam and a pellet of a second fraction in the reference beam. The positions of the pellets were reversed to obtain the complementary differential spectra. This technique greatly aided in the determination of a base line in the differential spectra.

LIGNIN AND CARBOHYDRATE MATERIALS SOLUBILIZED UPON STAGEWISE DELIGNIFICATION

GPC Fractionation Procedure

Liquors of the successive reaction stages were combined in pairs – stages 2 plus 3 (early reaction), 4 plus 5 (mid reaction), and 6 plus 7 (late reaction) – and eluted through the column, as described previously. Fractions of each were collected in the normal manner and then combined, in groups of five successive fractions, as indicated in Table XXII. Three groups of fractions were collected for carbohydrate determination, while five were used to determine both the optical rotation and the ultraviolet spectra of the eluting material. The fractions were freeze-dried after collection and later made up to appropriate concentrations for the various determinations.

TABLE XXII

GROUPS OF FRACTIONS USED IN CARBOHYDRATE ANALYSES AND POLARIMETRY AND UV SPECTRA

Determination	Fractions
Carbohydrate	9-13
	33-37
	47-51
Optical rotation and UV spectra	4-8
	19-23
	28-32
	38-42
	52-56

Lignin and Carbohydrate Analyses

Dilute solutions of the five groups of fractions indicated in Table XXII were made up quantitatively at 0.01% and at 0.001%, and direct UV spectra were obtained as described previously.

The specific rotation of five groups of lignin fractions was determined for early, mid, and late reaction stages using the Zeiss polarimeter at 546 nm. Samples were weighed out at 0.2 to 0.6% concentration in distilled water. A two-decimeter, narrow-bore polarimeter tube having a volume of approximately 1.8 ml. was used in all determinations. All readings were made at a room temperature of 19.0 $\pm$ 0.2°C. Twenty-five individual readings were averaged to determine the zero (solvent) rotation value; sixteen readings were averaged to obtain the observed rotation of each sample.

Three additional groups of fractions (Table XXII) were collected, each for early, mid, and late reaction stages, and analyzed for carbohydrate content by the method used in previously reported analyses (78).

CONCLUSIONS

The delignification of loblolly pinewood by peracetic acid was studied using a continuous flow reaction procedure in which the solubilized reaction products were removed from the reaction vessel directly after extraction from the wood. Several observations were made regarding the delignification reaction:

(1) A substantial increase in porosity as delignification proceeded was shown by the increase in the estimated median pore width.

(2) A shift in the GPC elution curves showed that there was an increase in the molecular size of the lignin extracted as delignification proceeded.

(3) An approximate correspondence was shown between the estimated median pore width and the midpoint in the elution curve at that yield.

(4) The literature was verified in that lignin oxidized by peracetic acid results in the formation of carboxyl groups and that 0.25-0.30 $COOH/C_9$ are required for water solubility. However, much of the lignin extracted in this study was shown to be oxidized to a much greater extent than apparently necessary for water solubility. The largest molecules extracted were the least oxidized.

The postulated explanation for these observations is as follows. Pore size serves as a restricting factor in the size of the lignin extracted. A physical, rather than a chemical mechanism would also explain why the rate of lignin extraction deviated from that predicted by apparent first-order kinetics. Overoxidation of water-solubile lignin fragments is suggested to occur because they are trapped within the restricting pore dimensions of the cell wall. The trapped lignin fragment may then be released or extracted by the simultaneous operation of two mechanisms. First, a physical mechanism, involving continued erosion or swelling of the cell

wall to increase the pore width. Second, a chemical mechanism, involving continued oxidation of the lignin fragments to yield smaller, more highly oxidized structures.

The changing shape of the elution curves may be explained in terms of these two mechanisms. Early in the reaction, porosity restrictions are the greatest resulting in extraction of small molecular size, highly oxidized lignins, at a relatively moderate rate. As the reaction continues, the porosity increases, resulting in a shift in favor of larger, less highly oxidized lignin fragments being extracted. This trend continues late in the reaction. Pore size has increased substantially and as a result larger lignin fragments are extracted. The degree of lignin oxidation is less because the fragments are trapped within the cell wall for a much shorter period of time, and the rate of extraction is still considerable since pore size restriction is no longer as important as earlier in the reaction.

SUGGESTIONS FOR FUTURE RESEARCH

Several areas of future research effort have been suggested by this investigation. In addition to further work involving peracetic acid, certain techniques which have evolved could be applied in studies involving other delignifying reagents.

More comprehensive studies of pore-size change with stagewise delignification would require a series of narrow molecular weight distribution polymers. Dextrans appear to be an acceptable polymer to use but would require preparative GPC fractionation on a rather large scale. Precision in solute exclusion experiments may be improved by increasing either the size of the wood sample or the initial polymer concentration. Solute exclusion studies might be extended into the study of the effects of water washing or extraction by alkali upon the porous structure of the cell wall.

Model compound studies of peracetic acid with ligninlike dimers would be expected to elucidate the oxidation mechanism and better define the likely points of lignin polymer scission.

The reactions of peracetic acid with isolated lignin preparations could be undertaken using the principles of a single-pass, continuous flow reaction apparatus. In studying isolated lignins, such as dioxane lignin, IR and UV spectroscopy could be applied to characterize the unreacted lignin, as well as the reaction products, in order to better define the chemical changes taking place during delignification.

Finally, relatively mild selective delignification with peracetic acid has yielded a solubilized lignin with which a small amount of carbohydrate always seems to be associated. The presence of a chemical linkage between the lignin

and carbohydrate portions of the reaction products could be investigated more thoroughly if a larger quantity of chemically uniform material were first isolated by GPC fractionation. Extended solubility studies, polarimetry at different wavelengths, and selective enzymatic cleavage might all prove useful in such an investigation.

ACKNOWLEDGMENTS

The author wishes to express his sincere appreciation for the assistance, encouragement, and guidance given by the members of his thesis advisory committee: Drs. G. A. Nicholls (chairman), R. H. Atalla, and H. A. Swenson. A special thanks goes to Dr. Nicholls for his advice in writing the manuscript.

The author would also like to thank various staff members for their contributions to the thesis research: especially, Messrs. M. C. Filz, Jr., P. F. Van Rossum, E. C. Koerner, and A. O. Johnson for their assistance in constructing various pieces of equipment; Mr. J. D. Hankey for the color photographs of the stained cross sections; Messrs. L. G. Borchardt and J. P. Rademacher for carbohydrate and sugar analyses, respectively; Mr. J. R. Taggart for lignin determinations; and Mr. F. R. Sweeney for the equipment photographs which appear in this manuscript.

The author would also like to thank the Forest Products Lab in Madison, Wisconsin, for cutting the log used into blocks and for loaning the wafer cutting tool; and Pope Scientific Co. for the custom blowing of certain components of the flow reactor.

Financial support from the Institute is gratefully acknowledged.

Above all, I am sincerely indebted to my wife, Carolyn, for her continued patience and encouragement throughout the work and especially for typing of the complete manuscript.

LITERATURE CITED

1. Poljak, A., Angew. Chem. 60A, no. 2:45(1948); ABIPC 19:389.

2. Haas, H., Schoch, W., and Strole, U., Das Papier 9, no. 19/20:469(1955); ABIPC 26:181.

3. Leopold, B., Tappi 44, no. 3:230(1961).

4. Poljak, A., Holzforschung 5, no. 2:31(1951); ABIPC 21:839.

5. Havel, S., Chem. Prumsyl 15, no. 2:68(1965); ABIPC 40:A3759.

6. Giguere, P. A., and Olmos, A. W., Can. J. Chem. 30:821(1952).

7. Brooks, W. V. F., and Haas, C. M., J. Phys. Chem. 71:650(1967).

7a. Benton, C. A., Lewis, T. A., and Llewellyn, D. R., J. Chem. Soc. 1956:1226.

8. Farrand, J. C. The peracetic acid oxidation of 4-methylphenols and their methyl ethers. Appleton, Wis., The Institute of Paper Chemistry, 1969. 206 p.

9. Hatakeyama, H., Nakano, J., and Migita, N., J. Chem. Soc. Japan, Ind. Chem. Sect. 68, no. 5:52A, 972(1965); ABIPC 36:3213.

10. Ishikawa, H., Oki, T., and Okubo, K., J. Jap. Tappi 20, no. 8:435(1966); ABIPC 37:A8913.

11. Kinoshita, Y., Oki, T., and Ishikawa, H., J. Jap. Wood Res. Soc. 13:319 (1967); ABIPC 38:A8316.

12. Sakai, K., and Kondo, T., J. Jap. Wood Res. Soc. 12, no. 1:57(1966); ABIPC 38:A7518.

13. Sarkanen, K. V., and Suzuki, J., Tappi 48, no. 8:459(1965).

14. Sarkanen, K. V., and Lai, Y.-Z., Tappi 51, no. 10:449(1968).

15. Ishikawa, H., Okubo, K., and Oki, T., J. Jap. Tappi 20, no. 9:485(1966); ABIPC 37:A8914.

16. Ishikawa, H., Kinoshita, Y., Oki, K., and Okubo, K., J. Jap. Tappi 21:494 (1967); ABIPC 38:A7503.

17. Kono, M., Sakai, K., and Kondo, T., J. Jap. Tappi 19, no. 1:27(1965); ABIPC 35:A8076.

18. Sakai, K., and Kondo, T., J. Jap. Wood Res. Soc. 12, no. 6:310(1966); ABIPC 38:A7518.

19. Sakai, K., and Kishimoto, S., J. Jap. Wood Res. Soc. 14, no. 8:411(1968); ABIPC 40:A1085.

20. Hatakeyama, H., Nakano, J., and Migita, N., J. Chem. Soc. Japan, Ind. Chem. Sect. 70, no. 6:957(1967); ABIPC 38:A7496.

21. Hatakeyama, H., Suzuki, K., Mishizuka, G., Nakano, J., and Migita, N., J. Chem. Soc. Japan, Ind. Chem. Sect. 70:1399(1967); ABIPC 39:A208.

22. Sarkanen, K. V., Chang, H.-M., and Allan, G. G., Tappi 50, no. 12:583(1967).

23. Dandarova-Vasatkova, M., Polcin, J., Kosikova, B., and Joniak, D., Holzforschung 23, no. 4:127(1969).

24. Hatakeyama, H., Nakano, J., and Migita, N., J. Chem. Soc. Japan, Ind. Chem. Sect. 70, no. 6:953(1967); ABIPC 38:A7335.

25. Endo, A., Saito, M., Yoshida, M., and Fusezaki, Y., J. Chem. Soc. Japan, Pure Chem. Sect. 88, no. 1:83(1967); ABIPC 38:A6908.

26. Cazes, J., J. Chem. Ed. 43:A567, A625(1966).

27. Cazes, J., J. Chem. Ed. 47:A461, A505(1970).

28. Bly, D. D., Science 168, no. 3931:527(1970).

29. Laurent, T. C., and Killander, J., J. Chromatog. 14:317(1964).

30. Ackers, G. K., J. Biol. Chem. 242, no. 13:3237(1967).

31. Yau, W. W., J. Poly. Sci., Part A-2, 7:483(1969).

32. Jensen, W., Fremer, K.-E., and Forss, K., Tappi 45, no. 2:122(1962).

33. Forss, K., and Fremer, K.-E., Tappi 47, no. 8:485(1964).

34. Forss, K., and Fremer, K.-E., Paperi Puu 47, no. 8:443(1965).

35. Forss, K., Fremer, K.-E., and Stenlund, B., Paperi Puu 48, no. 9:565, no. 11:669(1966).

36. Forss, K., and Stenlund, B., Paperi Puu 51, no. 1:93(1969).

37. Stenlund, B., Paperi Puu 52, no. 2:55(1970).

38. Stenlund, B., Paperi Puu 52, no. 3:121(1970).

39. Felicetta, V. F., Glennie, D., and McCarthy, J. L., Tappi 50, no. 4:170 (1967).

40. Gupta, P. R., and McCarthy, J. L., Macromolecules 1, no. 3:236(1968).

41. Gupta, P. R., and McCarthy, J. L., Macromolecules 1, no. 6:495(1968).

42. Pla, F. Ph.D. Thesis, Univ. de Grenoble, 1967; ABIPC 39:A3784.

43. Rinaude, M., and Pla, F., Chim. Anal. (Paris) 49, no. 6:320(1967); ABIPC 38:A6685.

44. Brown, W., Falkehag, S. I., and Cowling, E. B., Nature 214:410(1967).

45. Brown, W., Cowling, E. B., and Falkehag, S. I., Svensk Papperstid. 71, no. 2:811(1968).

46. Kirk, T. K., Brown, W., and Cowling, E. B., Biopolymers 7, no. 2:135(1969).

47. Loras, V., Tappi 48, no. 2:125(1965).

48. Kosikova, V., Polcin, J., and Dandarova-Vasatkova, M., Holzforschung 23, no. 2:37, 44(1969).

48a. Brownell, H. H., Tappi 54, no. 1:66(1971).

49. Kringstad, K. P., and Cheng, C. W., Tappi 52, no. 12:2382(1969).

50. Linnell, W. S., Thompson, N. S., and Swenson, H. A., Tappi 49, no. 11:491 (1966).

51. Linnell, W. S., and Swenson, H. A., Tappi 49, no. 11:494(1966).

52. Yean, W. Q., and Goring, D. A. I., Pulp Paper Mag. Can. 65:T127(1964).

53. McNaughton, J. G., Yean, W. Q., and Goring, D. A. I., Tappi 50, no. 11:548 (1967).

54. Szabo, A., and Goring, D. A. I., Tappi 51, no. 10:440(1968).

55. Proctor, A. R., Yean, W. Q., and Goring, D. A. I., Pulp Paper Mag. Can. 68:T445(1967).

56. Seely, T., J. Polymer Sci., Part A-1, 5:3029(1967).

57. Davies, G. W., Appita 21, no. 4:117(1968).

58. Stone, J. E., Scallan, A. M., and Aberson, G. M. A., Pulp Paper Mag. Can. 67:T263(1966).

59. Stone, J. E., and Scallan, A. M., J. Polymer Sci., Part C, 11:13(1965).

60. Stratton, W. O., J. Polymer Sci. 22:385(1956).

61. Hermans, P. H., Heikens, D., and Weidinger, A., J. Polymer Sci. 35:185 (1959).

62. Kellogg, R. M., and Wangaard, F. F., Wood Fiber 1, no. 3:180(1969).

63. Scott, J. A. N., Proctor, A. R., Fergus, B. J., and Goring, D. A. I., Wood Sci. and Technol. 3, no. 1:73(1969).

64. Fergus, B. J., and Goring, D. A. I., Pulp Paper Mag. Can. 70:T314(1969).

65. Stone, J. E., Pulp Paper Mag. Can. 65:T3(1964).

66. Stone, J. E., and Scallan, A. M., Tappi 50, no. 10:496(1967).

67. Stone, J. E., and Scallan, A. M., Pulp Paper Mag. Can. 69:T288(1968).

68. Stone, J. E., and Scallan, A. M., Cell. Chem. and Technol. 2:343(1968).

69. Adamson, A. W. Physical chemistry of surfaces. 2nd ed. p. 584. New York, Interscience, 1967.

70. Feist, W. C., Tarkow, H., and Southerland, C. F., Forest Prod. J. 16, no. 10:61(1966).

71. Feist, W. C., and Tarkow, H., Forest Prod. J. 17, no. 10:65(1967).

72. Feist, W. C., and Tarkow, H., Tappi 51, no. 2:80(1968).

73. FMC Corporation. The operation of a bench scale peracetic acid generator. New York, 1963.

74. Brauns, F. M., and Brauns, D. A. The chemistry of lignin. Supplemental Volume. p. 37. New York, 1960.

75. Adler, E., Bjorkqvist, K. J., and Haggroth, S., Acta Chem. Scand. 2:93 (1948).

76. Adler, E., and Ellmer, L. R., Acta Chem. Scand. 2:839(1948).

77. Buchanan, M. A., and Nicholls, G. A. Unpublished work.

78. Borchardt, L. G., and Piper, C. V., Tappi 53, no. 2:257(1970).

79. Barker, S. A., Hatt, B. W., Marsters, J. B., and Somers, P. J., Carbohyd. Res. 9, no. 4:373(1969).

80. Beau, R., Le Page, M., and De Vries, A. J., Appl. Poly. Symposia no. 8:137 (1969).

80a. Swenson, H. A., Kaustinen, H. M., and Almin, K. E., Polymer Letters 9:261 (1971).

81. Swenson, H. A. Private communication.

81a. Wilder, H. D., and Dalaski, E. J., Tappi 48, no. 5:293(1965).

82. Flory, P. J. Principles of polymer chemistry. p. 605. Ithaca, New York, Cornell Univ. Press, 1953.

83. Aulin-Erdtman, G., Svensk Papperstid. 57:745(1954).

84. Adler, E., Hernestam, S., and Wallden, I., Svensk Papperstid. 61:641(1958).

85. Gierer, J., Svensk Papperstid. 73, no. 18:571(1970).

86. Sarkanen, K. V. Wood lignins. In Browning's The chemistry of wood. p. 272. New York, John Wiley & Sons, 1963.

87. Olcay, A., Comm. de la Fac. des Sci. de l'Univ. D'Ankara 15, no. 7:85(1968).

88. Olcay, A., Holzforschung 24, no. 5:172(1970).

89. Aulin-Erdtman, G., Svensk Kem. Tidskr. 70:145(1958).

90. Wexler, A. S., Anal. Chem. 36, no. 1:213(1964).

91. Arseneau, D. F., and Pepper, J. M., Pulp Paper Mag. Can. 66:T415(1965).

92. Institute Method 18. 1951.

93. Polcin, J., and Rapson, W. H., Pulp Paper Mag. Can. 70:T555(1969).

94. Pew, J. C., J. Org. Chem. 28:1048(1963).

95. Pew, J. C., and Conners, W. J., Tappi 54, no. 2:245(1971).

96. Lin, S. Y., and Kringstad, K. P., Tappi 53, no. 9:1675(1970).

97. Norrstrom, H., and Teder, A., Svensk Papperstid. 73, no. 19:619(1971).

98. Polcin, J., and Rapson, W. H., Pulp Paper Mag. Can. 72, no. 3:T103(1971).

99. Silverstein, R. M., and Bassler, G. C. Spectrophotometric identification of organic compounds. p. 161. New York, John Wiley & Sons, 1968.

100. Rydholm, S. A. Pulping Processes. p. 182. New York, Interscience, 1965.

101. Azhar, M. R., and Wayman, M., Pulp Paper Mag. Can. 71:T81(1970).

102. Bolker, H. I., and Somerville, N. G., Pulp Paper Mag. Can. 64:T187(1963).

103. Harrington, K. J., Higgins, H. G., and Michell, A. J., Holzforschung 18:108(1964).

104. Michell, A. J., Watson, A. J., and Higgins, H. G., Tappi 48, no. 9:520 (1965).

105. Kolboe, S., and Ellefsen, O., Tappi 45, no. 2:163(1962).

106. Marton, J., Adler, E., and Persson, K., Acta Chem. Scand. 15, no. 2:384 (1961).

107. Hergert, H. L., J. Org. Chem. 25:405(1960).

108. Marton, J., and Sparks, H. E., Tappi 50, no. 7:363(1967).

109. Durie, I. A., Lynch, B. M., and Sternhell, S., Austral. J. Chem. 13:156 (1960).

110. Marchessault, R. H., Pure and Appl. Chem. 5:107(1962).

111. Vander Linden, N. G. Unpublished results.

112. Silverstein, R. M., and Bassler, G. C. Spectrophotometric identification of organic compounds. p. 64. New York, John Wiley & Sons, 1968.

113. Schuerch, C. The hemicelluloses. In Browning's The chemistry of wood. p. 220. New York, Interscience, 1963.

114. Lapinoja, V. Unpublished results.

115. Freudenberg, K., Science 148:595(1965).

116. Bolker, H. I., and Brenner, H. S., Science 170, no. 3954:173(1970).

117. Sully, B. D., and Williams, P. L., The Analyst 87:653(1962).

118. Institute Method 3, 1951.

119. Schroeder, L. R. The alcoholysis of 2,3,4,6-tetra-O-acetyl-β-D-glucopyranosyl bromide. Doctoral Dissertation. Appleton, Wis., The Institute of Paper Chemistry, 1965. 178 p.

120. Rinco Instrument Co., Inc. Automatic Fraction Collectors. Greenville, Illinois.

121. Waters Associates Inc. Porasil, A Controlled Support for Gas Chromatography. Framingham, Mass.

122. Granath, K. A., J. Colloid Sci. 13:308(1958).

APPENDIX I

GENERATION AND ANALYSIS OF PERACETIC ACID SOLUTIONS

GENERATION OF PERACETIC ACID

Peracetic acid was prepared by the hydrogen peroxide oxidation of acetic acid, with sulfuric acid as catalyst, using the method described by FMC Corporation (73).

$$CH_3COOH + H_2O_2 \xrightarrow{H_2SO_4} CH_3CO_3OH + H_2O$$

The peracetic acid generator apparatus was reconstructed and enclosed in a hood-vented, shatterproof, Plexiglas-wire mesh cage, as shown in Fig. 31. In order to minimize catalytic decomposition by trace metal ions, the generator was passivated according to FMC Corporation recommendations prior to initial production of peracetic acid.

The makeup of solutions used in the generator is shown in Table XXIII. Use of the 1000- and 1500-g. feed solutions generated approximately 1000 and 1500 g. of 35% peracetic acid, respectively, at a steady rate of about 1.5 to 2.0 ml./min. under the following operating conditions.

Bath temperature: 67-68°C.
Reaction temperature: 56-58°C.
Vapor temperature: 46-48°C.
Pressure: 40-50 mm.

The generator peracetic acid solutions were stored in vented brown-glass bottles at 5°C.

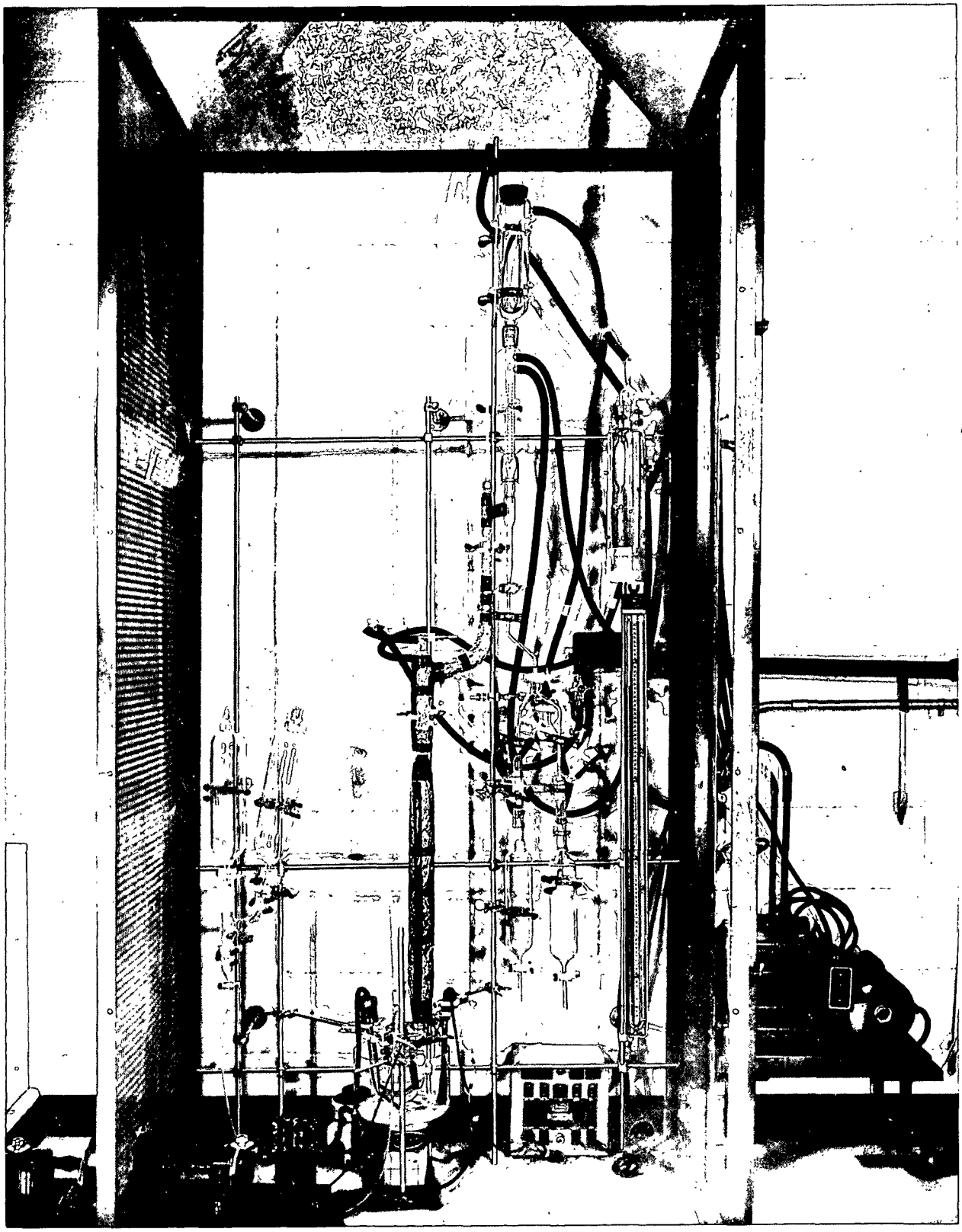

Figure 31. Peracetic Acid Generator According to FMC Corporation (73)

TABLE XXIII

PERACETIC ACID GENERATOR SOLUTIONS

	Pot Charge, g.	Continuous Feed Solutions	
		1000 g. Total	1500 g. Total
Distilled water	114	394	590
96% Sulfuric acid	115	--	--
Glacial acetic acid	51.2	294	440
50% Hydrogen peroxide	270	314	470
Dipicolinic acid	0.275	--	--

PERACETIC ACID AND HYDROGEN PEROXIDE ANALYSIS

REAGENTS

The following reagents were made up in aqueous solution:

Sodium thiosulfate solution, 0.100N
Acetic acid solution, approximately 0.1N
Potassium iodide solution, 15%, w/v
Ammonium molybdate solution, 10%, w/v

PROCEDURE

One hundred milliliters of acetic acid solution were placed in a 500-ml. Erlenmeyer flask and agitated by a magnetic stirring bar. An accurately weighed sample (approximately 5 g. of 3.0% peracetic acid) was added to the flask. Ten milliliters of potassium iodide were added, and, at the same moment, a stopwatch started. Initial buret reading (x_i) was recorded. The liberated iodine was titrated with thiosulfate, with thyodene indicator, until the first end point was overshot by about one drop. The buret reading (x_1) and the stopwatch reading (t_1) were noted when the blue color returned. The titration was continued as before, with an addition of about three more drops of thiosulfate. The second buret reading (x_2) and corresponding time (t_2) of reappearance of blue color were noted. Then several drops of ammonium molybdate solution were

added, and the titration continued to an end point (x_t) which remained stable for one minute.

The concentrations of peracetic acid and hydrogen peroxide were calculated using the following equations:

$$\text{Peracetic acid titer at time zero, } x_0 = x_1 - \frac{t_1 (x_2 - x_1)}{t_2 - t_1} \quad (27)$$

$$\text{Peracetic acid, \%} = 0.3803 (x_0 - x_i)/w \quad (28)$$

$$\text{Hydrogen peroxide, \%} = 0.1701 (x_t - x_0)/w \quad (29)$$

where w = solution weight (g.).

APPENDIX II

CONTINUOUS FLOW REACTION APPARATUS

The continuous flow reaction apparatus was designed essentially to incorporate four features: (1) a reaction vessel to hold the wood wafers in place in the stream of the reaction liquor, (2) a thermostatically controlled bath adjusted to the desired reaction temperature, (3) a device to allow constant-rate input of peracetic acid solution, and (4) a receiver for continuous collection of the solubilized reaction products. The continuous flow reaction apparatus is shown schematically in Fig. 32. All components of the flow system were made of either pyrex glass, teflon, stainless steel, or polyethylene, to minimize decomposition of the hot peracetic acid solution.

Dilute peracetic acid was kept in a 2000-ml. reservoir prior to reaction, and distilled water, for flushing the chips after reaction, was kept in a similar 1000-ml. vessel. Since flow through the apparatus was maintained by hydrostatic head alone, these vessels were placed high in the enclosing hood and were filled by gravity feed from above the hood. Constant flow of the reaction liquor through the apparatus was maintained by a constant head device located below the liquor reservoir. The constant head device, a three-liter round-bottom flask with a short exhaust tube extending below it, was specially blown by Pope Scientific. Variation in head with this device was only about one-quarter inch.

The liquor then passed up through a rotameter-type flowmeter and into 35 feet of heavy wall glass coil to allow it to heat up to constant reaction temperature before entering the reaction vessel. Constant temperature was maintained by submerging the coil and reaction vessel in a cylindrical constant temperature bath that could be raised and lowered using a CRC dual-drive jack. Temperature

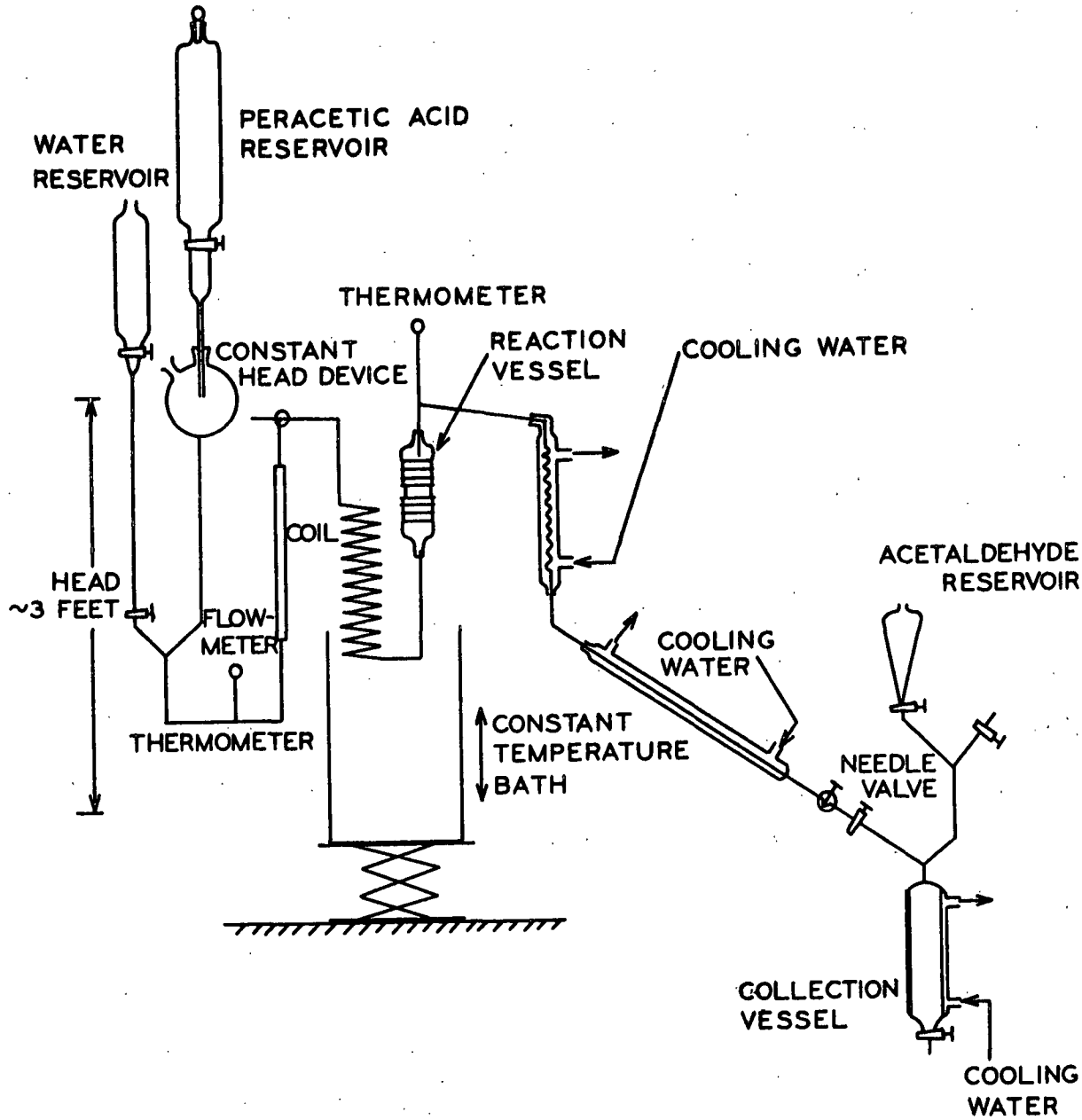

Figure 32. Continuous Flow Reaction Apparatus

control was regulated to 0.01°C. with a mercury thermoregulator and relay operating a 500-watt knife heater and an auxiliary 500-watt heater for quick warmup. A cold coil was also immersed in the bath, and circulation was maintained with a "Little Giant" submersible pump.

The reaction vessel itself was cylindrical, about five inches in height and three inches in diameter, and was custom blown from two 71/60 male standard taper joints by Pope Scientific. The wafers were held in place by two teflon plates perforated with 1/32-inch holes. A stainless steel rod, threaded at both ends, locked the porous plates against the cylindrical reaction vessel. A thermometer was fixed in place in an adaptor just above the reaction vessel.

After passing through the reaction vessel, the liquor was quickly cooled by passing through two condensers – first a Graham condenser, and then into a Liebig condenser. Following the needle valve, a stopcock was used to restrict flow so that the entire system between the constant head device and this point could be filled with fluid without disturbing the needle valve. Just above the collection vessel, acetaldehyde solution was added to quench the reaction, converting residual peracetic acid to acetic acid. The system was open to the atmosphere at this point, making the total head approximately three feet. Final cooling effects were achieved by using a jacketed separatory funnel for liquor collection.

A Tri-Flat Flowmeter, manufactured by the Fischer and Porter Company, was used for rapid measurement of the rate of flow of the liquor through the system. It was placed vertically in the flow line just prior to the submerged coil. The flowmeter selected provided accurate flow measurements between about 20 and 200 cc./min. Flow was estimated by directly reading a scale between one and twenty.

The scale reading was converted to volumetric flow rate at STP using a calibration procedure based on the viscosity and density of water at various temperatures. A thermometer was inserted in the flow line just prior to the flowmeter.

TABLE XXIV

PRELIMINARY FLOW REACTIONS WITH MIXED SUMMERWOOD-SPRINGWOOD WAFERS

Impregnation Period, hr.	Initial Peracetic Acid Concn., %	Initial Hydrogen Peroxide Concn., %	Chip Charge, g.	Temper-ature, °C.	Flow Rate, cc./min.	Time of Reaction, hr.:min.	Yield, %
1	2.15	0.030	30	40	50	1:10	105.5
1	1.97	0.023	30	40	25	2:30	94.0
24	1.96	0.018	40	49	25	2:45	92.1
24	2.84	0.163	40	50	25	2:45	89.5
24	2.87	0.087	40	50	25	5:10	89.9
24	2.82	0.075	40	60	20	3:55	90.9
24	2.83	0.146	40	60	25	4:25	92.1
24	3.52	0.070	40	60	25	10:15	74.2

APPENDIX IV

GENERAL MICROTECHNICAL METHODS OF EMBEDDING AND STAINING WOOD CHIPS

Microtome cross sections, approximately 12 μm. in thickness were prepared from (a) chips with no embedding material, (b) chips, solvent exchanged in increasing percentages of ethyl alcohol and embedded in butyl methacrylate, and (c) freeze-dried chips embedded in butyl methacrylate.

The cross sections were stained in one of the following stains after the removal of any embedding material.

(a) "C" Stain
(b) Jackson's Crystal Violet Stain
(c) Iodine – Malachite Green Stain
(d) Phloroglucinol Stain

The general microtechnical methods of embedding and staining were as follows:

A. Embedding

The submitted chip samples were embedded in butyl methacrylate according to the following schedule.

(1) The wood chips were placed in 70% ethyl alcohol for 24+ hours.
(2) The chips were transferred to 95% ethyl alcohol for 24+ hours.
(3) Absolute ethyl alcohol for 24+ hours.
(4) Absolute ethyl alcohol for 24+ hours.
(5) A 50/50 mixture of absolute alcohol and butyl methacrylate monomer for 24+ hours.
(6) Butyl methacrylate monomer for 24+ hours.
(7) Butyl methacrylate monomer for 24+ hours.
(8) Butyl methacrylate plus catalyst (benzoyl peroxide) in 55°C. oven overnight for polymerization of the methacrylate.

The freeze-dried samples were placed in butyl methacrylate monomer for 24+ hours and then transferred to No. 00 gelatin capsules containing catalyzed butyl

methacrylate monomer and placed in a 50°C. oven overnight for polymerization of the methacrylate.

Microtome sections 12 μm. in thickness were cut on a sliding microtome. The methacrylate was removed with the aid of acetone followed by a 50/50 mixture of absolute ethyl alcohol and ether.

B. Staining

The following staining schedules were employed to stain the microtome cross sections of the chip samples.

(1) "C" Stain (Prepared According to TAPPI Standard T 401 m-60). The sections were rinsed successively in (a) absolute alcohol, (b) 95% alcohol and (c) 70% alcohol. The sections were stained and mounted in "C" stain for preparation of photomicrographs (Fig. 33).

(2) Jackson's Crystal Violet Stain (Fig. 34)

Staining schedule:

(a) The sections were rinsed in absolute ethyl alcohol.
(b) Rinsed in 95% alcohol.
(c) Stained approximately 15 minutes in 1% aqueous crystal violet.
(d) Rinsed in distilled water.
(e) Dehydrated in 70%, 95%, and absolute ethyl alcohol.
(f) Stained approximately 10 minutes in a saturated solution of erythrosin B in clove oil.
(g) Rinsed thoroughly in 50/50 absolute alcohol and xylene.
(h) Cleared in xylene and mounted in Canada balsam for preparation of photomicrographs.

Nonlignified walls are stained red and lignified walls violet. The drawback to the staining procedure is that the erythrosin must be carefully controlled because it has a tendency to replace the violet in the lignified walls if allowed to act too long.

(3) Iodine – Malachite Green Stain

Staining procedure was as follows:

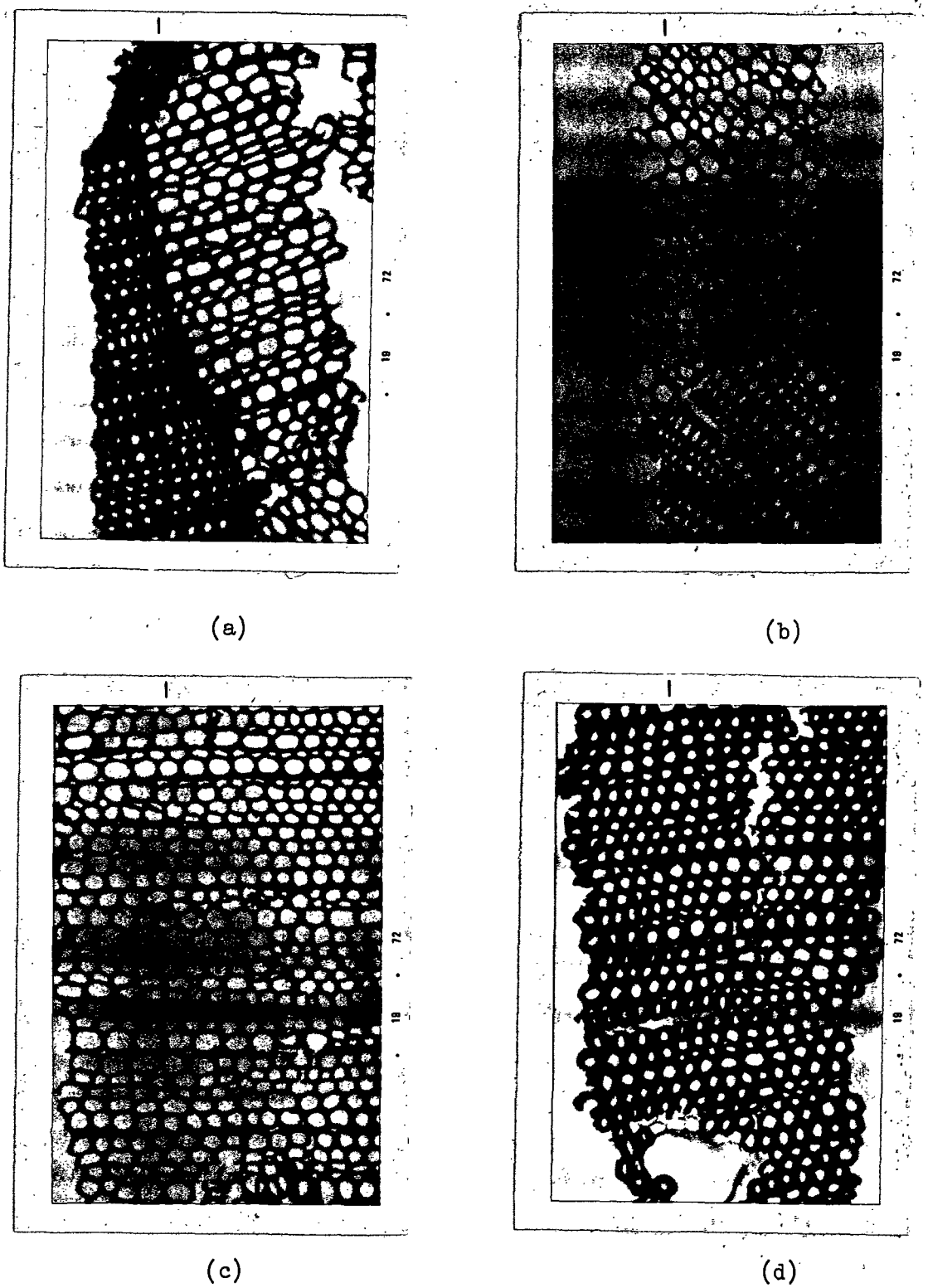

Figure 33. Cross Sections Stained with "C" Stain at Various Yields: (a) 100.0%, (b) 90.9%, (c) 88.1%, and (d) 74.2%

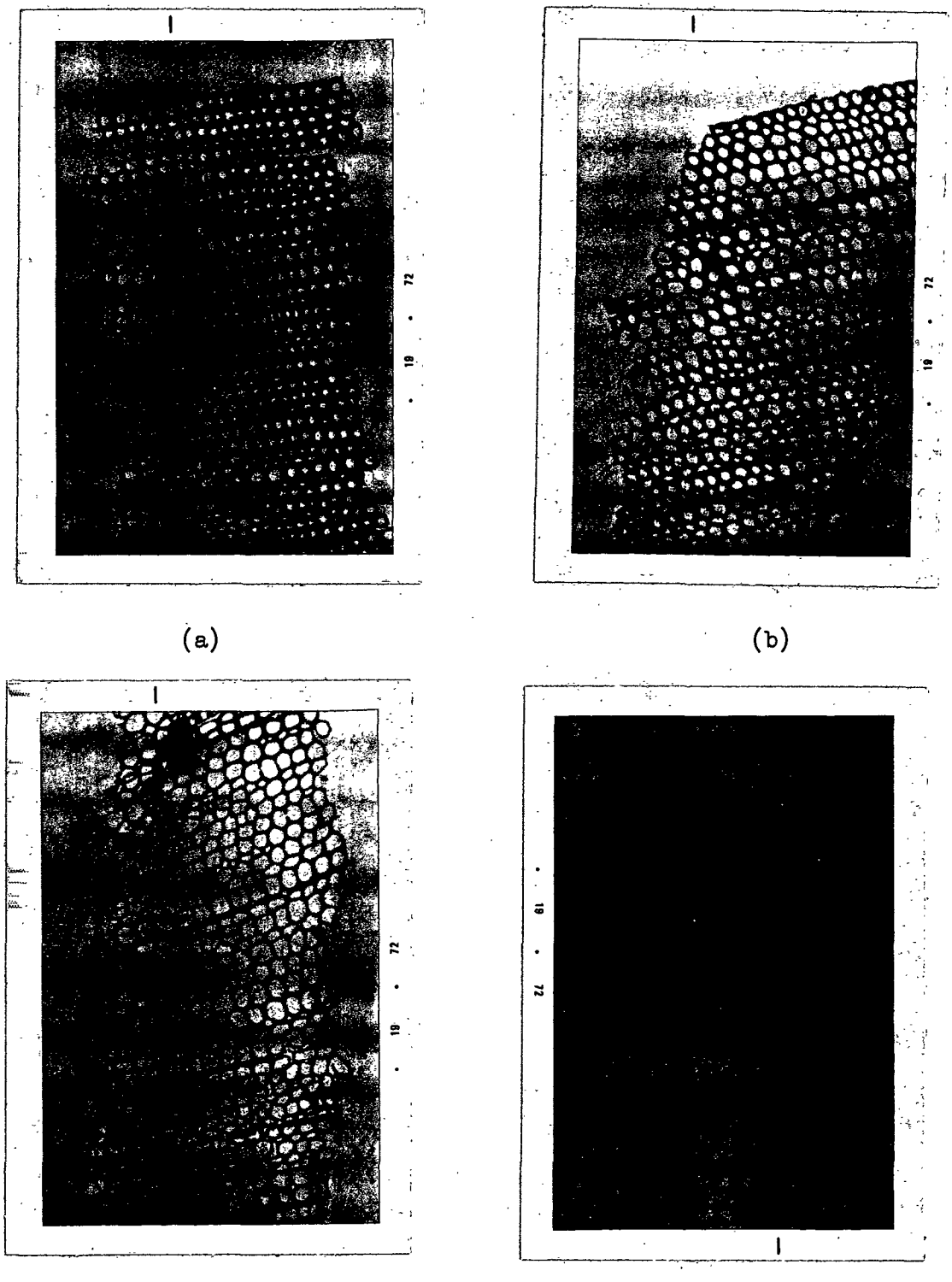

(a) (b)

(c) (d)

Figure 34. Cross Sections Stained with Jackson's Crystal Violet Stain at Various Yields: (a) 100.0%, (b) 92.1%, (c) 89.9%, and (d) 88.1%

(a) The dried sections, after removal of the butyl methacrylate, were placed on a glass slide and flooded with a solution of Malachite green acidified with acetic acid. The stain and specimen were heated to boiling on a small alcohol flame.
(b) The sections were washed thoroughly with distilled water and dried with the aid of filter paper.
(c) A drop of 48% stannic chloride acidified with hydrochloric acid was added and mixed with 1-2 drops of Herzberg stain. A cover glass was added to the preparation before taking photomicrographs.

Lignin free cells, walls, etc., stain intense blue, whereas lignified areas are stained deep brown.

(4) Phloroglucinol Stain (Prepared According to TAPPI Standard T 401 m-60)

The sections were rinsed successively in (a) absolute ethyl alcohol, (b) 95% ethyl alcohol, and (c) 70% ethyl alcohol. The sections were stained and mounted in the stain for preparation of photomicrographs.

Photomicrographs (35 mm. kodacolor) were prepared with a microscope equipped with 16 and 18 mm. objectives, 10X eyepiece, a microattachment, and Leica MD 35 mm. camera body.

APPENDIX V

GEL PERMEATION CHROMATOGRAPHY COLUMN APPARATUS

DESCRIPTION OF THE GPC COLUMN

The GPC column apparatus is shown schematically in Fig. 35. The column was obtained from Fischer-Porter (Lab Crest) and is of 50-mm. inside diameter. It has two sections, totalling 1750 mm. in length, and was equipped with a 2.0-mm. teflon stopcock and an exhaust adaptor for small diameter teflon tubing. The sections were coupled with double O-ring seals which do not disturb the flow pattern within the column.

Constant rate elution was accomplished simply by maintaining a constant hydrostatic head of degassed solvent water, using a solvent reservoir with a 14-mm. I.D. exhaust tube cut at a 45° angle. Flow rate was controlled by manipulating a teflon needle valve at the base of the column. Teflon spaghetti tubing of 1.06-mm. I.D. carried the eluate first to the flow cell in the Cary Model 15 spectrophotometer and then to the volumetric siphon assembly.

The flow cell inside the Cary spectrophotometer was made of Quarasil, a quartz material of high transmittance at short wavelengths. It was obtained from Precision Cells, Inc. and had a path length of 0.1 cm. Matching cells were obtained, and the reference cell was filled with distilled water and sealed. The flow cell was "permanently" fixed in place in one of the two cell holders of the Cary but could be moved out of the sample beam by simply adjusting the cell holder bracket.

A 237-tube, Model VE-2002-B24, fraction collector was obtained from Rinco, Inc. (120). It was equipped with both a timed circuit and a volumetric circuit.

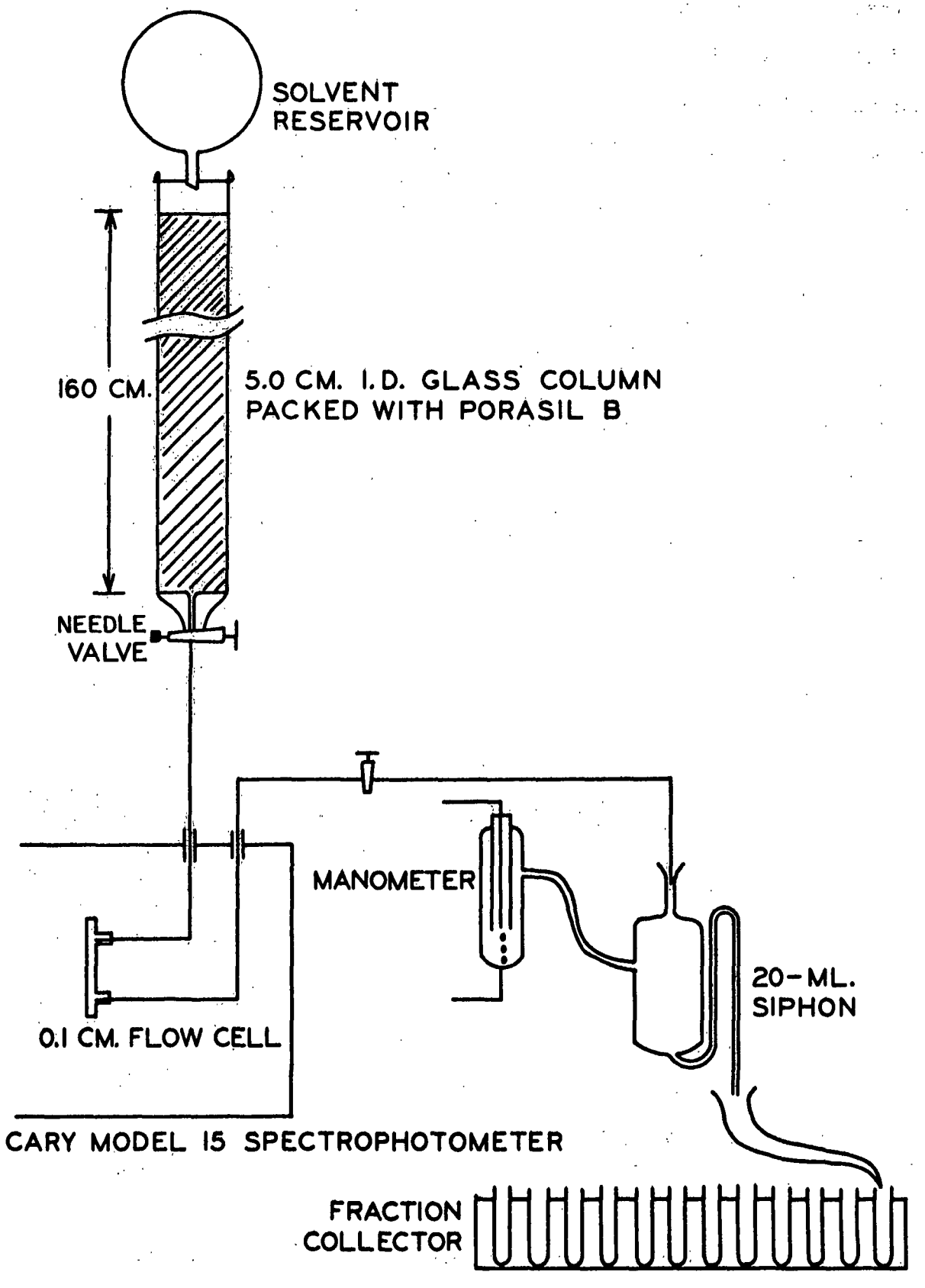

Figure 35. GPC Column Fractionation Apparatus

The volumetric circuit was activated by a siphon-manometer assembly. As the siphon filled to near the level at which it emptied, the potassium bicarbonate solution within the manometer completed the circuit and the fraction collector indexed once. When the siphon emptied, the circuit was broken, and collection of another fraction began. This simple and relatively inexpensive assembly proved to be both versatile and reliable.

The column was packed to a height of 160.0 cm. with deaerated Porasil B (1238.9 g.) submerged in water. A saturated fiberglass filter was placed on top of the Porasil. Porasil B has the second smallest porosity of the types of Porasil available. The surface area is 200 $m.^2/g.$, and the average pore diameter is given as 100-200 A. (121). The column packing procedure is presented in detail below.

The GPC fractionation apparatus was located in a constant temperature room maintained at 72°F. This eliminated the need for a water-jacketed column to maintain temperature control.

GPC COLUMN PACKING PROCEDURE

Forty-three units (of approximately 30 g. each) of Porasil B were obtained to pack the large GPC column. The Porasil obtained had a distinct contaminant present and became brown in water suspension. The Porasil was cleaned by baking at 500°C. for six hours in a muffle furnace. Treatment of all the Porasil for six hours resulted in considerably lightened dry particles, almost white in color. Based on the dry weight measured at 250°C., baking at 500°C. resulted in a 1.5% weight loss.

The approximate weight of Porasil required to pack the large column to 160 centimeters was calculated to be 1230 g. (dry density = 0.391 $g./cm.^3$).

A total of 1238.0 g. of Porasil B was weighed into two 2000-ml. globe funnels, and 1500 ml. of distilled water was added to each. Deaeration under vacuum proceeded for eight days.

First, the column was filled to the top with deaerated, distilled water. Then, two fiberglass filter papers were wetted and gently guided down the column to rest on the sintered glass base. The column was then ready to be packed, and the exhaust stopcock was opened. The deaerated Porasil was slowly added through the stopcock of the globe funnel, while a mechanical stirrer constantly agitated the Porasil suspension within the funnel.

Packing was completed in about five hours. The color of the packed column was pale beige. Not quite all the Porasil had been added by the time a height of 167 centimeters had been reached, and it became evident that air bubbles in the top half of the column accounted for this loose packing. These were removed by applying vacuum directly to the column. The column shrank, and the remainder of the Porasil was added, resulting in a final column height of 160 centimeters.

As the column was eluted with deaerated water, the eluant was slightly colored by some contaminant still in the Porasil. However, after several liters of washing, the eluant had become clear.

APPENDIX VI

RESULTS OF SOLUTE EXCLUSION STUDIES AND ERROR ANALYSIS

SORPTION VERSUS DIFFUSION OF DEXTRANS

TABLE XXV

YIELD = 100.0%, DEXTRAN T40

Sample Number	Chip Dry Weight (p), g.	Water With Chip (q), g.	Solution Weight (w), g.	Initial Concn., c_i, %	Final Concn., c_f, %	Inaccesible Water (δ), g./g. wood
1	3.2783	4.91	24.71	+0.04°	+0.065°	Obs. rotation
2	3.0495	4.60	24.75	+0.04°	+0.03 °	
3	3.2464	4.70	24.77	0.105	0.092	0.3659
4	3.3308	4.35	24.72	0.105	0.093	0.3482
5	3.1635	4.68	24.48	0.204	0.180	0.4480
6	2.8947	4.42	24.07	0.204	0.183	0.5728
7	3.1054	4.74	24.31	0.444	0.381	0.2320
8	3.4064	5.50	24.76	0.444	0.383	0.4566
9	3.3750	4.90	24.25	0.956	0.823	0.3171
10	3.7088	6.57	23.78	0.956	0.795	0.4780
11	2.9599	5.74	24.52	1.888	1.535	0.3036
12	3.4442	6.29	24.37	1.888	1.514	0.3125
Average at c_i = 1.838%						0.8080

TABLE XXVI

YIELD = 90.9%, DEXTRAN T10

Sample Number	Chip Dry Weight (p), g.	Water With Chip (q), g.	Solution Weight (w), g.	Initial Concn., c_i, %	Final Concn., c_f, %	Inaccessible Water (δ), g./g. wood
1	1.0837	3.866	24.830	0.000°	-0.003°	Obs. rotation
2	1.7254	6.994	24.624	0.000°	-0.002°	
3	1.9061	7.280	24.758	0.0983	0.0785	0.5429
4	1.7064	7.269	24.958	0.0983	0.0774	0.3115
5	2.4115	13.732	24.812	0.1843	0.1272	1.0757
6	1.8405	13.446	23.716	0.1843	0.1374	2.9075
7	1.7312	15.301	23.989	0.4726	0.3115	1.6726
8	2.1193	12.136	23.086	0.4726	0.3372	1.3528
9	2.5268	20.154	21.325	0.9326	0.5045	0.8142
10	2.3673	15.018	23.267	0.9326	0.6100	1.1466
11	2.9178	14.154	24.403	1.8653	1.2532	0.7664
12	2.6298	13.691	22.142	1.8653	1.2168	0.7194
Average at c_i = 1.8653%						0.7429

ERROR ANALYSIS

The extreme scatter, especially at low c_i, is due, for the main part, to the uncertainty in the precision of the polarimetry determinations. In the equation for "inaccessible water"

$$\delta = \frac{w + q}{p}\left[1 - \frac{w}{w + q}\left(\frac{c_i}{c_f}\right)\right] \qquad (13)$$

the critical factor is the term

$$\frac{w}{w + q}\left(\frac{c_i}{c_f}\right) \qquad (30)$$

which has a value of approximately 0.95.

The uncertainty in the term $(\underline{c}_i/\underline{c}_f)$ depends on the values of the individual terms; i.e., it is the sum of the relative errors in determining $\underline{c}_i$ and $\underline{c}_f$. Assume that the polarimeter may be read to $\pm$ 0.01° accuracy. Let the value of $\underline{c}_i/\underline{c}_f$ be 2.00. The error in determining $(\underline{c}_i/\underline{c}_f)$ can then be estimated at various values of $\underline{c}_i$:

	Relative Error	Error in Critical Term
$\underline{c}_i$ = 0.1%	0.01/0.470 = 0.0234	
$\underline{c}_f$ = 0.05%	0.01/0.235 = 0.0468	
	0.0702	0.9500 $\pm$ [0.0702 x 0.9500]
$\underline{c}_i$ = 2.0%	0.01/9.40 = 0.0011	
$\underline{c}_f$ = 1.0%	0.01/4.70 = 0.0021	
	0.0032	0.9500 $\pm$ [0.0032 x 0.9500]

This error is magnified in determining

$$1 - \frac{w}{w + q}\left(\frac{c_i}{c_f}\right) \qquad (31)$$

Thus, if $\underline{c}_i$ = 0.1%

$$(31) = 1 - 0.95 \pm 0.067$$
$$= 0.05 \pm 0.067$$

and if $\underline{c}_i$ = 2.0%

$$(31) = 1 - 0.95 \pm 0.003$$
$$= 0.050 \pm 0.003$$

From these simple calculations, it is seen that at very low initial dextran concentration, the uncertainty in the value of "inaccessible water" is greater than the value itself. Even at $\underline{c}_i$ = 2.0%, the error is more than 5% of the value of δ. Thus, this approach to studying the possible sorption of dextrans on wood is confounded by experimental error and would require a great number of determinations at low $\underline{c}_i$ to be certain of conclusion.

APPENDIX VII

APPLICATION OF THE POROUS SPHERE MODEL TO SOLUTE EXCLUSION STUDIES IN THE LITERATURE

The application of the solute exclusion technique to the study of the porous structure of wood requires an independent, and reliable, estimate of the size of the solute macromolecules in solution as a function of molecular weight. Stone and Scallan (67) employed the Einstein-Stokes equation to estimate the diameter, D, of an equivalent solid hydrodynamic sphere from its diffusion coefficient. Little evidence was given for the validity of this estimation of the size of dextran macromolecules in solution.

The porous sphere model by Seely (56) for a cross-linked polymer in solution, discussed in the literature review, has been applied to the dextrans obtained from Pharmacia. These dextrans contain 5-10% of non-1→6-linkages which are responsible for the branching of the molecule. Intrinsic viscosity and weight-average molecular weight data from six commercially available dextrans plus eight additional sets of data points taken from Granath (122) have been used to calculate A and B in Equation (9). A good linear plot was obtained (Fig. 36), indicating the validity of the model for these molecules.

$$A = 92.9 \text{ cc./g.}$$
$$B = 4.28 \times 10^{3}$$

From these values, the permeability, K, and the hydrodynamic radius, a, were calculated, using Equations (10) and (11), respectively:

$$K = 2.57 \times 10^{-13} \text{ cm.}^2$$
$$a = 2.45 \times 10^{-8} \bar{M}_w^{1/3} \text{ cm.} \qquad (32)$$

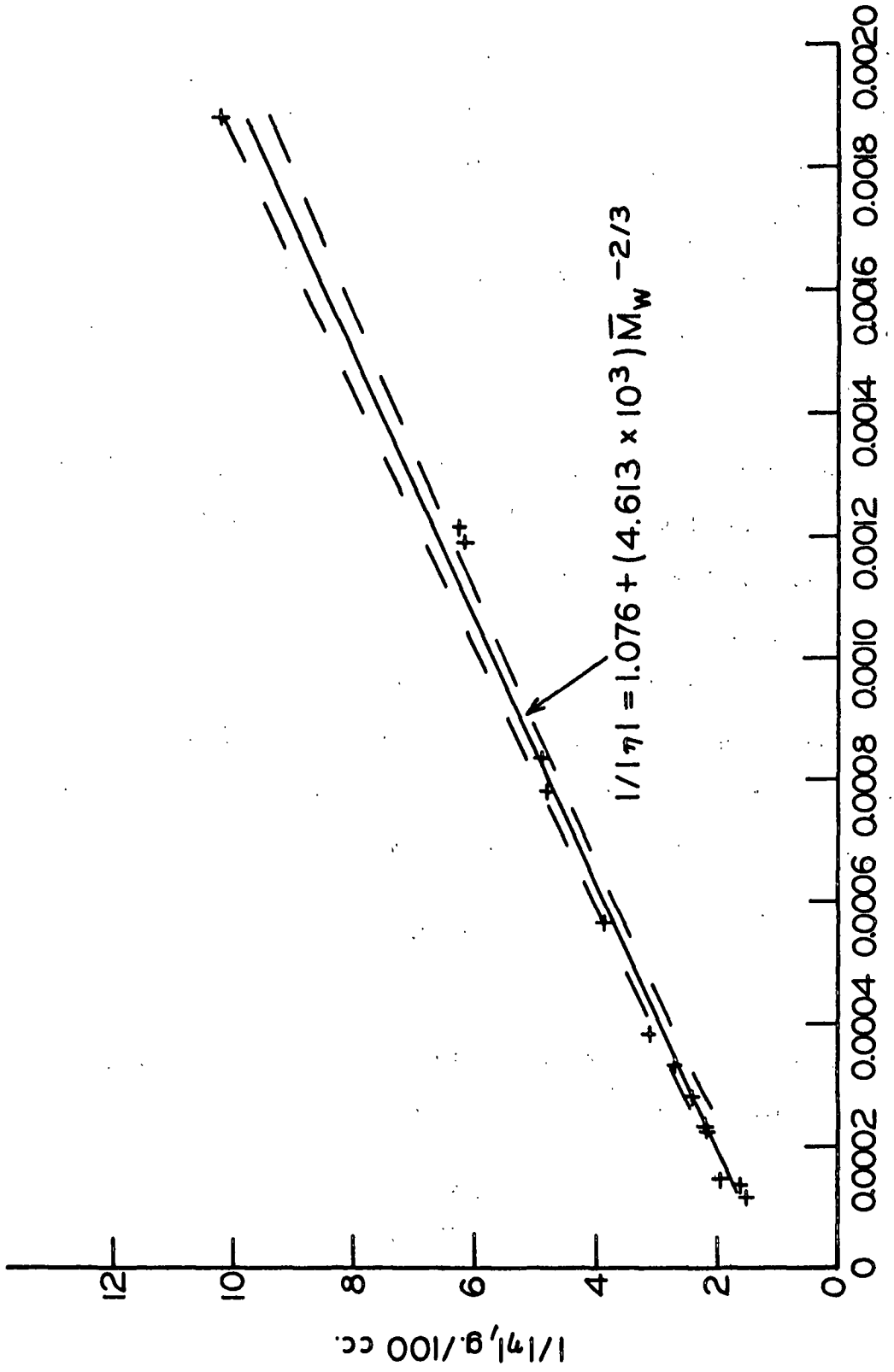

Figure 36. Inverse of Intrinsic Viscosity, $1/[\eta]$, Versus Weight-Average Molecular Weight to the Negative 2/3 for Combined Data of B512 Dextrans by Granath (122) and Commercially Available Pharmacia Dextrans

The diameter of dextran molecules in solution according to the Einstein-Stokes theory used by Stone and Scallan (67) is compared to that computed by Seely's porous sphere model for several dextrans in Table XXVII. The porous sphere model is probably a more accurate estimation of molecular diameter at weight-average molecular weights of 10,000 or more, but at lower molecular weights, independent intrinsic viscosity determinations would be required to verify the application of Equation (32). The true molecular diameter is probably intermediate between the two theories in the molecular weight range below 10,000, becoming closer to the Einstein-Stokes estimate as molecular weight decreases. Therefore, it is not possible to simply correct Stone's estimation of molecular diameter (or pore width) by using the porous sphere model for dextrans in solution. However, it may be stated, in view of this discussion, that qualitatively Stone's accessibility curves for kraft pulps (67) should be shifted to slightly higher molecular diameters.

TABLE XXVII

COMPARISON OF DEXTRAN MOLECULAR SIZE COMPUTED FROM EINSTEIN-STOKES (67) AND SEELY THEORIES

	Molecular Diameter	
$\bar{M}_w$	Solid Sphere Model (D), A.	Porous Sphere Model (2a), A.
1,400	20	55
2,600	26	67
5,400	36	86
8,800	45	101
11,200	51	110
21,800	68	137
39,800	90	167
100,500	140	228
420,000	270	367
2×10^6	360	618

A review of the solute exclusion studies in the literature has suggested that both sulfite pulping (66) and sodium chlorite holopulping (72) result in

considerable swelling of the cell wall of softwood chips. However, an increase in cell wall volume of only about 10% was observed in the early stages of kraft pulping (67). In light of recent work on holopulping, it appears that swelling of the cell wall by any of these processes is no more than 10% (114). The observed swelling with sodium chlorite holopulping actually occurred upon washing of the delignified chips rather than during the delignification reaction itself. This same observation may explain the apparent swelling with sulfite pulping, as well. Swelling of the cell wall was largely attributed to changing electrokinetic effects which occurred upon washing (114). With these observations in mind, and the data presented in Table X (p. 51), it appears that at high yields the pore volume change in the cell wall which occurred during peracetic acid delignification of loblolly pine wafers most closely parallels that which has been measured for kraft pulping.

Therefore, for lack of a more direct measurement, the change in median pore width of loblolly pine springwood wafers with progressive delignification by peracetic acid has been estimated and is presented in Fig. 9 (p. 53). The curve shows a slightly greater median pore width than that given by Stone and Scallan (67) for kraft pulps to take into account the change in the determined size of the dextran molecules.

APPENDIX VIII

RESULTS OF ABSORPTIVITY (275 NM.) DETERMINATION AND GENERATION OF BEST FIT SOLUTION

ABSORPTIVITY DATA COLLECTED

TABLE XXVIII

SPECTROPHOTOMETRICALLY DETERMINED ABSORPTIVITY DATA

Fraction Number	Absorbance at 275 nm.	Concentration, g./l.	a_{275}, l./g.cm.
1-2[a]	0.255	0.1469	1.74
5-6	0.873	0.1078	4.91
7	1.225	0.2210	5.55
8[a]	0.915	0.1544	5.93
10[a]	0.851	0.1415	6.02
15	0.763	0.1145	6.66
17	0.703	0.1022	6.88
19	1.670	0.2450	6.14
20[a]	0.838	0.1150	7.29
21[a]	0.573	0.0825	6.95
22	0.706	0.0980	7.20
24	1.525	0.2170	7.03
26[a]	0.578	0.1005	6.81
26[a]	1.021	0.1447	7.06
28	0.788	0.1070	7.36
29[a]	0.580	0.0833	6.95
30	0.831	0.1133	7.34
33[a]	0.908	0.1206	7.53
34[a]	0.884	0.1213	7.30
36	0.780	0.1112	7.01
40[a]	0.737	0.0994	7.41
41	0.812	0.1114	7.29
43	0.615	0.0900	6.83
44[a]	0.732	0.1051	6.96
45[a]	0.696	0.0881	7.91
45	1.610	0.2880	5.57
47	0.714	0.1172	6.10
49	0.776	0.1248	6.22
50[a]	0.466	0.0760	6.13
50	0.756	0.1172	6.45
50[a]	0.600	0.0954	6.29
51-52	1.620	0.2550	6.35
53-54[a]	0.630	0.0930	6.78
55-56	0.855	0.1382	5.77
57-58[a]	0.339	0.0671	5.05
59-60[a]	0.452	0.0922	5.54
61-62	1.325	0.2460	5.39

See end of table for footnote.

TABLE XXVIII (Continued)

SPECTROPHOTOMETRICALLY DETERMINED ABSORPTIVITY DATA

Fraction Number	Absorbance at 275 nm.	Concentration, g./l.	$\underline{a}_{275}$, l./g.cm.
65	0.368	0.1428	2.58
67	0.920	0.4070	2.16
71	0.830	0.2580	3.22
73	0.589	0.2682	2.20
75	1.025	0.3530	2.87
77	0.557	0.2286	2.44
84	0.855	0.2430	3.52
88-91	1.920	0.6120	3.14
100-103	1.240	0.4500	2.76

[a]These determinations were made on freeze-dried lignins.

VALUES OF BEST FIT SOLUTIONS

TABLE XXIX

VALUES OF BEST FIT SOLUTIONS OF $\underline{a}_{275}$ VERSUS FRACTION NUMBER

Fraction Number	$\underline{a}_{275}$	Fraction Number	$\underline{a}_{275}$
1-2	1.77	26	7.09
		27	7.14
3-4	3.63	28	7.18
		29	7.22
5-6	4.87	30	7.25
		31	7.28
7	5.50	32	7.30
8	5.81	33	7.31
9	6.05	34	7.32
10	6.24	35	7.32
11	6.38	36	7.30
12	6.48	37	7.28
13	6.56	38	7.25
14	6.63	39	7.20
15	6.67	40	7.15
16	6.71	41	7.09
17	6.75	42	7.02
18	6.78	43	6.94
19	6.81	44	6.86
20	6.85	45	6.77

Table continued next page.

TABLE XXIX (Continued)

VALUES OF BEST FIT SOLUTIONS OF a_{-275} VERSUS FRACTION NUMBER

Fraction Number	a_{-275}	Fraction Number	a_{-275}
21	6.88	46	6.68
22	6.92	47	6.59
23	6.96	48	6.49
24	7.00	49	6.39
25	7.05	50	6.30
51-52	6.16	76	2.73
53-54	5.99	77	2.75
55-56	5.82	78	2.76
57-58	5.66	79	2.78
59-60	5.49	80	2.80
61-62	5.27	81	2.81
63-64	4.95	82	2.83
		83	2.84
		84	2.86
		85	2.88
65	2.56	86-87	2.90
66	2.57	88-91	2.95
67	2.59	92-95	3.01
68	2.60	96-99	3.07
69	2.62	100-103	3.14
70	2.64		
71	2.65		
72	2.67		
73	2.68		
74	2.70		
75	2.72		

APPENDIX IX

SUMMARY OF INTRINSIC VISCOSITY DATA

TABLE XXX

INTRINSIC VISCOSITY AT 30°C.

Fraction Number	t, sec.	t_0, sec.	c, g./100 ml.	$[(t-t_0)/t_0]/c$, dl./g.	$[\eta]_{30} \pm$ 95% Limits, dl./g.
1-2	481.3	240.3	4.045	0.2479	
	425.2		3.236	0.2378	
	382.9		2.697	0.2200	
	349.4		2.312	0.1964	
	335.0		2.023	0.1948	0.1374 ± 0.0200
3-4	248.2	216.3	1.537	0.0959	
	241.2		1.230	0.0936	
	234.5		1.025	0.0821	
	232.8		0.878	0.0868	
	230.0		0.769	0.0824	0.0684 ± 0.0094
5-6	263.5	230.5	1.283	0.1116	
	255.4		1.027	0.1052	
	251.1		0.856	0.1045	
	247.7		0.733	0.1018	
	245.2		0.642	0.0994	0.0884 ± 0.0003
5-6	306.9	240.3	1.793	0.1546	
	292.7		1.434	0.1521	
	283.8		1.195	0.1515	
	276.1		1.024	0.1455	
	271.7		0.896	0.1458	0.1365 ± 0.0046
8	240.7	216.3	1.4131	0.0798	
	235.0		1.131	0.0765	
	231.9		0.942	0.0766	
	228.9		0.808	0.0721	
	226.9		0.707	0.0694	0.0612 ± 0.0045
10	260.7	240.3	1.383	0.0614	
	255.3		1.106	0.0564	
	252.7		0.922	0.0560	
	250.3		0.790	0.0527	
	249.0		0.692	0.0524	0.0431 ± 0.0024

TABLE XXX (Continued)

INTRINSIC VISCOSITY AT 30°C.

Fraction Number	t, sec.	t_0, sec.	C, g./100 ml.	$[(t-t_0)/t_0]/C$, dl./g.	$[\eta]_{30}$ ± 95% Limits, dl./g.
12	254.2	230.5	1.353	0.0760	
	250.8		1.083	0.0813	
	245.2		0.902	0.0707	
	243.4		0.773	0.0724	
	241.4		0.677	0.0699	0.0629 ± 0.0107
13	227.0	216.3	1.166	0.0424	
	224.4		0.933	0.0401	
	223.2		0.777	0.0410	
	221.7		0.666	0.0375	
	221.1		0.583	0.0381	0.0334 ± 0.0030
13	258.5	240.3	1.424	0.0532	
	254.0		1.139	0.0501	
	252.1		0.949	0.0517	
	249.6		0.814	0.0476	
	248.8		0.712	0.0497	0.0448 ± 0.0043
15	260.4	240.3	1.144	0.0731	
	256.6		0.915	0.0741	
	253.3		0.763	0.0709	
	251.0		0.654	0.0681	
	249.8		0.572	0.0691	0.0635 ± 0.0042
17	226.6	216.3	1.042	0.0457	
	224.7		0.833	0.0466	
	223.4		0.694	0.0473	
	221.8		0.595	0.0427	
	220.0		0.521	0.0417	0.0392 ± 0.0057
18	227.5	216.3	1.176	0.0441	
	224.8		0.940	0.0418	
	222.0		0.672	0.0392	
	221.1		0.588	0.0378	0.0320 ± 0.0012
20	224.3	216.3	1.223	0.0302	
	222.7		0.979	0.0302	
	221.2		0.816	0.0278	
	220.2		0.699	0.0258	
	219.7		0.612	0.0257	0.0206 ± 0.0026
22	242.3	230.5	1.020	0.0502	
	239.6		0.816	0.0484	
	238.3		0.680	0.0498	
	236.9		0.583	0.0476	
	235.9		0.510	0.0459	0.0435 ± 0.0031

TABLE XXX (Continued)

INTRINSIC VISCOSITY AT 30°C.

Fraction Number	t, sec.	t_0, sec.	c, g./100 ml.	$[(t-t_0)/t_0]/c$, dl./g.	$[\eta]_{30} \pm$ 95% Limits, dl./g.
25	241.1	230.5	1.343	0.0342	
	237.9		1.075	0.0299	
	236.8		0.896	0.0305	
	236.2		0.768	0.0322	
	236.0		0.672	0.0355	0.0325 ± 0.0072
25	242.2	230.5	1.053	0.0482	
	240.0		0.842	0.0490	
	273.3		0.702	0.0420	
	236.8		0.601	0.0455	
	235.8		0.526	0.0437	0.0383 ± 0.0020
26	231.8	216.3	1.165	0.0615	
	228.3		0.932	0.0595	
	226.6		0.777	0.0613	
	224.2		0.666	0.0549	
	223.1		0.583	0.0540	0.0479 ± 0.0064
27	251.8	240.3	1.189	0.0403	
	248.6		0.951	0.0363	
	247.5		0.793	0.0378	
	246.0		0.680	0.0355	
	245.6		0.595	0.0378	0.0335 ± 0.0043
28	224.4	216.3	1.098	0.0341	
	222.6		0.878	0.0332	
	221.2		0.732	0.0310	
	220.4		0.627	0.0302	
	220.1		0.549	0.0320	0.0276 ± 0.0029
29	243.5	230.5	1.033	0.0546	
	240.2		0.827	0.0509	
	237.4		0.636	0.0471	
	235.6		0.517	0.0428	0.0322 ± 0.0039
30	250.0	240.3	1.146	0.0352	
	247.2		0.917	0.0313	
	246.1		0.764	0.0316	
	245.3		0.655	0.0318	
	244.4		0.573	0.0298	0.0257 ± 0.0029
31	248.6	230.5	1.179	0.0666	
	244.8		0.943	0.0658	
	242.6		0.786	0.0668	
	240.2		0.674	0.0625	0.0601 ± 0.0073

TABLE XXX (Continued)

INTRINSIC VISCOSITY AT 30°C.

Fraction Number	$\underline{t}$, sec.	$\underline{t}_0$, sec.	$\underline{c}$, g./100 ml.	$[(\underline{t}-\underline{t}_0)/\underline{t}_0]/\underline{c}$, dl./g.	$[\eta]_{30} \pm$ 95% Limits, dl./g.
31	258.8	240.3	1.260	0.0611	
	253.7		1.008	0.0553	
	250.8		0.840	0.0520	
	249.4		0.720	0.0526	0.0391 ± 0.0078
33	251.4	240.3	1.073	0.0431	
	249.1		0.858	0.0427	
	247.2		0.715	0.0402	
	246.0		0.613	0.0387	
	245.0		0.536	0.0365	0.0310 ± 0.0030
36	224.7	216.3	1.244	0.0312	
	223.3		0.995	0.0325	
	221.4		0.829	0.0284	
	220.8		0.711	0.0293	
	220.5		0.622	0.0312	0.0283 ± 0.0046
36	248.2	240.3	1.069	0.0308	
	246.6		0.855	0.0307	
	245.6		0.712	0.0310	
	244.7		0.611	0.0300	
	243.8		0.534	0.0273	0.0263 ± 0.0034
39	239.3	230.5	1.097	0.0348	
	238.0		0.878	0.0371	
	236.5		0.732	0.0356	
	235.6		0.627	0.0353	
	234.7		0.549	0.0332	0.0332 ± 0.0039
41	250.7	240.3	1.145	0.0378	
	248.3		0.916	0.0363	
	246.9		0.764	0.0360	
	246.2		0.654	0.0375	
	245.1		0.573	0.0349	0.0339 ± 0.0028
41	245.7	230.5	1.254	0.0526	
	241.3		1.003	0.0467	
	238.8		0.836	0.0431	
	237.2		0.717	0.0406	
	236.6		0.627	0.0422	0.0287 ± 0.0041
43	226.4	216.3	0.886	0.0527	
	224.3		0.709	0.0522	
	222.6		0.591	0.0493	
	220.8		0.443	0.0470	0.0414 ± 0.0041

TABLE XXX (Continued)

INTRINSIC VISCOSITY AT 30°C.

Fraction Number	t, sec.	t_0, sec.	C, g./100 ml.	$[(t-t_0)/t_0]/C$, dl./g.	$[\eta]_{30} \pm$ 95% Limits, dl./g.
43	256.8	240.3	1.412	0.0486	
	254.7		1.130	0.0531	
	251.5		0.941	0.0495	
	249.3		0.807	0.0464	
	248.5		0.706	0.0483	0.0459 ± 0.0068
45	252.4	240.3	1.197	0.0421	
	250.1		0.957	0.0426	
	248.0		0.798	0.0402	
	246.6		0.684	0.0384	
	245.5		0.598	0.0362	0.0315 ± 0.0038
47	253.0	240.3	1.084	0.0488	
	250.2		0.867	0.0475	
	247.7		0.722	0.0426	
	246.8		0.619	0.0437	
	245.2		0.542	0.0376	0.0299 ± 0.0058
49	226.7	216.3	1.186	0.0405	
	224.5		0.949	0.0400	
	223.2		0.791	0.0403	
	222.0		0.678	0.0389	
	220.8		0.593	0.0351	0.0331 ± 0.0047
49	259.4	240.3	1.257	0.0633	
	255.1		1.005	0.0613	
	252.2		0.838	0.0591	
	250.0		0.718	0.0562	
	248.4		0.628	0.0537	0.0455 ± 0.0031
51-52	246.5	230.5	0.854	0.0813	
	242.5		0.683	0.0762	
	240.8		0.569	0.0785	
	237.5		0.427	0.0711	0.0637 ± 0.0117
51-52	230.1	216.3	1.307	0.0488	
	226.7		1.046	0.0460	
	224.5		0.871	0.0435	
	222.9		0.747	0.0409	
	221.6		0.653	0.0375	0.0281 ± 0.0031
53-54	260.3	240.3	1.741	0.0478	
	255.5		1.393	0.0454	
	252.5		1.161	0.0437	
	250.9		0.995	0.0443	
	249.0		0.871	0.0416	0.0369 ± 0.0023

TABLE XXX (Continued)

INTRINSIC VISCOSITY AT 30°C.

Fraction Number	t, sec.	t_0, sec.	c, g./100 ml.	$[(t-t_0)/t_0]/c$, dl./g.	$[\eta]_{30} \pm$ 95% Limits, dl./g.
55-56	273.9	230.5	1.469	0.1282	
	264.6		1.175	0.1259	
	258.8		0.979	0.1271	
	254.6		0.840	0.1245	
	251.3		0.735	0.1229	0.1193 ± 0.0033
57-58	280.5	216.3	1.558	0.1905	
	267.1		1.247	0.1884	
	258.5		1.039	0.1878	
	251.9		0.891	0.1848	
	247.5		0.779	0.1851	0.1792 ± 0.0021
59-60	276.0	230.5	1.599	0.2234	
	265.7		1.279	0.1194	
	258.9		1.066	0.1156	
	253.7		0.914	0.1101	
	250.7		0.800	0.1096	0.0948 ± 0.0034
63-64	277.8	230.5	1.240	0.1655	
	267.3		0.992	0.1609	
	260.9		0.827	0.1595	
	256.1		0.709	0.1567	
	252.6		0.620	0.1546	0.1441 ± 0.0022
65	255.5	230.5	1.438	0.0755	
	249.8		1.150	0.0728	
	246.4		0.958	0.0720	
	243.3		0.821	0.0676	
	241.2		0.719	0.0646	0.0560 ± 0.0046
68	258.4	216.3	1.927	0.1010	
	249.1		1.542	0.0984	
	243.5		1.285	0.0979	
	238.9		1.101	0.0949	
	235.9		0.964	0.0941	0.0875 ± 0.0021
70	280.5	216.3	1.769	0.1678	
	266.1		1.415	0.1627	
	257.0		1.179	0.1596	
	250.4		1.011	0.1560	
	245.7		0.884	0.1537	0.1401 ± 0.0015
71	286.2	216.3	1.608	0.2010	
	271.7		1.286	0.1992	
	262.1		1.072	0.1976	
	255.2		0.919	0.1958	
	249.9		0.804	0.1933	0.1870 ± 0.0024

TABLE XXX (Continued)

INTRINSIC VISCOSITY AT 30°C.

Fraction Number	t, sec.	t_0, sec.	c, g./100 ml.	$[(t-t_0)/t_0]/c$, dl./g.	$[\eta]_{30} \pm$ 95% Limits, dl./g.
73	302.7	230.5	2.198	0.1425	
	286.2		1.758	0.1374	
	275.3		1.465	0.1327	
	267.6		1.256	0.1282	
	264.4		1.099	0.1259	0.1094 ± 0.0023
75	339.6	230.5	1.908	0.2481	
	313.2		1.526	0.2350	
	296.9		1.272	0.2265	
	286.8		1.090	0.2240	
	279.0		0.954	0.2206	0.1918 ± 0.0044
77	351.9	230.5	2.025	0.2600	
	321.9		1.620	0.2447	
	304.6		1.350	0.2381	
	290.6		1.157	0.2253	
	282.4		1.013	0.2223	0.1839 ± 0.0060
79	295.0	216.3	2.018	0.1803	
	279.1		1.614	0.1798	
	266.7		1.345	0.1732	
	258.3		1.153	0.1684	
	252.1		1.009	0.1640	0.1496 ± 0.0078
82	283.3	216.3	2.420	0.1280	
	269.8		1.936	0.1277	
	259.3		1.614	0.1232	
	251.6		1.383	0.1180	
	246.3		1.210	0.1146	0.1029 ± 0.0072
86-87	326.3	216.3	2.752	0.1848	
	298.0		2.201	0.1716	
	281.2		1.834	0.1636	
	270.1		1.572	0.1582	
	262.1		1.376	0.1539	0.1228 ± 0.0011
96-99	236.5	216.3	2.544	0.0367	
	231.8		2.035	0.0352	
	228.8		1.696	0.0341	
	227.2		1.454	0.0347	
	225.8		1.272	0.0345	0.0319 ± 0.0015

APPENDIX X

OPERATION OF THE MECHROLAB MEMBRANE OSMOMETER AND ANALYSIS OF THE DATA BY A DYNAMIC METHOD

OPERATION OF THE OSMOMETER

The Mechrolab 501 Membrane Osmometer operates by balancing a small air bubble, located within a capillary on the solvent side of the membrane, between the osmotic pressure of the solution and the hydrostatic head of the solvent cup. A light beam continuously detects the bubble within the capillary and activates the servo mechanism to move the solvent cup in the direction necessary to balance the osmotic pressure and keep the bubble in a steady position.

Readout of the instrument is in centimeters of head of solvent. When lignin solution was added, hydrostatic head decreased rapidly from a high value, due to instrument lag. Readings were taken at half-minute intervals over the first six minutes after addition of solution, then in minute intervals to about ten minutes. Within usually three to five minutes, the rate of descent decreased to a more gradual rate. During this time, diffusion of the solute molecule was occurring. When the solution was replaced with solvent, the instrument began a sharp increase from a low pressure, reaching a steady rate of ascent again in three to five minutes. Further change was gradual and apparently due to back diffusion of solute.

ANALYSIS OF OSMOTIC PRESSURE DATA

When the polymer being studied is small enough in solution to diffuse through the membrane, analysis by a dynamic method is required. No universally accepted method has been published for picking the solution or solvent value under dynamic conditions. However, many hours of examining the plots of

hydrostatic head versus time have led to the development of a rather consistent technique of analysis. Essentially, an attempt was made to determine the beginning of a steady rate of change of solution or solvent value, which generally occurred at about three to five minutes after introduction of the solution. An extension of this steady rate, or a tangent drawn at about this time interval, was drawn back to the time equals zero axis, and the solution ($\underline{P}$) or solvent ($\underline{P}_o$) value was taken to be the intercept.

It was assumed that a plot of $(\underline{P} - \underline{P}_o)/\underline{c}$ versus concentration would yield a straight line whose slope was positive but generally not steep. The tangent lines were drawn using as good judgment as possible, taking into account the full family of ten solution and ten solvent curves (5 concentrations, each run twice). Finally, the various families of curves of the fractions were compared. Account was taken of the fact that higher concentrations diffused more readily. In addition, the faster rate of diffusion of the later (presumably smaller) molecules was observed.

Number-average molecular weight was calculated from van't Hoff's law, Equation (19) as follows:

$$\overline{M}_n = RT/(\pi/c)_o =$$

$$\frac{(0.08205 \text{ l. atm./deg.mole})(1033.2 \text{ g./cm.}^2\text{atm.})(1000 \text{ cm.}^3/\text{l.})(1 \text{ cm.}^3/0.9957 \text{ g.})(298°)}{(\pi/c)_o}$$

$$= \frac{25,372}{(\pi/c)_o}$$

where π = osmotic pressure, cm.

$\underline{c}$ = concentration, g./l.

APPENDIX XI

SUMMARY OF NUMBER-AVERAGE MOLECULAR WEIGHT DATA

TABLE XXXI

NUMBER-AVERAGE MOLECULAR WEIGHT BY MEMBRANE OSMOMETRY

Fraction Number	P, cm.	P_o, cm.	Concn., g./l.	π/c	$(\pi/c)_o \pm$ 95% Limits	$\bar{M}_n$	$\bar{M}_n$ Range
1-2	19.47	16.15	2.938	1.130			
	19.31	16.00	2.938	1.127			
	18.71	16.00	2.350	1.153			
	18.62	15.99	2.350	1.119			
	18.08	16.34	1.763	0.987			
	18.09	16.27	1.763	1.033			
	17.50	16.43	1.175	0.911			
	17.65	16.43	1.175	1.038			
	17.28	16.72	0.588	0.953			
	17.23	16.77	0.588	0.783	0.819 ± 0.034	31,291	30,033-32,659
8	19.00	15.42	1.358	2.636			
	19.32	15.37	1.358	2.909			
	18.40	15.45	1.086	2.715			
	18.55	15.50	1.086	2.807			
	17.95	15.92	0.815	2.491			
	17.74	16.02	0.815	2.111			
	17.61	16.18	0.543	2.633			
	17.61	16.25	0.543	2.504			
	17.05	16.54	0.272	1.878			
	17.10	16.60	0.272	1.841	1.847 ± 0.133	13,873	12,944-14,945
14	18.37	15.76	0.928	2.811			
	18.20	15.73	0.928	2.661			
	17.94	15.91	0.743	2.733			
	17.89	15.69	0.743	2.962			
	17.46	16.00	0.557	2.621			
	17.37	16.48	0.371	2.396			
	17.41	16.56	0.371	2.289			
	17.17	16.78	0.186	2.100			
	17.17	16.75	0.186	2.262	2.053 ± 0.078	12,481	12,022-12,976
15	18.65	15.06	1.247	2.879			
	19.00	15.14	1.247	3.095			
	18.44	15.58	0.998	2.867			
	18.53	15.53	0.998	3.007			
	18.05	15.85	0.748	2.940			
	18.05	15.95	0.748	2.806			
	18.00	16.51	0.499	2.987			
	17.90	16.58	0.499	2.646			
	17.28	16.72	0.249	2.245			
	17.30	16.76	0.249	2.165	2.259 ± 0.113	11,343	10,802-11,941

TABLE XXXI (Continued)

NUMBER-AVERAGE MOLECULAR WEIGHT BY MEMBRANE OSMOMETRY

Fraction Number	P, cm.	P_o, cm.	Concn., g./l.	π/c	$(\pi/c)_o \pm$ 95% Limits	$\bar{M}_n$	$\bar{M}_n$ Range
19	18.90	15.50	1.441	2.359			
	18.92	15.37	1.441	2.463			
	18.30	15.50	1.153	2.429			
	18.30	15.53	1.153	2.403			
	17.95	15.82	0.865	2.463			
	17.90	15.83	0.865	2.394			
	17.57	16.30	0.577	2.203			
	17.69	16.22	0.577	2.550			
	17.17	16.58	0.288	2.047			
	17.27	16.66	0.288	2.117	2.133 ± 0.073	12,009	11,610-12,436
21	19.77	15.55	1.594	2.648			
	19.47	15.08	1.594	2.755			
	18.85	15.50	1.275	2.628			
	18.90	15.50	1.275	2.667			
	18.47	15.94	0.956	2.646			
	18.55	16.10	0.956	2.563			
	17.80	16.32	0.637	2.322			
	17.86	16.38	0.637	2.322			
	17.51	16.73	0.319	2.447			
	17.57	16.75	0.319	2.573	2.345 ± 0.059	10,926	10,657-11,209
22	18.50	15.40	1.206	2.571			
	18.70	15.40	1.206	2.737			
	18.50	15.44	0.965	3.173			
	18.55	15.57	0.965	3.090			
	17.90	15.85	0.723	2.834			
	17.88	15.96	0.723	2.655			
	17.38	16.53	0.482	1.763			
	17.40	16.53	0.482	1.804			
	17.28	16.84	0.241	1.763			
	17.23	16.84	0.241	1.618	1.418 ± 0.201	18,066	15,822-21,052
26	18.93	15.60	1.358	2.452			
	18.86	15.52	1.358	2.460			
	18.50	15.73	1.086	2.550			
	18.48	15.73	1.086	2.531			
	17.82	16.06	0.815	2.160			
	17.88	16.10	0.815	2.185			
	17.45	16.45	0.543	1.841			
	17.47	16.51	0.543	1.767			
	17.20	16.69	0.272	1.878			
	17.14	16.69	0.272	1.657	1.514 ± 0.077	16,921	16,107-17,821

TABLE XXXI (Continued)

NUMBER-AVERAGE MOLECULAR WEIGHT BY MEMBRANE OSMOMETRY

Fraction Number	P, cm.	P_o, cm.	Concn., g./l.	π/c	$(\pi/c)_o \pm$ 95% Limits	$\bar{M}_n$	$\bar{M}_n$ Range
26	19.37	15.47	2.009	1.941			
	18.92	15.13	2.009	1.886			
	18.37	15.27	1.607	1.929			
	18.16	15.25	1.607	1.804			
	17.85	15.43	1.206	2.007			
	17.78	15.44	1.206	1.941			
	17.57	16.18	0.804	1.730			
	17.57	16.25	0.804	1.642			
	17.15	16.55	0.402	1.493			
	17.10	16.65	0.402	1.120	1.331 ± 0.101	19,252	17,892-20,834
30	18.50	15.66	1.109	2.562			
	18.42	15.55	1.109	2.589			
	17.94	15.90	0.887	2.300			
	17.97	15.96	0.887	2.266			
	17.33	16.40	0.665	1.398			
	17.64	16.45	0.665	1.789			
	17.31	16.46	0.443	1.917			
	17.31	16.53	0.443	1.759			
	17.25	16.84	0.222	1.849			
	17.25	16.87	0.222	1.714	1.405 ± 0.145	18,239	16,535-20,333
33	19.29	15.22	2.411	1.688			
	19.14	15.12	2.411	1.667			
	18.86	15.46	1.929	1.763			
	18.68	15.37	1.929	1.716			
	18.38	15.67	1.447	1.873			
	18.36	15.67	1.447	1.859			
	17.65	16.09	0.964	1.616			
	17.75	16.24	0.964	1.566			
	17.38	16.66	0.482	1.493			
	17.38	16.69	0.482	1.431	1.493 ± 0.067	17,155	16,417-17,964
35	18.46	15.75	1.247	2.173			
	18.40	15.65	1.247	2.205			
	18.36	15.78	0.998	2.586			
	18.30	15.75	0.998	2.556			
	17.76	16.21	0.748	2.071			
	17.73	16.26	0.748	1.965			
	17.36	16.43	0.499	1.864			
	17.41	16.45	0.499	1.924			
	17.17	16.78	0.249	1.564			
	17.26	16.78	0.249	1.925	1.613 ± 0.120	15,879	14,782-17,152

TABLE XXXI (Continued)

NUMBER-AVERAGE MOLECULAR WEIGHT BY MEMBRANE OSMOMETRY

Fraction Number	P, cm.	P_o, cm.	Concn., g./l.	π/c	$(\pi/c)_o \pm$ 95% Limits	$\bar{M}_n$	$\bar{M}_n$ Range
38	19.23	15.12	1.871	2.202			
	18.88	15.01	1.871	2.069			
	18.45	15.11	1.497	2.232			
	18.73	15.07	1.497	2.446			
	18.17	15.78	1.123	2.123			
	18.26	15.78	1.123	2.209			
	17.69	15.83	0.748	2.486			
	17.73	16.13	0.748	2.138			
	17.25	16.55	0.374	1.871			
	17.25	16.61	0.374	1.710	1.934 ± 0.119	13,245	12,475-14,117
40	18.32	15.25	1.344	2.284			
	18.57	15.30	1.344	2.433			
	19.01	16.85	0.807	2.678			
	18.99	16.73	0.807	2.802			
	18.33	17.03	0.538	2.418			
	18.35	17.02	0.538	2.474			
	17.97	17.37	0.269	2.232			
	18.01	17.37	0.269	2.381	2.426 ± 0.119	10,566	10,107-11,111
44	19.17	16.60	0.956	2.688			
	19.25	16.53	0.956	2.845			
	19.11	16.67	0.765	3.190			
	19.21	16.70	0.765	3.282			
	18.44	16.90	0.574	2.684			
	18.51	16.90	0.574	2.806			
	18.17	17.19	0.383	2.562			
	18.28	17.21	0.383	2.797			
	17.89	17.38	0.191	2.667			
	17.92	17.32	0.191	3.138	2.781 ± 0.141	9,212	8,768-9,703
44	19.07	15.62	1.607	2.146			
	18.66	15.52	1.607	1.954			
	18.38	15.73	1.286	2.061			
	18.57	15.91	1.286	2.069			
	17.96	15.95	0.965	2.084			
	17.85	16.06	0.965	1.856			
	17.80	16.30	0.643	2.333			
	17.67	16.53	0.643	1.773			
	17.47	16.71	0.322	2.364			
	17.12	16.56	0.322	1.742	2.036 ± 0.122	12,581	11,868-13,384
48	19.55	15.88	1.206	3.044			
	19.37	15.83	1.206	2.936			
	19.18	16.30	0.965	2.986			
	19.11	16.27	0.965	2.945			

TABLE XXXI (Continued)

NUMBER-AVERAGE MOLECULAR WEIGHT BY MEMBRANE OSMOMETRY

Fraction Number	P, cm.	P_o, cm.	Concn., g./l.	π/c	$(\pi/c)_o \pm$ 95% Limits	$\bar{M}_n$	$\bar{M}_n$ Range
	18.53	16.75	0.723	2.461			
	18.71	16.75	0.723	2.710			
	18.19	17.16	0.482	2.136			
	18.34	17.16	0.482	2.447			
	17.98	17.32	0.241	2.738			
	17.99	17.33	0.241	2.779	2.377 ± 0.120	10,778	10,197-11,430
50	18.80	15.57	1.413	2.285			
	18.50	15.38	1.413	2.207			
	18.05	15.44	1.131	2.308			
	19.07	16.65	1.131	2.141			
	18.07	16.20	0.848	2.205			
	18.31	16.12	0.848	2.582			
	17.68	16.30	0.565	2.441			
	17.41	16.63	0.565	1.380			
	17.17	16.52	0.283	2.299			
	17.22	16.60	0.283	2.193	2.110 ± 0.181	12,142	11,184-13,280
53-54	19.30	15.95	1.178	2.844			
	19.10	15.83	1.178	2.776			
	18.94	16.17	0.942	2.940			
	18.73	16.24	0.942	2.643			
	18.55	16.65	0.707	2.689			
	18.57	16.70	0.707	2.646			
	18.30	17.07	0.471	2.611			
	18.30	17.13	0.471	2.484			
	17.90	17.43	0.236	1.995			
	18.07	17.35	0.236	3.056	2.424 ± 0.152	10,567	9,945-11,272
57-58	19.19	16.16	1.150	2.635			
	18.72	16.94	0.920	1.935			
	18.75	16.54	0.920	2.402			
	18.44	16.98	0.690	2.116			
	18.56	17.00	0.690	2.261			
	17.94	17.22	0.460	1.565			
	18.28	17.22	0.460	2.304			
	17.82	17.40	0.230	1.826			
	17.99	17.34	0.230	2.826	2.056 ± 0.242	12,459	11,148-14,119
57-58	17.65	15.67	0.707	2.802			
	17.96	15.76	0.707	3.113			
	17.31	16.23	0.471	2.293			
	17.60	16.40	0.471	2.547			
	17.36	16.75	0.236	2.589			
	17.46	16.73	0.236	3.099	2.627 ± 0.342	9,753	8,630-11,213

APPENDIX XII

PROCEDURE FOR THE DETERMINATION OF FREE PHENOLIC HYDROXYL BY REACTION WITH 1-NITROSO-2-NAPHTHOL

As received, 1-nitroso-2-naphthol was a black powder, containing a small amount of the desired yellow crystals. The impure reagent (6.48 g.) was dissolved in 250-ml. ethanol. The deep red-brown solution color was removed by repeated washing with decolorizing carbon, with filtering through Celite filter acid. The resulting solution was clear yellow. When crystallization could not be achieved, the solution was taken to dryness overnight under vacuum. About 30 mg. of yellow material was obtained (m.p. 108°C., lit. 112°C.) and made up in 95% ethanol solution at 0.1%. The reagent solution was clear yellow.

Nitric acid solution was prepared by diluting chemically pure nitric acid (sp.gr. 1.42) with distilled water to 2.5N. Concentrated hydrochloric acid (sp.gr. 1.19) was used. Model compound solutions in a solvent mixture of 40 parts ethylene glycol and 60 parts ethyl alcohol (96%) were made up at 0.05 mg./ml. Lignin fractions were made up quantitatively at about 0.1 to 0.2% in glycol-ethanol.

The procedure for the color reaction was as follows: In one of two pyrex test tubes was placed a five-milliliter sample of model compound or lignin solution, and in the other, five milliliters of solvent. To each tube was added 1.0 ml. of 1-nitroso-2-naphthol solution, 0.25 ml. of nitric acid solution, and 1.5 ml. of hydrochloric acid. The contents of the tubes were well mixed by shaking and then heated in an oil bath maintained at 85.0 ± 0.5°C. Color development (red-orange) occurred in about ten minutes for the model compounds. The tubes were cooled to room temperature, then put in an ice bath, and finally stored in the refrigerator prior to absorption measurement. Visible spectra

were obtained on the Cary Model 15 spectrophotometer, using 1.0-cm. silica cells, with the solvent (blank) in the reference cell. Concentration of free phenolic hydroxyl was calculated from the absorbance maximum at 505 nm. using the value 1670 l./mole·cm. for molar absorptivity.

APPENDIX XIII

SUMMARY FROM THE LITERATURE OF INFRARED BAND ASSIGNMENTS OF LIGNIN AND CARBOHYDRATE MATERIALS

TABLE XXXII

SUMMARY FROM THE LITERATURE OF INFRARED BAND ASSIGNMENTS OF LIGNIN AND CARBOHYDRATE MATERIALS

3600-3000 $cm.^{-1}$

Frequency, $cm.^{-1}$	Band Assignment	Reference
Hydroxyl Group O-H		
3440-3430	Phenolic and alcoholic groups (strong H-bonding indicated by shift from normal 3600 of free hydroxyls)	(102,104)
3400	O-H peak of differential spectra shifted slightly from above	(102)
3380	Same	(109)
3300	Same (all indicate lack of differentiation between phenols and alcohols)	(103)
3600-3200	Overall spread of H-bonded O-H	(110)
3400, 3150sh	Broadness of band indicates degree of H-bonding	(107)
Carboxyl Group O-H		
3505	Appears as shoulder in presence of alcohol and phenol groups	(102)
Water		
3448	Broad absorption	
Aromatic C-H		
3000		(104)
3030	Expected C-H stretch of aromatic rings, but not observed in lignins	(109)

3000-2600 $cm.^{-1}$

Aliphatic C-H		
2890-2880	Tertiary C-H groups of alkyl side chains	(102,104)
2885-2900	Also present in differential spectra; since this is also a strong carbohydrate band, assignment is uncertain (poor compensation possible)	(102,103)
2920,2850	Methoxyl groups and side-chain methylene	(107)
2920,2830	Same	(109)
2860-2850	Methoxyl groups	(102)
2845	Methoxyl groups or CH_2 symmetrical stretching vibration	(104)

TABLE XXXII (Continued)

SUMMARY FROM THE LITERATURE OF INFRARED BAND ASSIGNMENTS OF LIGNIN AND CARBOHYDRATE MATERIALS

Frequency, $cm.^{-1}$	Band Assignment	Reference
	1800-1600 $cm.^{-1}$	
Carbonyl, C=O		
1730-1725	Acetyl groups or carboxylic acid groups	(110)
1720	β-Keto, carboxyl, and acetyl groups	(106)
1713	Nonconjugated (to ring) carboxyl groups (observed in kraft lignins)	(107)
1705-1700	Carboxyl groups	(90,109)
1720-1700	Two possibilities: 1) β-keto groups and 2) carboxyl groups	(102)
1735	Nonconjugated carboxylic acid esters; peak parallels 1375 peak, therefore is acetyl group attached to the lignin (unstable to $NaBH_4$, so not a lactone)	(22)
1715	Often obscured in pine lignins by 1735 peak; esters of C_6C_1 and C_6C_3 acids suggested	(22)
1730-1720	β-Keto groups	(104,90)
1726	β-Keto groups (stable to $NaBH_4$)	(106)
1725	β-Keto groups (decreases in alkali upon conversion to enolic form; keto (yellow)←→enol (colorless)	(23)
1712	β-Keto groups (unstable to $NaBH_4$; shifts to 1575 in alkali, reappears upon acidification; re-acidified group now stable to $NaBH_4$ and suggested to be aliphatic COOH)	(107)
1670-1665	α-Keto groups (conjugated to ring) plus small amounts of coniferyl aldehyde groups	(105,106, 22,100)
1660	α-Keto groups	(102,104)
1660	α-Keto groups with paraposition etherified and oxygen in β-position	(107)
1655	Same (this peak found to be unstable to $NaBH_4$, but some disagreement by various authors as to the borohydride stability of 1720 peak above)	(90)
1650	α-Keto with paraphenolic OH (peak shifts to 1635 in alkali)	(107)
1650	In a model cpd. with paraphenolic OH, a similar shift (1675 to 1650) was noted in alkali	(23)
Carbohydrate Carbonyl Bands		
1730	Acetyl ester groups in hemicellulose which were not adequately compensated for in differential spectra	(102)
1730	Carboxyl and acetyl groups on xylans	(103)

TABLE XXXII (Continued)

SUMMARY FROM THE LITERATURE OF INFRARED BAND ASSIGNMENTS OF LIGNIN AND CARBOHYDRATE MATERIALS

Frequency, $cm.^{-1}$	Band Assignment	Reference
	1600-1400 $cm.^{-1}$	
Aromatic C=C		
1606-1595,1515-1500	Two bands, always present	(102,105,106,108,110)
1600	Intensity of this band seems to parallel the amount of conjugation to the ring, models	(23)
1600	In a model cpd. system with α-carbonyl group, treatment with alkali shifted this peak to 1585 and decreased its intensity	(23)
1500	This aromatic band appears to have minimal intensity variation with structure	(22)
1590	An aromatic C=C band that appears to be at least partly due to the presence of the α-carbonyl group (1590 seems to parallel 1660 band)	(102)
1590	Partially attributed to diphenyl groups (5-5')	(105)
1585-1580	Conjugated aromatic C=C	(107)
1465-1460	Partly due to benzene vibration (C=C)	(103,105,110)
1495	A moderate absorption attributed to the coumaran unit, located between much stronger 1515 and 1465 peaks	(105)
C-H Bending		
1462-1452	Doublet characteristic of softwood lignins	(102)
1462	Asymmetric deformation	(107)
1465	Both $-CH_2-$ (bending) and $-OCH_3$ (sym. bending) contribute	(109)
1430	Includes considerable contribution from methoxyl groups	(110)
1425-1420	Same	(102,104)
1425	CH_3 sym. bending vibration in methoxyl groups	(109)
1423	Unassigned guaiacyl absorption	(107)
Carbonyl, C=O		
1600	Carboxylate ion	(110)
1590-1580	Carboxylate ion (on side chain)	(107)
Carbohydrate Bands		
1460	Xylan (in part); $-CH_2-$ sym. bending on pyran ring	(103,110)
	1400-1200 $cm.^{-1}$	
O-H Bands-Alcoholic		
1400-1350	General region of alcoholic O-H absorption, shifting to 980 upon deuteration	(105)

TABLE XXXII (Continued)

SUMMARY FROM THE LITERATURE OF INFRARED BAND ASSIGNMENTS OF LIGNIN AND CARBOHYDRATE MATERIALS

Frequency, $cm.^{-1}$	Band Assignment	Reference
1370	A bending vibration (in plane)	(102)
1360	Same (hardwood)	(104)
O-H Bands-Phenolic		
1225-1215	Phenolic groups	(102,103, 107,109)
Ether Bands; C-O-C		
1270	Aryl-alkyl ether bonds (methoxyl)	(102,107,110)
1265	Asym. stretch vibration of aryl ether linkages	(104,100)
1265	Phenolic ether groups (these all seem to refer to the same general Ar-O-R groups)	(109)
1230	Same (hardwoods)	(104)
Ester Bands; C-O		
1375	Specific for acetyl groups (like 1735 peak, unstable to $NaBH_4$)	(22)
C-H Bending		
1380	Symmetric deformation	(110)
1365	Same	(107)
Ring Substitution		
1300	Condensed (5-position) phenylpropane units	(22)
1275	Uncondensed phenylpropane units (also at 1040)	(22)
1265	Uncondensed guaiacyl groups	(100)
Carbohydrate Bands		
1350	O-H deformation in xylan	(103)
1335	O-H deformation in cellulose	(103)
1330,1320	Probably carbohydrate	(103)
1315	$-CH_2-$ wagging mode in cellulose	(103)
1310	$-CH_2-$ wagging mode in polysaccharides	(103)
1235	Principally xylan	(103)
1205	O-H deformation in cellulose	(103)
	1200-900 $cm.^{-1}$	
Ether Bands; C-O-C		
1190	Unassigned methoxyl	(107)
1140,1040	Doublet, dialkyl ether linkages	(102)
1125	Unassigned aromatic ether	(107)
1120	Asym. stretching in dialkyl ether linkages (hardwood)	(104)
1115	Stretching in methyl-aryl ethers	(109)

TABLE XXXII (Continued)

SUMMARY FROM THE LITERATURE OF INFRARED BAND ASSIGNMENTS OF LIGNIN AND CARBOHYDRATE MATERIALS

Frequency, $cm.^{-1}$	Band Assignment	Reference
1087-1082	Aliphatic ether or secondary O-H	(107)
1031	Methoxyl group	(107)
1030	Sym. stretching in dialkyl ether linkages (hardwood)	(104)
O-H Bands		
1145	Characteristic of 1,3,4 substitution on softwood lignins	(100)
1160sh,1145-1140d, 1135-1130d	Complex pattern characteristic of softwood lignins	(90)
1130	Secondary or tertiary alcoholic groups	(109)
1043	Primary alcoholic groups	(107)
Ethylenic C=C		
970	Very weak band of aromatic conjugated (α-β) double bonds	(107)
Carbohydrate Bands		
1055,1030,990	All partially attributable to cellulose and xylan polysaccharides; assigned to C-O stretching	(103)
1160	C-O-C antisymmetric bridge stretching mode	(103)
1200-1000	Differential spectra in this region could not be interpreted due to strong cellulose absorption	(102)
	900→650 $cm.^{-1}$	
C-H Out-of-plane Bending Vibrations		
860,825	Two bands characteristic of softwood lignins	(102)
870,810	Same	(103)
860,815	Same	(90)
817	Deformation of two adjacent hydrogens (5 and 6)	(107)
858	Deformation of monohydrogen (2)	(107)
Carbohydrate Bands		
895	Anomeric (C_1) carbon group frequency in carbohydrates	(103)
893	Same (characteristic of β-anomeric linkage)	(108)
Note: 560,470	Two bands noted in all softwood lignins	(102)